

**BULLETIN 250**

This document was produced  
by scanning the original publication.

Ce document est le produit d'une  
numérisation par balayage  
de la publication originale.

**DEGREE OF DIAGENESIS, STRATIGRAPHIC  
CORRELATIONS AND POTENTIAL SEDIMENT  
SOURCES OF LOWER CRETACEOUS SHALE  
OF NORTHEASTERN BRITISH COLUMBIA**

A.E. Foscolos and D.F. Stott

1975

**DEGREE OF DIAGENESIS, STRATIGRAPHIC  
CORRELATIONS AND POTENTIAL SEDIMENT  
SOURCES OF LOWER CRETACEOUS SHALE  
OF NORTHEASTERN BRITISH COLUMBIA**

Critical readers

G.R. Davies  
R.O. Van Everdingen

Technical Editor

E.J.W. Irish



Énergie, Mines et  
Ressources Canada

Energy, Mines and  
Resources Canada

**GEOLOGICAL SURVEY  
BULLETIN 250**

**DEGREE OF DIAGENESIS, STRATIGRAPHIC  
CORRELATIONS AND POTENTIAL SEDIMENT  
SOURCES OF LOWER CRETACEOUS SHALE  
OF NORTHEASTERN BRITISH COLUMBIA**

A.E. Foscolos and D.F. Stott

© Crown Copyrights reserved  
Available by mail from *Information Canada*, Ottawa, K1A 0S9

from the Geological Survey of Canada  
601 Booth St., Ottawa, K1A 0E8

and

*Information Canada* bookshops in

HALIFAX — 1683 Barrington Street  
MONTREAL — 640 St. Catherine Street W.  
OTTAWA — 171 Slater Street  
TORONTO — 221 Yonge Street  
WINNIPEG — 393 Portage Avenue  
VANCOUVER — 800 Granville Street

or through your bookseller

A deposit copy of this publication is also available  
for reference in public libraries across Canada

Price - Canada: \$3.50                      Catalogue No. M42-250  
Other Countries: \$4.20

Price subject to change without notice

*Information Canada*  
Ottawa  
1975

## P R E F A C E

This report records the results of detailed mineralogical and inorganic geochemical studies on fifteen Lower Cretaceous shale formations in northeastern British Columbia. The work was done to assess the degree of diagenesis, to differentiate and correlate zones within the thick shale sequence and to assess potential sediment sources.

The results of this research have opened up new horizons for the application of inorganic geochemistry in the study of sedimentary rocks. In addition, mineralogical indicators are used, for the first time, to define the diagenetic stages of shale successions, thus bridging the classification gap between the very early sedimentogenesis and early metamorphism. Finally, the work establishes the basis for future studies concerning the evolution of oil- and gas-generating potential of source rocks.

Ottawa, April 1975

D.J. McLaren,  
Director General,  
Geological Survey of Canada.



## CONTENTS

	Page
Introduction .....	1
Acknowledgments .....	1
Stratigraphy .....	1
Sample treatment and methods .....	5
Analytical results .....	7
Moosebar Formation, Peace River .....	7
Commotion Formation, North Wolverine Ridge .....	7
Hasler Formation, Dokie Ridge .....	9
Cruiser Formation, Young Creek .....	9
Gething Formation, Besa River .....	9
Gething Formation, Prophet River .....	15
Gething Formation, Bat Creek .....	15
Buckinghorse Formation, Tetsa River .....	16
Buckinghorse Formation, Muskwa River .....	17
Middle Scatter Formation, Bear Island, Liard River .....	17
Middle Scatter Formation, north of Scatter River .....	18
Scatter Formation, Scatter River .....	18
Garbutt Formation .....	18
Lepine Formation, Liard River .....	18
Lepine, Sikanni and Sully Formations, Scatter River .....	19
Discussion and interpretation of the results .....	19
Inorganic geochemistry, mineralogy and layer lattice silicates .....	19
Peak migration of mixed layers, illite polymorphs, sharpness ratio-crystallinity index, presence of 1:1 layer silicates .....	20
Peak migration of mixed layers .....	20
Illite polymorphs .....	21
Crystallinity index and sharpness ratio .....	21
Presence of kaolinite in shale .....	21
Diagenesis .....	22
Stratigraphic relationships .....	24
Possible sediment sources .....	24
Bibliography .....	27

### Illustrations

Table 1.	References, geographic and topographic locations, sample numbers, total thickness and thickness intervals of the studied formations .....	4
Table 2.	Stratigraphic succession, thicknesses and general lithologies of Cretaceous beds between Tetsa and Scatter Rivers .....	5
Table 3.	Stratigraphic succession, thicknesses and general lithologies of Cretaceous beds in the vicinity of Prophet River .....	5
Table 4.	Stratigraphic succession, thicknesses and general lithologies of Cretaceous beds in the vicinity of Pine and Peace Rivers .....	6
Table 5.	Crystallinity index, sharpness ratio, percentage of 2M illite polymorphs and ratio of illite/kaolin and/or chlorite of fifteen Lower Cretaceous shale formations of northeastern British Columbia .....	9
Table 6.	Mineralogy and clay mineralogy of fifteen Lower Cretaceous shale formations of northeastern British Columbia as determined by X-ray methods .....	10
Table 7.	Exchangeable cations, cation exchange capacity, exchange acidity, base saturation, pH, inorganic carbon and sulphur, and ratio of sulphur to inorganic carbon of fifteen Lower Cretaceous shale formations of northeastern British Columbia .....	11
Table 8.	Total elemental analyses of fifteen Lower Cretaceous shale formations of northeastern British Columbia after lithium saturation and removal of soluble salts .....	12
Table 9.	Percentages of quartz, K-feldspar, Na-feldspar, organic matter, CO <sub>2</sub> evolved from carbonates, sulphur and free Fe <sub>2</sub> O <sub>3</sub> of salt-free Li <sup>+</sup> -saturated samples in fifteen Lower Cretaceous shale formations of northeastern British Columbia .....	13



	Page
Table 10. Elemental analyses and molar ratios of SiO <sub>2</sub> to sesquioxides (R <sub>2</sub> O <sub>3</sub> ) in salt-free Li <sup>+</sup> -saturated samples after the removal of quartz and feldspars in fifteen Lower Cretaceous shale formations of northeastern British Columbia .....	14
Table 11. Crystallinity indices of illites, their relation to sharpness ratio of illites, and their use in evaluating the stages of diagenesis and early metamorphism .....	22
Table 12. A tentative scheme for correlating the crystallinity index, sharpness ratio, percentage of 2M illite polymorphs, percentage of illite in the illite-2:1 expandables random mixed layers, presence and absence of discrete layer lattice silicates and regular interstratified layer silicates with diagenetic stages .....	23
Figure 1. Bullhead-Fort St. John-Dunvegan sequence along the Foothills between Pine and Scatter Rivers .....	2
Figure 2. Index map showing location of sampled sections .....	3
Figure 3. Flow chart of the chemical and mineralogical analyses performed on shale samples .....	8
Figure 4. X-ray diffraction patterns of the whole rock, Ca <sup>2+</sup> and K <sup>+</sup> saturated <.2μ oriented specimens from Moosebar Formation, Peace River (Section 1) .....	31
Figure 5. X-ray diffraction patterns of the whole rock, Ca <sup>2+</sup> and K <sup>+</sup> saturated <.2μ oriented specimens from Commotion Formation, North Wolverine Ridge (Section 2) .....	31
Figure 6. X-ray diffraction patterns of the whole rock, Ca <sup>2+</sup> and K <sup>+</sup> saturated <.2μ oriented specimens from Hasler Formation, Dokie Ridge (Section 3) .....	32
Figure 7. X-ray diffraction patterns of the whole rock, Ca <sup>2+</sup> and K <sup>+</sup> saturated <.2μ oriented specimens from Cruiser Formation (Section 4) .....	32
Figure 8. X-ray diffraction patterns of the whole rock, Ca <sup>2+</sup> and K <sup>+</sup> saturated <.2μ oriented specimens from the lower zone of Gething Formation, Besa River (Section 5, I) .....	33
Figure 9. X-ray diffraction patterns of the whole rock, Ca <sup>2+</sup> and K <sup>+</sup> saturated <.2μ oriented specimens from the middle zone of Gething Formation, Besa River (Section 5, II) .....	33
Figure 10. X-ray diffraction patterns of the whole rock, Ca <sup>2+</sup> and K <sup>+</sup> saturated <.2μ oriented specimens from the upper zone of Gething Formation, Besa River (Section 5, III) .....	34
Figure 11. X-ray diffraction patterns of the whole rock, Ca <sup>2+</sup> and K <sup>+</sup> saturated <.2μ oriented specimens from the lower zone of Gething Formation, Prophet River (Section 6, I) .....	34
Figure 12. X-ray diffraction patterns of the whole rock, Ca <sup>2+</sup> and K <sup>+</sup> saturated <.2μ oriented specimens from the upper zone of Gething Formation, Prophet River (Section 6, II) .....	35
Figure 13. X-ray diffraction patterns of the whole rock, Ca <sup>2+</sup> and K <sup>+</sup> saturated <.2μ oriented specimens from the lower zone of Gething Formation, Bat Creek (Section 7, I) .....	35
Figure 14. X-ray diffraction patterns of the whole rock, Ca <sup>2+</sup> and K <sup>+</sup> saturated <.2μ oriented specimens from the upper zone of Gething Formation, Bat Creek (Section 7, II) .....	36
Figure 15. X-ray diffraction patterns of the whole rock, Ca <sup>2+</sup> and K <sup>+</sup> saturated <.2μ oriented specimens from Buckinghorse Formation, Tetsa River (Section 8, I) .....	36
Figure 16. X-ray diffraction patterns of the whole rock, Ca <sup>2+</sup> and K <sup>+</sup> saturated <.2μ oriented specimens from Buckinghorse Formation, Tetsa River (Section 8, II) .....	37
Figure 17. X-ray diffraction patterns of the whole rock, Ca <sup>2+</sup> and K <sup>+</sup> saturated <.2μ oriented specimens from Buckinghorse Formation, Tetsa River (Section 8, III) .....	37
Figure 18. X-ray diffraction patterns of the whole rock, Ca <sup>2+</sup> and K <sup>+</sup> saturated <.2μ oriented specimens from Buckinghorse Formation, Tetsa River (Section 8, IV) .....	38
Figure 19. X-ray diffraction patterns of the whole rock, Ca <sup>2+</sup> and K <sup>+</sup> saturated <.2μ oriented specimens from Buckinghorse Formation, Tetsa River (Section 8, V) .....	38

	Page
Figure 20. X-ray diffraction patterns of the whole rock, Ca <sup>2+</sup> and K <sup>+</sup> saturated <.2μ oriented specimens from Buckinghorse Formation, Tetsa River (Section 8, VI) .....	39
Figure 21. X-ray diffraction patterns of the whole rock, Ca <sup>2+</sup> and K <sup>+</sup> saturated <.2μ oriented specimens from Buckinghorse Formation, Muskwa River (Section 9, I) .....	39
Figure 22. X-ray diffraction patterns of the whole rock, Ca <sup>2+</sup> and K <sup>+</sup> saturated <.2μ oriented specimens from Buckinghorse Formation, Muskwa River (Section 9, II) .....	40
Figure 23. X-ray diffraction patterns of the whole rock, Ca <sup>2+</sup> and K <sup>+</sup> saturated <.2μ oriented specimens from Buckinghorse Formation, Muskwa River (Section 9, IIIa) .....	40
Figure 24. X-ray diffraction patterns of the whole rock, Ca <sup>2+</sup> and K <sup>+</sup> saturated <.2μ oriented specimens from Buckinghorse Formation, Muskwa River (Section 9, IIIb) .....	41
Figure 25. X-ray diffraction patterns of the whole rock, Ca <sup>2+</sup> and K <sup>+</sup> saturated <.2μ oriented specimens from Garbutt Formation (Section 10) .....	41
Figure 26. X-ray diffraction patterns of the whole rock, Ca <sup>2+</sup> and K <sup>+</sup> saturated <.2μ oriented specimens from the lower zone of Scatter Formation, Scatter River (Section 11, I) .....	42
Figure 27. X-ray diffraction patterns of the whole rock, Ca <sup>2+</sup> and K <sup>+</sup> saturated <.2μ oriented specimens from the middle zone of Scatter Formation, Scatter River (Section 11, II) .....	42
Figure 28. X-ray diffraction patterns of the whole rock, Ca <sup>2+</sup> and K <sup>+</sup> saturated <.2μ oriented specimens from the upper zone of Scatter Formation, Scatter River (Section 11, III) .....	43
Figure 29. X-ray diffraction patterns of the whole rock, Ca <sup>2+</sup> and K <sup>+</sup> saturated <.2μ oriented specimens from Middle Scatter Formation, Bear Island, Liard River (Section 12) .....	43
Figure 30. X-ray diffraction patterns of the whole rock, Ca <sup>2+</sup> and K <sup>+</sup> saturated <.2μ oriented specimens from Middle Scatter Formation, north of Scatter River (Section 13) .....	44
Figure 31. X-ray diffraction patterns of the whole rock, Ca <sup>2+</sup> and K <sup>+</sup> saturated <.2μ oriented specimens from the lower zone of Lepine Formation, Liard River (Section 14, I) .....	44
Figure 32. X-ray diffraction patterns of the whole rock, Ca <sup>2+</sup> and K <sup>+</sup> saturated <.2μ oriented specimens from the middle zone of Lepine Formation, Liard River (Section 14, II) .....	45
Figure 33. X-ray diffraction patterns of the whole rock, Ca <sup>2+</sup> and K <sup>+</sup> saturated <.2μ oriented specimens from the lower zone of Lepine, Sikanni and Sully Formations, Scatter River (Section 14, III, and 15, I) .....	45
Figure 34. X-ray diffraction patterns of the whole rock, Ca <sup>2+</sup> and K <sup>+</sup> saturated <.2μ oriented specimens from the middle zone of Lepine, Sikanni and Sully Formations, Scatter River (Section 15, II) .....	46
Figure 35. X-ray diffraction patterns of the whole rock, Ca <sup>2+</sup> and K <sup>+</sup> saturated <.2μ oriented specimens from the upper zone of Lepine, Sikanni and Sully Formations, Scatter River (Section 15, III) .....	46
Figure 36. Columnar sections illustrating the mineralogy and clay mineralogy in fifteen Lower Cretaceous shale formations of northeastern British Columbia .....	25
Figure 37. Columnar sections of fifteen Lower Cretaceous shale formations of northeastern British Columbia. The various patterns indicate sediments having different source characteristics .....	26



## ABSTRACT

Detailed mineralogical and chemical analyses have been carried out on Lower Cretaceous shale of northeastern British Columbia in order to evaluate the degree of diagenesis, to differentiate and correlate zones within the thick shale sequences, and to assess potential sediment sources.

The degree of sediment diagenesis was studied by examining five indicators in combination in the <math>2\mu</math> clay size fraction. These are: a) layer lattice silicate assemblages; b) percentage of illite in illite-2:1 expandable interstratified clays; c) percentage of 2M illite polymorphs; d) sharpness ratio of illites (Weaver's index); and e) crystallinity index of illites (Kubler's index). With information derived from this work and from data obtained from the studies of Weaver (1961), Kubler (1966), Burst (1969) and Dunoyer de Seconzac (1970), a classification is proposed which relates the five indicators to diagenetic stages. Based on this scheme, the Gething Formation and the lowermost part of the Buckingham Formation at Tetsa River are classified as being in the early stages of diagenesis, while the Lepine, Sikanni and Sully Formations are allocated to the early middle stage of diagenesis. The Moosebar, Commotion, Hasler and Cruiser Formations of Peace River, the Buckingham Formation at Muskwa River and the lower and upper Buckingham Formation at Tetsa River are allocated to the intermediate middle stage of diagenesis.

Stratigraphic correlations based on mineralogy, inorganic geochemistry, and the five diagenetic indicators suggest that the lower Gething Formation at Besa River is correlative with the lower Gething Formation at Bat Creek and with the basal Buckingham Formation at Tetsa River. The middle part of the Gething Formation at Besa River is similar to the upper Gething Formation at Bat Creek. The upper zone of the Gething Formation at Besa River is related to the upper Gething at Prophet River and the second lowest zone of the Buckingham Formation at Tetsa River. The middle Buckingham Formation at Tetsa River is correlative with the lower zone of the Scatter Formation at Scatter River. The upper zone of the Buckingham Formation at Tetsa River is similar to the lower zone of the middle Buckingham Formation at Muskwa River, and to the middle Scatter Formation both at and north of Scatter River. The upper zone of the Buckingham Formation shale at Muskwa River is related to the upper zone of shale of the Lepine Formation at Liard River, and to the lowermost part of the Lepine-Sully-Sikanni Formations at Scatter River. The lower zone of the Lepine Formation at Liard River is correlated with the middle and upper part of the Lepine, Sikanni and Sully Formations at Scatter River. The shales of the Cruiser, Hasler, Commotion and Moosebar Formations of Peace River are unrelated to each other and to any other shale formation encountered in this study.

Combined mineralogical and chemical data indicate that the formations can be divided into three groups, each with different source characteristics: a) the Cruiser, Hasler, Commotion and Moosebar Formations at Peace River; b) the Gething Formation and the lowermost Buckingham Formation

## RÉSUMÉ

Des analyses minéralogiques et chimiques détaillées ont été effectuées sur l'argilite de Crétacé inférieur dans le nord-ouest de la Colombie-Britannique afin d'en évaluer le degré de diagénèse, d'établir des distinctions et des corrélations entre les zones à l'intérieur des épaisses séquences de schistes argileux et de fixer les origines possibles des sédiments.

Le degré de diagénèse sédimentaire a été étudié par l'examen de 5 indices existants dans les particules d'argile inférieures à 2 microns. Ce sont: a) les assemblages en couches de silicate treillisés; b) le pourcentage d'illite dans les argiles expansibles interstratifiées contenant de l'illite 2:1; c) le pourcentage d'illite 2M polymorphes; d) le rapport d'acuité des illites (indice de Weaver); et e) l'indice de cristallinité des illites (indice de Kubler). Au moyen des renseignements obtenus par ce travail et à l'aide des données tirées des études de Weaver (1961), de Kubler (1966), de Burst (1969) et de Dunoyer de Seconzac (1970), on propose une classification qui établit un rapport entre les cinq indices et les stades de la diagénèse. Selon ce système, la formation de Gething et la partie inférieure de la formation de Buckingham de la rivière Tetsa sont classifiées comme étant aux premiers stades de la diagénèse, tandis que les formations de Lepine, Sikanni et Sully sont considérées comme ayant atteint le stade intermédiaire moyen de la diagénèse. On situe les formations de Moosebar, Commotion, Hasler et Cruiser de la rivière de la Paix, la formation de Buckingham de la rivière Muskwa et les parties inférieure et supérieure de la formation de Buckingham de la rivière Tetsa au stade intermédiaire moyen de la diagénèse.

Les corrélations stratigraphiques basées sur la minéralogie, la géochimie minérale et les cinq indices de la diagénèse semblent indiquer que la partie inférieure de la formation de Gething de la rivière Besa se trouve en corrélation avec la partie inférieure de la formation de Gething du ruisseau Bat et la formation basale de Buckingham de la rivière Tetsa. La partie médiane de la formation de Gething de la rivière Besa est semblable à la partie supérieure de la formation de Gething du ruisseau Bat. La zone supérieure de la formation de Gething de la rivière Besa est apparentée à la partie supérieure de la formation de Gething de la rivière Prophète et à l'avant dernière zone inférieure de la formation de Buckingham de la rivière Tetsa. La partie médiane de la formation de Buckingham de la rivière Tetsa est en corrélation avec la zone inférieure de la formation de Scatter de la rivière Scatter. La zone supérieure de la formation de Buckingham de la rivière Tetsa est semblable à la zone inférieure de la partie médiane de la formation de Buckingham de la rivière Muskwa et à la partie médiane de la formation de Scatter; ces deux formations sont toutes deux situées dans la région de la rivière Scatter et au nord de celle-ci. Les schistes argileux de la zone supérieure de la formation de Buckingham de la rivière Muskwa s'apparente aux schistes argileux de la zone supérieure de la formation de Lepine de la rivière Liard et à la partie inférieure des formations de Lepine, Sully et Sikanni de la rivière Scatter. La zone

at Tetsa River; and c) the Lepine, Sully, Sikanni, Garbutt, and Buckinghorse Formations at Muskwa River and the Middle and upper Buckinghorse Formation at Tetsa River.

inférieure de la formation de Lepine de la rivière Liard est en corrélation avec les parties médianes et supérieures de formations de Lepine, Sikanni et Sully de la rivière Scatter. Les schistes argileux des formations de Cruiser, Hasler, Commotion et Moosebar de la rivière de la Paix ne s'apparentent pas les unes aux autres non plus qu'avec toute autre formations de schistes argileux rencontrées au cours de cette étude.

L'ensemble des données minéralogiques et chimique indique que les formations peuvent être classées en trois groupes, chacun présentant des particularités qui indiquent des origines différentes: a) les formations de Cruiser, Hasler, Commotion et Moosebar de la rivière de la Paix; b) la formation de Gething et la formation de Buckinghorse la plus basse de la rivière Tetsa; et c) les formations de Lepine, Sully, Sikanni, Garbutt et Buckinghorse de la rivière Muskwa et les parties médianes et supérieures de la formation de Buckinghorse de la rivière Tetsa.

# "Degree of diagenesis, stratigraphic correlations and potential sediment sources of Lower Cretaceous shale of northeastern British Columbia"

## INTRODUCTION

Clay mineralogy is used in geological studies for various reasons, some of which are summarized by Parham (1966). Recently, layer lattice silicates have been used to reconstruct the geochemical history of sedimentary basins and to assess the degree of sediment alteration upon deep burial and incipient metamorphism (Weaver, 1960, 1961, 1967; Powers, 1959, 1967; Khitarov and Pugin, 1966; Long and Neglia, 1968; Muffler and White, 1969; Perry and Hower, 1970, 1972; Weaver and Wampler, 1970; Mirchink *et al.*, 1971; Teodorovich and Konyukhov, 1970; van Moort, 1971; Weaver *et al.*, 1971; Cordell, 1972; and Sarkisjan, 1972).

Weiss (1969) has shown that a ton of montmorillonite may adsorb very large amounts of protein, amino acids, fats, fatty acids or carbohydrates. In addition, it has been demonstrated experimentally that when organic compounds, which are adsorbed on clays, are heated to 200°C in an oxygen-deprived atmosphere, a mixture of liquid and gaseous hydrocarbons is produced simultaneously with the expulsion of interlayer water from the clays (Weiss and Roloff, 1965). This hydrocarbon mixture contains compounds almost identical to those encountered in petroleum. Galwey (1972) has studied experimentally the catalytic properties of clay surfaces in the genesis of petroleum and concluded that the above reactions make substantial contributions to the formation of natural hydrocarbon deposits. Louis and Tissot (1967), Tissot *et al.*, (1971), and Tissot *et al.*, (1974) have pointed out that, when a sediment is heated to 60°C, its organic components form petroleum products (particularly hydrocarbons) at the expense of kerogen.

Burst (1969) has shown that, during the transformation of montmorillonite to illite, a dehydration process takes place which is closely associated with the production of hydrocarbons. During this transformation, which occurs at temperatures not greater than 150°C, large amounts of water are produced from the clays (Perry and Hower, 1972). Price (1973) concluded, from his work, that deeply buried water at 150°C could dissolve large amounts of hydrocarbons. It appears, therefore, that, during the initial stages of transformation of montmorillonite to illite, hydrocarbons are generated on the clay surfaces. As this process of transformation continues, a large volume of water is released from

the clays, thus triggering primary oil migration (Colombo, 1967; Andreev *et al.*, 1968; Kartsev *et al.*, 1971; and Yerofeyev, 1972).

Clay minerals, therefore, adsorb and embed organic matter, catalyze organic reactions which produce petroleum compounds, and release interlayer water from the expandable clay minerals which is important in primary oil migration. These reactions are temperature and pressure dependent and, since these factors affect also the type, concentration and structure of clay minerals, it is obvious that parameters derived from the study of layer silicates can be used in evaluating the degree of diagenesis and hydrocarbon-generating potential of sediments.

In the present study, the degree of sediment diagenesis is evaluated by the combined use of five indicators derived from the study of clays. Data from this work have been combined with those of other studies to devise a scheme for the classification of the degree of diagenesis. In addition, general mineralogy, clay mineralogy, and inorganic geochemistry have been used to correlate stratigraphically zones of thick shale sequences and to assess potential sediment sources.

## ACKNOWLEDGMENTS

The authors wish to thank Drs. G.R. Davies and R.O. van Everdingen for their constructive criticism of the paper and for reviewing the manuscript. Appreciation is expressed also to Messrs. R.R. Barefoot and A.G. Heinrich for their technical assistance in inorganic chemistry and X-ray diffractometry.

## STRATIGRAPHY

The stratigraphy of Lower Cretaceous rocks at Peace River and southward along the Foothills was described in considerable detail by Stott (1968b). The succession north of Peace River is outlined in preliminary reports (Stott, 1967, 1968a) and is described in more detail by Stott (1973). A brief summary of the stratigraphy follows, in order to provide a basic framework for this study of clay mineralogy.

Lower Cretaceous sediments of northeastern British Columbia were deposited in a vast inland sea that developed through the interior of the North American continent during late Neocomian to Albian time. During the initial phases of this inundation, boreal marine water covered the region that is now northeastern British Columbia. In this region, the embayment was bordered on the west by

---

Manuscript received: May 14, 1974  
Authors' address: Institute of Sedimentary and  
Petroleum Geology  
3303 - 33rd Street N.W.  
Calgary, Alberta  
T2L 2A7

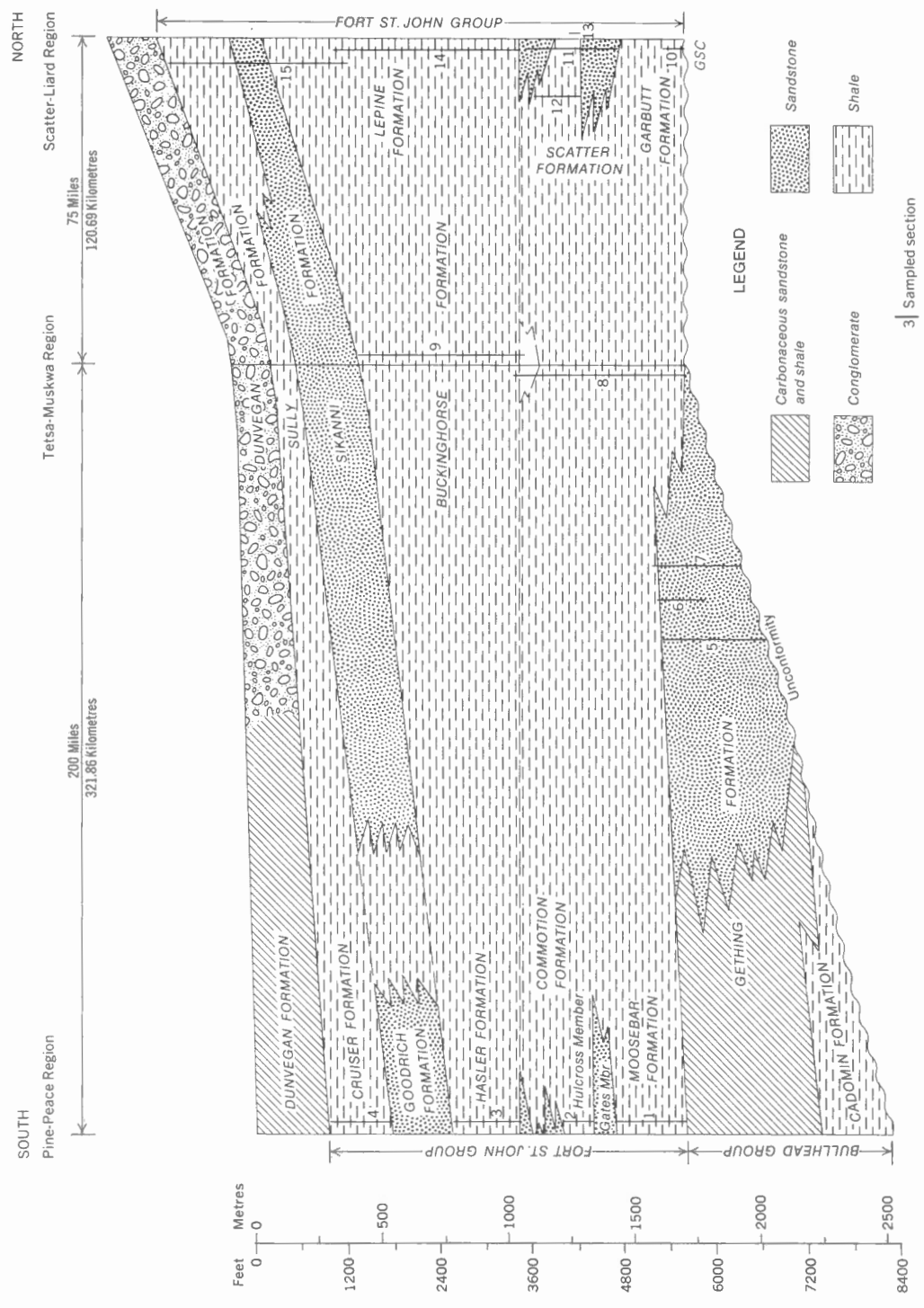


FIGURE 1. Bullhead-Fort St. John-Dunvegan sequence along the Foothills between Pine and Scatter Rivers

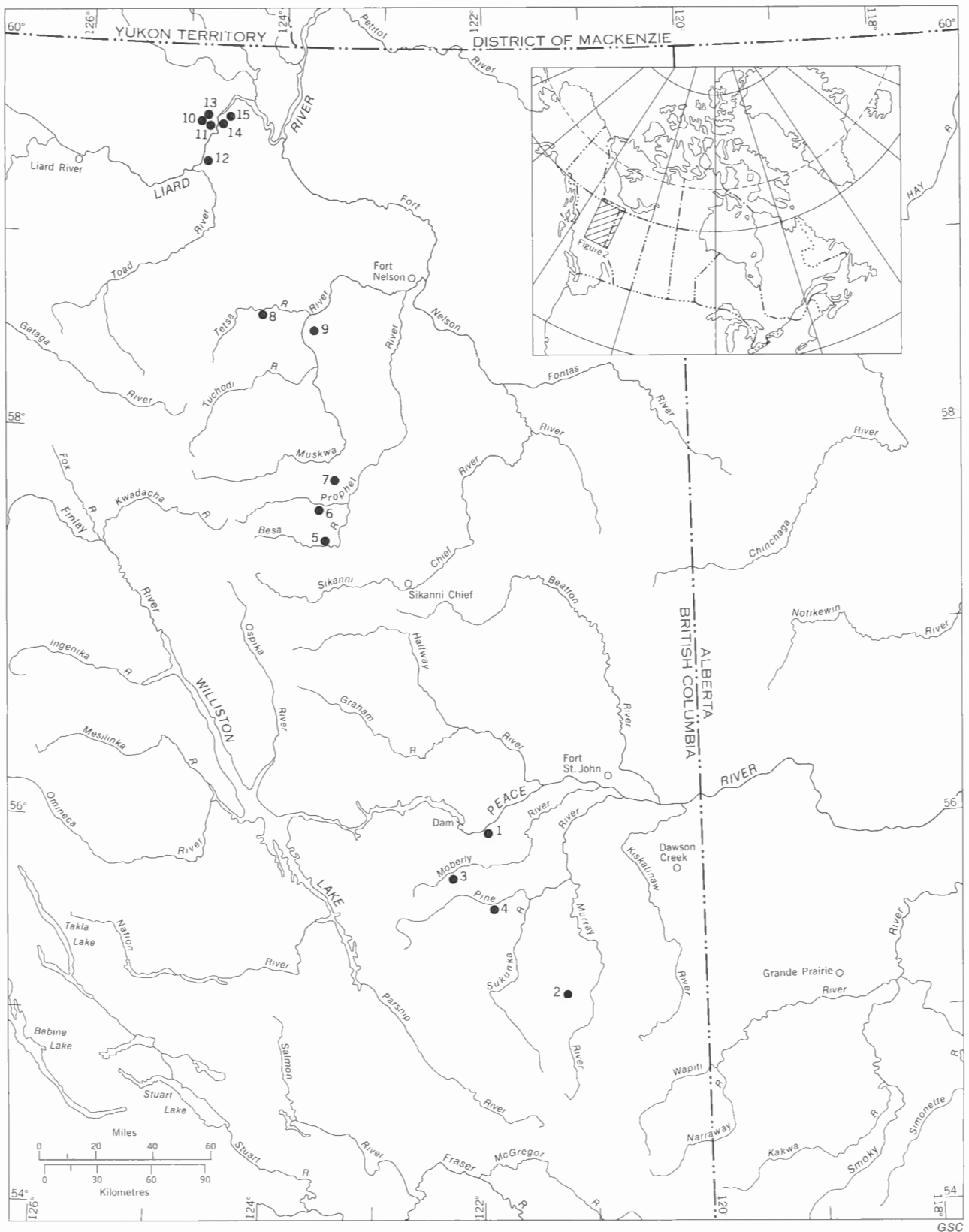


FIGURE 2. Index map showing location of sampled sections. Sections are listed in Table 1



	Formation or Member	Geographic Location	Topographic Location	References	Sample Number	Total Thickness of Formation in feet	Thickness of sampled interval in feet
1.	Moosebar	Peace River	55°58'N, 122°06'W	Stott, 1968a, p. 48, type section	61-282 to 61-308	957	957
2.	Hulcross	Ridge near Wolverine River	55°05'N, 121°23'W	Stott, 1968a, p. 159, type section, Sec. 59-11	59-68 to 59-96	388	388
3.	Hasler	Dokie Ridge	55°42'N, 122°18'W	Stott, 1968a, p. 90; type section	60-124 to 60-140	868	868
4.	Cruiser	Young Creek	55°36'N, 121°46'W	Stott, 1968a, p. 101, type section	60-310 to 60-320	742	742
5.	Gething	Besa River	57°28'N, 123°31'W	Stott, 1973; Section 64-15	64-437 to 64-465	1,330+	1,330+
6.	Gething and basal	Prophet River	57°39'N, 123°34'W	Stott, 1973; Section 62-20	64-505 to 64-596	Buckinghorse -3,500± Gething -1,200 to 1,300	Basal 65' of Buckinghorse Upper 550" of Gething
7.	Buckinghorse	Bat Creek	57°46'N, 123°31'W	Stott, 1973; Section 64-22	64-647 to 64-673	Buckinghorse -3,500± Gething -887	Basal 75' of Buckinghorse 887
8.	Buckinghorse	Tetsa River	58°40'N, 124°07'W	Stott, 1967, p. 53, Section 64-3	64-88 to 64-291 65-125 to 65-165	4,000±	Lower 2,200
9.	Buckinghorse	Muskwa River	58°33'N, 123°45'W	Stott, 1967, p. 61, Section 64-25	64-748 to 64-1,092	4,000±	Upper 2,100
10.	Garbutt	Tributary of Scatter River	59°38'N, 124°58'W	Stott, unpublished; Section 65-12	65-721 to 65-765 65-766 to 65-769	970±	Basal 275
11.	Scatter	Scatter River	59°37'N, 124°44'W	Stott, unpublished; type section, Section 65-11	65-628 to 65-710	1,143	Lower 1,045
12.	Middle and Upper Scatter	"Bear Island" Liard River	59°25'N, 124°50'W	Stott, unpublished; Section 65-16	65-680 to 65-904	655	Lower 525
13.	Middle Scatter	Canyon north of Scatter River	59°38'N, 124°44'W	Stott, unpublished	65-794 to 65-809	545	Lower 80
14.	Lepine	Liard River	59°29'N, 124°46'W	Stott, unpublished; Section 65-9	65-234 to 65-411	3,000±	Lower 2,292
15.	Lepine, Sikanni and Sully	Liard River	59°37'N, 124°40'W	Stott, unpublished; Section 65-10	65-412 to 65-621	Upper Lepine 930 Sikanni 433 Sully 997	2,360

TABLE 1. References, geographic and topographic locations, sample numbers, total thickness and thickness intervals of the studied formations

GSC

the Columbian Orogen and on the east by the Canadian Shield, and clastic material derived from those sources was deposited both within the marine basin and along its bordering alluvial-deltaic plain. The marine sediments deposited during that boreal invasion were investigated during this study. Within northeastern British Columbia, these sediments are included in the Fort St. John Group. The vertical and lateral relationships of the formations within the group are shown schematically in Figure 1.

Samples collected from 15 outcrop sections (Fig. 2, Table 1) were analysed, and these provided representative profiles in three major regions: 1) Pine and Peace Rivers, 2) Tetsa and Muskwa Rivers, and 3) Scatter and Liard Rivers, with supplemental sections from intervening areas.

The most northerly sections from which samples were analysed are in the vicinity of the junction of Scatter and Liard Rivers near the British Columbia-Yukon border. There, the Fort St. John Group comprises mid-basin marine shales separated by two major wedges of fine-grained, epineritic to neritic sandstone. The succession, in ascending order, comprises the Garbutt (shale), Scatter (a major wedge of two sandstone members and intervening shale), Lepine (shale), Sikanni (major sandstone), and Sully (shale) Formations (Table 2).

In the vicinity of Muskwa and Tetsa Rivers, some 75 miles (125 km) south of Scatter River, similar facies are found within the Fort St. John Group although the lower major sandstone wedge (Scatter) is poorly developed. As a result, only three formations are recognized. These are, in ascending order, the Buckinghorse (shale), Sikanni (sandstone), and Sully (shale) Formations (Table 2).

Farther south in the region between Prophet and Peace Rivers, basal shale grades laterally into sandstone which in turn grades into the coal-bearing facies of the deltaic plain. The sandstone is assigned to the Gething Formation and the overlying shale to the Buckinghorse Formation (Table 3). The Sikanni and Sully Formations are present in the eastern part of the region, but their shales were not analysed during this investigation.

At Peace River, 275 miles (460 km) south of Scatter River, part of the succession comprises sediments deposited in the alluvial-deltaic plain that flanked the marine embayment. In that region, a well-developed basal conglomeratic facies and a lower coal-bearing facies are included in the Cadomin and Gething Formations, respectively, of the Bullhead Group. In addition, two other clastic wedges containing sandstone and coal occur. The sequence, in ascending order, comprises the Cadomin (conglomerate) Gething (sandstone and coal), Moosebar (shale), Commotion (sandstone and coal with a middle member of marine shale), Hasler (shale), Goodrich (sandstone), and Cruiser (shale) Formations (Table 4).

#### SAMPLE TREATMENT AND METHODS

Rock samples were ground in a Bleuler mill for 20 seconds. The powdered samples were used in the following analyses.

SERIES	GROUP	FORMATION	THICKNESS IN FEET	LITHOLOGY
UPPER CRETACEOUS	Unconformity			
		DUNVEGAN	500-600	Massive conglomerate; fine- to coarse-grained sandstone; carbonaceous shale and mudstone; coal seams
LOWER CRETACEOUS	FORT ST. JOHN 4,500-6,500 feet	SULLY	300-1,000	Dark grey, marine shale with sideritic concretions; flaky, black shale
		SIKANNI	350-1,000	Fine-grained, laminated, marine sandstone; silty mudstone
		LEPINE	3,000-3,600	Dark grey, marine shale with sideritic concretions; fine-grained silty sandstone
		SCATTER	1,143	Fine-grained, highly glauconitic sandstone and siltstone; silty marine shale
		GARBUTT	950	Silty shales and mudstone, and siltstone; sideritic concretions
Regional erosional unconformity bevels rock of succeeding older age northward and eastward				

TABLE 2. Stratigraphic succession, thicknesses, and general lithologies of Cretaceous beds between Tetsa and Scatter Rivers

SERIES	GROUP	FORMATION	THICKNESS IN FEET	LITHOLOGY
UPPER CRETACEOUS		DUNVEGAN	350-600	Massive conglomerate; fine- to coarse-grained sandstone; some carbonaceous shale
		SULLY	250-700+	Dark grey, marine shale with sideritic concretions; prominent marker bed of fish remains
LOWER CRETACEOUS	FORT ST. JOHN	SIKANNI	350-900	Fine-grained, crossbedded, marine sandstone; rusty weathering, silty mudstone
		BUCKINGHORSE	3,000-3,500	Dark grey, marine shale with sideritic concretions; fine-grained, thin- to thick-bedded sandstone
		GETHING	0-1,300	Fine-grained, cherty, marine sandstone; rusty weathering, rubbly to blocky shales; minor conglomerate and carbonaceous shale; rare coal seams
Regional erosional unconformity bevels rock of succeeding older age northward and eastward				

TABLE 3. Stratigraphic succession, thicknesses, and general lithologies of Cretaceous beds in vicinity of Prophet River

GSC

SERIES	GROUP	FORMATION	THICKNESS IN FEET	LITHOLOGY
UPPER CRETACEOUS		DUNVEGAN	300-1200	Marine and nonmarine sandstone and shale
	LOWER CRETACEOUS	SHAFTSBURY 400-900'	CRUISER	350-800
GOODRICH			50-1,350	Fine-grained, crossbedded sandstone; shale and mudstone
HASLER			500? -1,500	Silty, dark grey marine shale with sideritic concretions; siltstone and sandstone in lower part; minor conglomerate
COMMOTION 1080-1600'		Boulder Creek Member	240-560	Fine-grained, well-sorted sandstone; massive conglomerate; nonmarine sandstone and mudstone
		Hulcross Member	0-450	Dark grey marine shale with sideritic concretions
		Gates Member	220-900	Fine-grained, marine and nonmarine sandstones; conglomerate; coal, shale and mudstone
		MOOSEBAR	100-1,000	Dark grey marine shale with sideritic concretions; glauconitic sandstone and pebbles at base
BULLHEAD		GETHING	75-1,000	Fine- to coarse-grained, brown, calcareous, carbonaceous sandstone; coal, carbonaceous shale, and conglomerate
		CADOMIN	45-600	Massive conglomerate containing chert and quartzite pebbles

GSC

TABLE 4. Stratigraphic succession, thicknesses, and general lithologies of Cretaceous beds in vicinity of Pine and Peace Rivers

All crystalline minerals present in the rock were determined by X-ray diffraction. One portion of the powdered sample was pelletized on a cellulose substrate and X-rayed with  $\text{CoK}\alpha$  radiation, iron filter, settings of 45Kv - 20ma, scanning speed of  $1^\circ 20'/\text{min}/2$  cm, time constant 2, and range  $2^\circ$  to  $40^\circ 20'$ . A second portion of the sample was sieved between 60 and 250 mesh sieves to obtain fine and very fine sand fractions. These fractions were pelletized on a cellulose substrate and X-rayed with  $\text{CuK}\alpha$  radiation, nickel filter setting of 40Kv - 20ma, scanning speed of  $1^\circ 20'/\text{min}/2$  cm, time constant of 2, and range  $2^\circ$  to  $40^\circ 20'$ . The aim was to identify in these fractions the presence of heavy and other minerals. In a third portion of the powdered sample, the clays were analysed as follows. A sample was diluted with water at 1:10 ratio (10 grams of powdered sample with 100 ml distilled water) and sonicated with  $22 \pm 3$  KHZ frequency for 30 minutes. If the clay fraction was flocculating quickly, 1 ml of a 1N  $(\text{NaPO}_3)_6$  + 0.08 M  $\text{Na}_2\text{CO}_3$  mixture was added to stabilize the suspension. After 7 hours, 52 minutes, the  $<2\mu$  fraction was collected, and 200 ml of Javex (trade name for 6%  $\text{NaClO}$ ) was added with constant stirring. The suspension was left overnight on a steam bath to destroy the organic matter and homionically saturate the sample with sodium (Cassidy and Mankin, 1960). The excess salt was washed out and a small portion of the sodium-saturated clay was used to prepare oriented specimens for identification of discrete layer lattice silicates in the less than  $2\mu$  fraction. The sample was X-rayed using  $\text{CuK}\alpha$  radiation with nickel filter, settings of 40Kv - 20ma, scanning speed  $1^\circ 20'/\text{min}/2$  cm, time constant of 2, and range  $2^\circ$  to  $40^\circ 20'$ .

Free iron was removed following the technique of Aguilera and Jackson (1953), and free silica and aluminum were removed by digestion with 0.5 NaOH

following the method of Jackson (1965). The remainder of the sodium-saturated sample was converted to lithium form by saturating with LiCl. The salt-free,  $<2\mu$  lithium-saturated sample was separated by centrifugation following the method of Jackson (1956). A portion of this sample was used to perform the Greene-Kelly (1953) test in order to identify the dioctahedral or trioctahedral nature of expandable minerals. Another portion of the  $<2\mu$  lithium sample was converted to  $\text{K}^+$  form to identify the vermiculitic or montmorillonitic nature of expandable minerals and/or to differentiate chlorite from vermiculite. A third portion was converted to  $\text{Ca}^{2+}$  form to undergo six intensive treatments in order to establish the type of mixed layers following criteria of Kodama and Brydon (1968), and to determine the quantity of the end members following the solution and graphical presentation of Hendricks-Teller formula (Hendricks and Teller, 1942) by MacEwan, Ruiz Amil and G. Brown (Fig. X1.19 in Brown, 1961). All  $<2\mu$  clay samples were X-rayed using  $\text{CoK}\alpha$  radiation with nickel filter, settings of 40Kv - 20ma, scanning speed  $1^\circ 20'/\text{min}/2$  cm, time constant of 2, and range  $2^\circ$  to  $40^\circ 20'$ .

The crystallite size was determined following the method of Jones (1938) in order to avoid discrepancies on measured d-spacings as reported by Reynolds (1968). The use of  $\text{Ca}^{2+}$  in absorbed positions was necessary in order to use Figure X1.19 of Brown (1961) and because montmorillonite, beidellite or vermiculite give almost the same basal spacing at 50 per cent relative humidity (Barshad, 1948, 1950; Mooney, Keenan and Wood, 1952), thus differentiating the expandable 2:1 layer silicates from the non-expandable ones.

The portion between  $1\mu$  and  $.2\mu$  was collected by centrifugation following Jackson's (1956) method and then divided into two portions. One was

saturated with  $K^+$  and the oriented clays were X-rayed with  $CuK\alpha$  radiation, iron filter, settings of 45Kv - 20ma, scanning speed  $1^\circ 2\theta/\text{min}/2\text{ cm}$ , time constant 2, range  $2^\circ$  to  $15^\circ 2\theta$ , and 50 per cent relative humidity. The purpose was to study the sharpness ratio according to Weaver's (1961) technique and the crystallinity index following Kubler's (1966) method. After heating the sample to  $230^\circ\text{C}$ , the peak-area ratio of  $d_{001}$  illite to  $d_{001}$  kaolinite +  $d_{002}$  chlorite was measured. Another portion of the fraction between  $1\mu$  and  $.2\mu$  was treated with 2N HCl overnight to ensure removal of biotite and chlorite (Brown, 1961), then washed and treated with KOH to remove kaolinite and ensure  $K^+$  saturation following the method of Dudas and Harward (1971). This treatment yields  $K^+$ -saturated illites upon which the 2M vs 1M + 1Md polymorph ratios can be studied following either Velde and Hower's (1967) method or Maxwell and Hower's (1967) method. In our work, the Velde and Hower technique is used because of the similarity of the particle size.

Chemical analyses were carried out on the crushed rock sample. Measurements of pH were obtained on a paste at 1:1 ratio of sample to water as described by Peech (1965). Extraction of water soluble ions, measurement of conductivity, and determination of ions in water extract were carried out by the Bower and Wilcox (1965) method in order to obtain the exchangeable cations. Adsorbed cations were measured by modifying Chapman's (1965a, b) method to use LiCl salt as a leaching salt. The standard method of leaching with ammonium or potassium salts was avoided for two reasons. (i) If vermiculite is a component of the mixed layers, or if it occurs as a discrete mineral in the shales, then  $Ca^{2+}$ ,  $Mg^{2+}$  and  $Na^+$  are found to be "trapped" in the interior surfaces of the vermiculitic layers upon replacement of the most accessible portions with  $NH_4^+$  or  $K^+$  (Barshad, 1954). This leads to erroneous measurement of the cation exchange capacity. (ii) By total chemical analysis of the Li-saturated sample, cation exchange capacity is determined immediately by measuring  $Li_2O$ . As a result, the modified method is not only faster, but more accurate if vermiculite is present in the clay fraction.

Total chemical analysis on the whole rock was used to supplement the mineralogical studies. The determination of major constituents was carried out by decomposing the sample with  $HF:HNO_3$  (Brooks, 1960) and measuring the elements by following the method of Foscolos and Barefoot (1970b). To obtain more meaningful chemical results which can be used in the study of diagenetic alterations [for example, correlation between cation exchange capacity (C.E.C.) and per cent concentration of illite in the illite-expandable layer lattice silicate mixed layers, or per cent  $K_2O$  content with per cent of 2M vs 1M + 1Md illite polymorphs], quartz, feldspars and organic matter were quantitized and their elemental contributions were subtracted from the initial chemical analysis. Quartz and feldspar concentrations were determined by modifying the method of Jackson (1965). Thus, the amount of  $SiO_2$  was determined and the factors for the recovery of quartz and feldspars for the whole rock sample were based on a weighed average obtained from the mechanical analysis of the sample after verifying the presence of each

constituent in each size range by X-rays. Carbon and sulphur determinations were carried out following the method of Foscolos and Barefoot (1970a) and organic matter was calculated by multiplying the organic carbon by a factor of 1.22 (Forsman and Hunt, 1958; Gehman, 1962).

The integral analysis of the shale sample is presented in Figure 3.

#### ANALYTICAL RESULTS

Most of the mineralogical data are shown in Figures 4 to 35 and all results are summarized in Tables 5 and 6. The chemical analyses are reported in Tables 7, 8, 9 and 10. The mineralogy and chemistry of each formation are as follows.

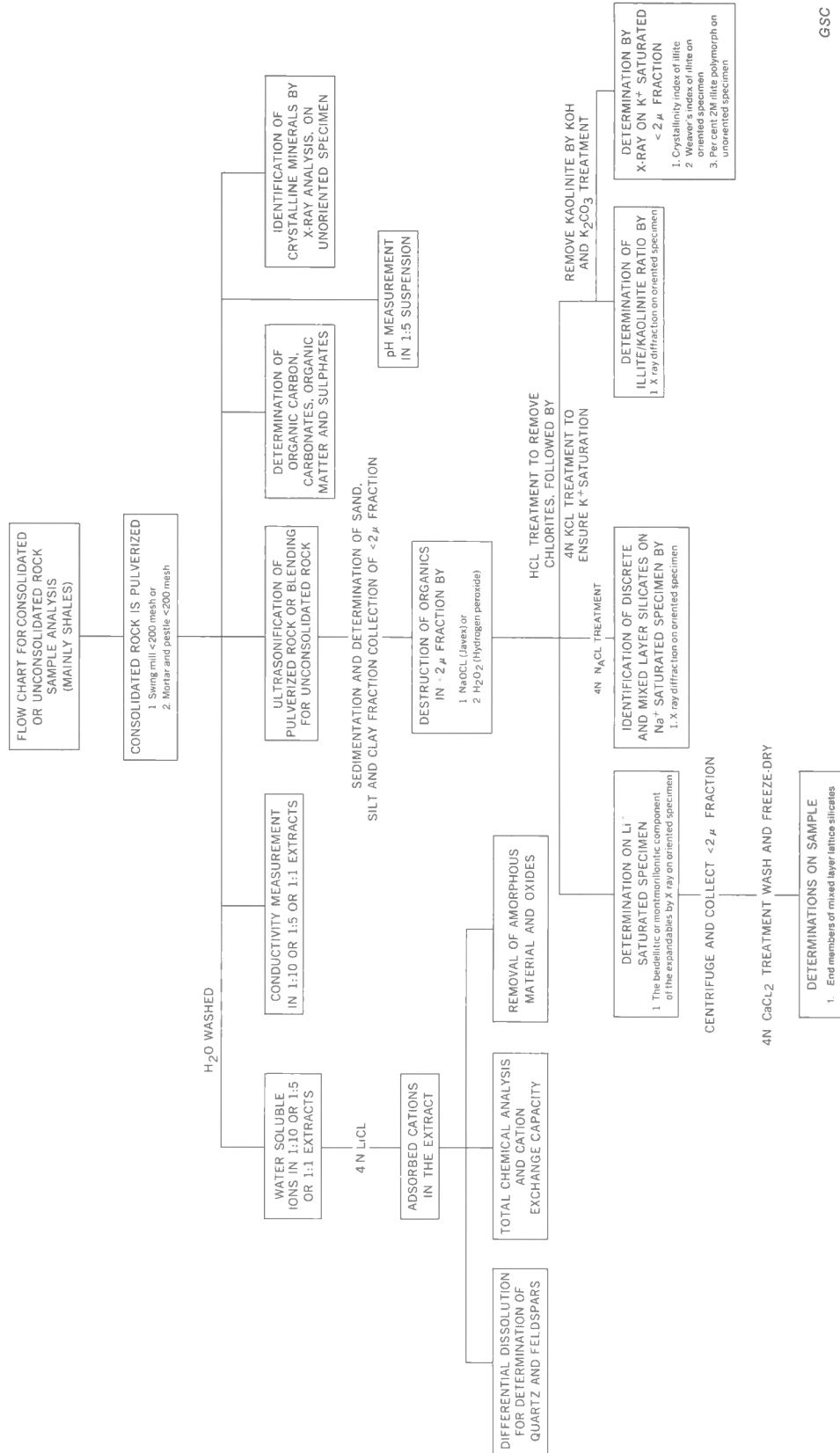
#### MOOSEBAR FORMATION, PEACE RIVER (SECTION 1)

The mineralogy of this shale formation is as follows: 29.3 per cent quartz, 0.52 per cent K-feldspar, 2.84 per cent Na-feldspar, with dolomite, siderite, pyrite, illite and chlorite. Kaolinite is absent. The illite and 2:1 expandable clays in the mixed layers are combined at a ratio of 80:20 as shown by the 10.8A spacing of the  $d_{001}$  peak position (Table 6). Discrete illite is composed of 30 per cent 2M illite polymorphs and the  $d_{001}$  illite to  $d_{002}$  chlorite ratio is 6.6 (Table 5). The pH value (Table 7) of the shale is alkaline which is in agreement with the presence of dolomite, the per cent base saturation and the ratio of sulphur to inorganic carbon (Table 7). The importance of the sulphur to inorganic carbon ratio will be discussed later when the interaction between the oxidative products of sulphur, the mineralogy, and the layer silicates will be presented. Also, in this formation the molar ratio of  $SiO_2$  to  $R_2O_3^*$  is above 4.00, indicating that some amorphous  $SiO_2$  might be present.

#### COMMOTION FORMATION, NORTH WOLVERINE RIDGE (SECTION 2)

In this formation the mineralogy is as follows: 23.72 per cent quartz, 0.52 per cent K-feldspar, 2.84 per cent Na-feldspar with illite, chlorite and kaolinite. The percentage composition of the end member in the mixed layers is fairly close to that of the Hasler Formation (Table 6), whereas the percentage of 2M illite polymorphs, in the discrete illite, decreases to 25 per cent (Table 5). The  $d_{001}$  illite to  $d_{001}$  kaolinite +  $d_{002}$  chlorite ratio increases to 16.7 which indicates that illite is the most predominant layer lattice silicate. The pH value (7.7) of the shale unit is slightly alkaline (Table 7) and, therefore, hydrogen and/or hydroxyaluminum are absent from the clay surface. The same conclusion is reached from the per cent base saturation (Table 7). In this formation, the percentages of  $Al_2O_3$  and  $Fe_2O_3$  are high and the molar ratio of  $SiO_2$  to  $R_2O_3$  indicates that free  $Al_2O_3$  and  $Fe_2O_3$  exist in an amorphous state because they cannot be identified by X-rays. In addition,

\*  $R_2O_3 = Fe_2O_3 + Al_2O_3$



GSC

FIGURE 3. Flow chart of the chemical and mineralogical analyses performed on shale samples

due to the high value of L.O.I. (Table 10), it may be assumed that some of the amorphous  $Al_2O_3$  and  $Fe_2O_3$  exist in a hydrous state.

HASLER FORMATION,  
DOKIE RIDGE (SECTION 3)

This formation has 36.88 per cent quartz, 0.46 per cent K-feldspar, 0.62 per cent Na-feldspar, with illite, chlorite and kaolinite. In the mixed layers, illite and 2:1 expandable layer silicates are combined at a proportion of 81:19 whereas 2M illite polymorphs in the discrete illite increase to 30 per cent. The  $d_{001}$  illite to  $d_{001}$  kaolinite +  $d_{002}$  chlorite ratio increases to 4.3. The pH value of the rock is 4.3 (Table 7), which indicates that the clays are acidic. The same is deduced from the per cent base saturation (Table 7).  $K_2O$  content is 4.10 per cent, indicating that illite is in higher proportion in this formation than in the Cruiser Formation, as discussed in a following section. The same conclusion is indicated by the ratio of  $d_{001}$  illite to  $d_{001}$  kaolinite +  $d_{002}$  chlorite (Table 5).

CRUISER FORMATION, YOUNG CREEK  
(SECTION 4, SAMPLES 60/310 to 60/320)

The shale of this formation contains 41.65 per cent quartz, 0.91 per cent K-feldspars, 1.69 per cent Na-feldspars, with illite, chlorite and kaolinite. In the mixed layers, illite and 2:1 expandable clay minerals are in a proportion of 79:21 as indicated by the  $10.9\text{\AA}$  position of the  $d_{001}$  peak of the mixed system (Table 6). The percentage of 2M illite polymorphs in the discrete illite amounts to 35 and the ratio of  $d_{001}$  illite to  $d_{001}$  kaolinite +  $d_{002}$  chlorite is 3.4. The pH value of the formation (6.2) is slightly acidic, indicating that hydroxyaluminum and/or hydrogen ions occur on the clay surfaces. The difference between the measured absorbed cations and cation exchange capacity, which is expressed also as per cent base saturation, indicates the same. In this formation, the percentage of  $Al_2O_3$  is high (Table 10), indicating that free  $Al_2O_3$  exists probably in an amorphous state, since it cannot be detected by X-rays.

GETHING FORMATION,  
BESA RIVER (SECTION 5)

The Gething Formation is characterized by high quartz and relatively high Na-feldspar content. The formation is divided into three zones which have different mineralogy and chemistry.

The lower part of the Gething Formation (5, I; sample 64/437 to 64/452)\* contains 38.25 per cent quartz, 0.91 per cent K-feldspars, 1.33 per cent Na-feldspar and illite. In the mixed layers, illite and 2:1 expandable layer silicates are in the proportion of 88:12 as indicated by the  $d_{001}$  peak

\* In the text and figures, the section is referred to by Arabic numerals and the zone or assemblage by Roman numerals.

FORMATION	SAMPLE NO.	Crystallinity index in mm	Sharpness ratio	Per cent 2M illite polymorphs	2:1 1:1 and/or 2:2	
<i>Cruiser</i>	60/318	19	1.6	35	3.4	
<i>Hasler</i>	60/138	19	1.5	30	4.3	
<i>Commotion</i>	59/89	17	1.7	25	16.7	
<i>Moosebar</i>	61/301	18	1.4	30	6.6	
<i>Gething</i>	<i>Besa River</i> *	64/437	13	2.2	45	∞
		64/453	13	2.6	40	30.1
		64/465	14	2.1	40	16.9
	<i>Prophet River</i> *	64/515	13	1.8	50	∞
		64/542	14	2.1	40	16.9
	<i>Bat Creek</i> *	64/653	15	1.8	55	∞
64/670		13	3.0	40	7.5	
<i>Buckinghorse</i>	<i>Tetsa River</i> *	64/88-92	15	1.8	55	∞
		64/109	15	1.8	50	∞
		64/201	20	1.5	40	2.1
		65/128	18	1.6	30	2.1
		64/223	22	1.3	30	1.0
	<i>Muskwa River</i> *	64/278	19	1.4	30	2.9
		64/757	19	1.4	30	2.9
		64/822	26	1.2	30	2.7
		64/999	24	1.2	30	6.7
		64/1063	26	1.2	20	3.9
<i>Middle Scatter</i>	<i>Bear Island, Liard River</i>	65/869	24	1.3	25	10.7
	<i>North of Scatter River</i>	65/800	21	1.4	25	6.3
<i>Scatter</i>		65/634	42	1.1	20	3.5
		65/666	22	1.3	20	10.2
		65/691	19	1.5	20	4.4
<i>Garbutt</i>		65/756	22	1.4	25	3.0
<i>Lepine</i>		65/241	27	1.2	25	3.8
		65/291	25	1.3	25	3.2
<i>Lepine-Sikanni-Sully</i>		65/389	24	1.4	25	3.7
		65/469	26	1.4	20	1.9
		65/592	28	1.2	20	3.5

\* Localities

GSC

TABLE 5. Crystallinity index, sharpness ratio, per cent 2M illite polymorphs and ratio of illite/kaolin and/or chlorite on fifteen formations of Lower Cretaceous shale of northeastern British Columbia

FORMATION	SAMPLE NO.	Non-Layer Lattice Silicates	Layer Lattice Silicates				
			Discrete	Mixed			
				% Illite	% Expandables*	d <sub>001</sub> in Å	
<i>Cruiser</i>	60/318	Quartz, Feldspars	Illite, Chlorite, Kaolinite	79	21	10.9	
<i>Hasler</i>	60/138			81	19	10.7	
<i>Commotion</i>	59/89			82	18	10.6	
<i>Moosebar</i>	61/301	Quartz, Feldspars, Dolomite, Siderite, Pyrite	Illite, Chlorite	80	20	10.8	
Gething	<i>Besa River</i> **	64/437	Quartz, Feldspars	Illite	88	12	10.2
		64/453		Illite, Chlorite in trace	87	13	10.3
		64/465	Quartz, Feldspars, Dolomite, Calcite, Siderite, Pyrite	Illite, Chlorite	85	15	10.4
	<i>Prophet River</i> **	64/515	Quartz, Feldspars, Dolomite, traces of Siderite, Pyrite	Illite, Chlorite in trace	87	13	10.3
		64/542	Quartz, Feldspars, Dolomite, Calcite, Siderite, Pyrite	Illite, Chlorite	87	13	10.3
	<i>Bat Creek</i> **	64/653	Quartz, Feldspars, Dolomite and traces of Siderite	Illite	88	12	10.2
		64/670	Quartz, Feldspars	Illite, Chlorite	87	13	10.3
	Buckinghorse	<i>Tetsa River</i> **	64/88-92	Quartz, Feldspars, Dolomite, Siderite	Illite	87	13
64/109			Quartz, Feldspars, Dolomite, Siderite, Pyrite	Illite, Chlorite in trace	84	16	10.5
64/201			Quartz, Feldspars, Siderite, Pyrite	Illite, Chlorite, Kaolinite	79	21	10.9
65/128			Quartz, traces of Feldspars, Calcite, Siderite, Pyrite	Illite, Vermiculite, Kaolinite	78	22	11.1
64/223			Quartz, Feldspars	Illite, Chlorite	77	23	11.2
64/278		77			23	11.2	
64/757		77			23	11.2	
<i>Muskwa River</i> **		64/822	Quartz, Feldspars, Dolomite, Siderite, Pyrite	Illite, trace of Chlorite, Kaolinite	77	23	11.2
		64/999			76	24	11.7
		64/1063			Quartz, Feldspars, traces of Dolomite, Siderite, Pyrite	Illite, Chlorite, Kaolinite	76
Middle Scatter	<i>Bear Island, Liard River</i>	Quartz, Feldspars	Illite, Chlorite, Kaolinite	77	23	11.2	
	<i>North of Scatter River</i>			Illite, Chlorite	77	23	11.2
Scatter	65/634	Quartz, Feldspars, Dolomite, Calcite, Pyrite, Gypsum	Illite, Montmorillonite, Kaolinite	32	68	14.7	
	65/666	Quartz, Feldspars	Illite, Chlorite, Kaolinite	77	23	11.2	
	65/691		Illite, Chlorite	78	22	11.1	
<i>Garbutt</i>	65/756		Illite, Chlorite, Kaolinite	76	24	11.7	
<i>Lepine</i>	65/241	Quartz, Feldspars, Gypsum	Illite, Verm., Kaolinite	76	24	11.7	
	65/291	Quartz, Feldspars	Illite, trace of Chlorite, Vermiculite, Kaolinite	74	26	11.8	
<i>Lepine-Sikanni-Sully</i>	65/389	Quartz, Feldspars, Dolomite	Illite, Chlorite, Vermiculite, Kaolinite	74	26	11.8	
	65/469	Quartz, Feldspars		70	30	12.3	
	65/592			76	24	11.7	

\* The expandable layer silicates are montmorillonite and vermiculite

GSC

\*\* Localities

TABLE 6. Mineralogy and clay mineralogy of fifteen Lower Cretaceous shale formations of northeastern British Columbia as determined by X-ray methods

FORMATION	SAMPLE NO.	Exchangeable Cations in meq/100 gm				Exchange Acidity in meq/100 gm	Cation Exchange Capacity in meq/100 gm**	Per Cent Base Saturation	pH in 1:1 paste	Per Cent Inorganic Carbon	Per Cent Sulphur	Ratio of Sulphur to Inorganic Carbon	
		Na <sup>+</sup>	K <sup>+</sup>	Ca <sup>2+</sup>	Mg <sup>2+</sup>								
<i>Cruiser</i>	60/318	.00	1.44	5.50	2.27	2.79	11.98	76.87	6.2	.08	.15	1.87	
<i>Hasler</i>	60/138	.07	2.00	4.77	1.78	2.70	11.32	76.14	4.5	.13	.14	1.07	
<i>Commotion</i>	59/89	.00	.82	1.31	.08	0.00	2.21	100.00	7.7	.25	.14	.56	
<i>Moosebar</i>	61/301	.17	1.37	7.11	2.78	0.00	11.33	100.00	8.0	.36	.19	.52	
<i>Gething</i>	<i>Besa River</i> ***	64/437	.00	.00	1.13	.24	3.25	4.62	29.65	3.2	.11	.65	5.90
		64/453	.09	.63	10.61	.00	0.00	11.33	100.00	7.3	.10	.06	.60
		64/465	.05	.24	5.73	.64	0.00	6.66	100.00	8.1	1.25	.20	.16
	<i>Prophet River</i> ***	64/515	.00	.21	4.07	4.39	0.00	8.67	100.00	8.5	.42	.12	.28
		64/542	.00	.73	6.24	5.67	0.00	12.64	100.00	7.7	.35	.24	.68
	<i>Bat Creek</i> ***	64/653	.00	.19	3.08	3.39	0.00	6.66	100.00	7.4	.95	.90	.94
64/670		.04	1.64	7.15	1.74	0.76	11.33	93.29	6.7	.06	.28	4.66	
<i>Buckinghorse</i>	<i>Tetsa River</i> ***	64/88-92	.02	1.13	5.65	3.14	0.06	10.00	100.00	6.9	.30	.14	.46
		64/109	.02	.54	3.93	.84	0.00	5.33	100.00	8.3	.24	.19	.79
		64/201	6.26	.65	2.28	.29	3.19	12.67	74.82	4.4	.25	.32	1.28
		65/128	4.93	.49	1.87	.14	.57	8.00	92.87	4.1	.35	.93	2.65
		64/223	.76	.37	3.20	.54	.46	5.33	91.36	5.5	.15	.18	1.20
		64/278	1.96	.32	2.88	.58	1.58	7.32	78.41	6.8	.09	.08	.89
	<i>Muskwa River</i> ***	64/757*	—	—	—	—	—	—	—	3.5	.02	.33	16.50
		64/822	.00	.51	1.33	.87	7.29	10.00	27.10	2.8	.03	.66	22.00
		64/999	.04	1.59	6.40	6.37	1.58	15.98	90.11	6.0	.40	.29	.72
		64/1063	.02	3.84	6.38	4.43	1.34	15.98	91.61	6.7	.53	.33	.62
<i>Middle Scatter</i>	<i>Bear Island, Liard River</i>	65/869	.01	2.62	3.30	1.66	5.08	12.67	59.90	4.7	.09	.16	1.78
	<i>North of Scatter River</i>	65/800	.00	1.73	1.63	.91	7.06	11.33	37.68	4.5	.12	.15	1.25
<i>Scatter</i>	65/634	.00	.82	3.55	.00	12.97	17.34	25.20	2.7	.25	1.21	4.84	
	65/666	.00	1.20	5.21	.06	4.86	11.33	57.10	4.5	.03	.12	4.00	
	65/691	.02	1.42	4.83	1.74	3.32	11.33	70.69	4.8	.15	.19	1.26	
<i>Garbutt</i>	65/756	.00	.86	2.28	.12	10.81	14.67	26.31	3.9	.20	.40	2.00	
<i>Lepine</i>	65/241	.00	1.08	2.24	.29	9.06	12.67	28.41	3.0	.10	.64	6.40	
	65/291	.00	.71	1.48	.21	14.26	16.66	14.40	3.4	.15	.47	3.13	
<i>Lepine-Sikanni-Sully</i>	65/389	.00	1.41	4.63	1.94	6.02	14.00	57.00	3.8	.10	.17	1.70	
	65/469	.00	1.14	4.93	.87	5.73	12.67	54.71	4.0	.05	.13	2.60	
	65/582	.00	.79	10.29	4.27	1.38	16.67	91.72	6.8	.20	.38	1.90	

GSC

\*Not determined

\*\*Obtained from total chemical analysis by dividing Li<sub>2</sub>O by its equivalent weight

\*\*\* Localities

TABLE 7. Exchangeable cations, cation exchange capacity, exchange acidity, base saturation, pH, inorganic carbon and sulphur, and ratio of sulphur to inorganic carbon of fifteen Lower Cretaceous shale formations of northeastern British Columbia



FORMATION	SAMPLE	PER CENT												TOTAL	
		SiO <sub>2</sub> *	Al <sub>2</sub> O <sub>3</sub>	TiO <sub>2</sub>	Fe <sub>2</sub> O <sub>3</sub> **	MnO	MgO	CaO	K <sub>2</sub> O	Na <sub>2</sub> O	Li <sub>2</sub> O	H <sub>2</sub> O	L.O.I.		
<i>Cruiser</i>	60 318	60.95	25.94	.67	2.79	.06	.74	.31	2.16	.32	.18	1.00	4.88	100.00	
<i>Hasler</i>	60/138	68.14	15.56	.59	3.62	.03	.90	.42	2.52	.24	.17	1.50	6.30	100.00	
<i>Commotion</i>	59/89	51.58	22.08	.67	9.74	.03	.57	.25	2.52	.42	.03	1.10	11.01	100.00	
<i>Moosebar</i>	61/301	66.74	12.98	.67	5.15	.05	1.62	1.27	2.52	.53	.17	1.30	7.00	100.00	
<i>Gething</i>	<i>Besa River</i> ****	64/437,440,441,443,450	72.47	12.23	.67	4.15	.03	.60	.07	2.84	.24	.07	.94	5.69	100.00
		64/458	79.14	8.97	.67	1.57	.03	.37	.14	1.80	.26	.17	.63	6.25	100.00
		64 465	71.04	9.98	.50	2.79	.05	2.12	3.05	1.76	.61	.10	.75	7.25	100.00
	<i>Prophet River</i> ***	64 515	69.35	13.61	.67	1.29	.05	1.38	2.41	3.06	.55	.13	.63	6.87	100.00
		64 542	67.15	15.12	.67	3.57	.05	1.00	.76	3.06	.43	.19	1.19	6.81	100.00
	<i>Bat Creek</i> ****	64 653	62.59	13.61	.67	1.14	.04	.70	.11	3.43	.11	.10	1.00	16.50	100.00
64 670		66.72	16.48	.75	3.57	.04	1.21	.29	3.36	.53	.17	.81	6.07	100.00	
<i>Buckinghorse</i>	<i>Tetsa River</i> ****	64/88-92	69.58	14.47	.75	2.29	.03	.84	.65	3.20	.55	.15	1.20	6.29	100.00
		64/109	75.10	10.98	.84	2.43	.04	.93	1.00	2.32	.78	.08	.75	4.75	100.00
		64/201	65.34	13.48	.84	7.73	.06	.90	1.60	1.96	.27	.19	1.13	6.50	100.00
		65/128	54.38	12.23	.67	14.87	.09	.68	4.48	1.80	.18	.12	1.88	8.62	100.00
		64/223	87.00	5.52	.50	2.36	.03	.48	.29	.92	.57	.08	.38	1.87	100.00
		64/278	79.88	9.48	.67	2.86	.04	.74	.21	1.68	.58	.11	.69	3.06	100.00
	<i>Muskwa River</i> ****	64 757***	—	—	—	—	—	—	—	—	—	—	—	—	—
		64/822	63.12	15.78	.67	4.57	.04	.98	.06	3.06	.32	.15	1.88	9.37	100.00
		64 999	61.42	16.97	.84	6.44	.12	1.14	.32	2.32	.50	.24	1.25	8.44	100.00
		64 1063	71.36	13.48	.67	2.72	.02	.85	.39	2.20	.26	.24	1.13	6.68	100.00
<i>Middle Scatter</i>	<i>Bear Island Liard River</i>	65 869	70.98	12.98	.59	3.57	.02	.98	1.12	2.40	.42	.19	1.25	5.50	100.00
	<i>North of Scatter River</i>	65/800	69.36	13.97	.50	3.79	.02	1.00	.98	2.68	.34	.17	1.44	5.75	100.00
<i>Scatter</i>	65/634	64.19	13.97	.75	4.87	.02	.95	.70	2.32	.28	.26	2.13	9.56	100.00	
	65/666***	—	—	—	—	—	—	—	—	—	—	—	—	—	
	65/691	77.46	9.98	.50	3.79	.02	.86	.17	2.16	.39	.17	.50	4.00	100.00	
<i>Garbutt</i>	65/756	74.10	12.23	.50	2.58	.02	.67	.15	1.96	.38	.22	1.38	5.81	100.00	
<i>Lepine</i>	65/241	72.79	12.23	.59	2.15	.02	.66	.08	1.92	.31	.19	1.25	7.81	100.00	
	65/291	67.27	15.98	.75	3.50	.02	.96	.06	2.56	.40	.25	1.25	7.00	100.00	
<i>Lepine-Sikanni-Sully</i>	65/388	62.93	17.97	.84	4.08	.04	.96	.06	2.67	.36	.21	1.56	8.32	100.00	
	65/469	69.81	13.97	.75	4.40	.02	.90	.11	2.16	.69	.19	1.25	5.75	100.00	
	65 592	66.28	15.48	.67	4.22	.04	1.24	.43	2.68	.27	.25	1.69	6.75	100.00	

GSC

\* SiO<sub>2</sub> calculated by difference

\*\* All iron reported as ferric

\*\*\* Analysis not carried out due to lack of sample

\*\*\*\* Localities

TABLE 8. Total elemental analyses of fifteen formations from Lower Cretaceous shale of northeastern British Columbia after lithium saturation and removal of soluble salts

FORMATION	SAMPLE	PER CENT									
		Qtz.	K-Fdsp	Na-Fdsp	Organic C	Min. C	Organic Matter	CO <sub>2</sub> <sup>**</sup>	S	Free Fe <sub>2</sub> O <sub>3</sub>	
<i>Cruiser</i>	60/318	41.65	.91	1.69	1.21	.07	1.49	.26	.16	.60	
<i>Hasler</i>	60/138	36.88	.46	.62	1.39	.13	1.71	.48	.08	1.36	
<i>Commotion</i>	59/89	23.72	.91	1.60	1.35	.20	1.66	.73	.14	.57	
<i>Moosebar</i>	61/301	29.37	.52	2.84	2.05	.31	2.52	1.13	.22	1.39	
<i>Gething</i>	<i>Besa River</i> *****	61/437, 440, 441, 443, 450	38.25	.91	1.33	1.58	.10	1.94	.37	.56	2.63
		64/458	40.78	.33	1.42	2.94	.08	3.61	.29	.04	.89
		64/465	39.21	.26	3.73	1.25	1.05	1.54	3.85	.18	.79
	<i>Prophet River</i> *****	64/515	36.46	.20	2.40	2.18	.41	2.68	1.51	.14	.37
		64/542	25.23	.00	1.42	1.64	.19	2.02	.70	.30	1.59
	<i>Bat Creek</i> *****	64/653	34.42	.78	.62	10.21	.00	12.56	.00	.90	.44
64/670		25.81	.26	2.49	1.75	.00	2.15	.00	.20	.81	
<i>Buckinghorse</i>	<i>Tetsa River</i> *****	64/88-92	34.38	.26	3.38	2.61	.27	3.21	.99	.18	.89
		64/109	44.77	.52	4.71	1.78	.10	2.19	.37	.24	.73
		64/201	30.83	.26	1.16	1.61	.20	1.98	.73	.22	1.57
		65/128	24.52	.33	.62	1.38	.10	1.70	.37	.98	3.91
		64/223	60.74	.33	3.73	.23	.10	.28	.37	.16	.31
	<i>Muskwa River</i> *****	64/278	41.58	.10	1.28	.60	.00	.74	.00	.08	.66
		64/757***	—	—	—	—	—	—	—	—	—
		64/822	25.59	.00	1.07	3.28	.00	4.03	.00	.48	1.86
		64/999	22.03	.26	3.11	1.61	.36	1.98	1.32	.28	1.73
64/1063	34.15	.52	2.04	1.18	.43	1.45	1.58	.34	.26		
<i>Middle Scatter</i>	<i>Bear Island, Liard River</i>	65/869	33.65	.20	1.95	.98	.07	1.21	.26	.08	.79
	<i>North of Scatter River</i>	65/800	30.91	.20	1.69	1.28	.10	1.58	.37	.14	.92
<i>Scatter</i>	65/634****	31.68	1.04	1.95	1.62	.22	2.00	.81	2.32	1.57	
	65/666***	—	—	—	—	—	—	—	—	—	
<i>Garbutt</i>	65/691	47.60	.91	2.75	.59	.13	.73	.48	.18	.84	
<i>Lepine</i>	65/756	40.74	.00	2.49	1.31	.16	1.61	.59	.12	.73	
	65/241	38.25	.00	2.04	2.85	.08	3.46	.29	.38	.63	
	65/291	29.10	.00	3.02	2.02	.10	2.49	.37	.44	.92	
<i>Lepine-Sikanni-Sully</i>	65/389	14.97	.26	3.64	1.60	.07	1.97	.26	.16	1.13	
	65/469	37.94	2.34	5.60	1.21	.04	1.49	.15	.12	1.11	
	65/592	29.87	1.23	2.04	1.55	.12	1.91	.44	.40	.79	

\* Calculated by multiplying organic carbon by 1.22

\*\*\*\* S reported as SO<sub>2</sub> ↑ because of gypsum

\*\* Calculated by multiplying mineral carbon by 3.67

\*\*\*\*\* Localities

\*\*\* Analysis not carried out due to lack of sample

GSC

TABLE 9. Per cent quartz, K-feldspar, Na-feldspar, organic matter, CO<sub>2</sub> evolved from carbonate sulphur, and free Fe<sub>2</sub>O<sub>3</sub> of salt-free Li+-saturated samples in fifteen Lower Cretaceous shale formations of northeastern British Columbia

FORMATION	SAMPLE	PER CENT												L.O.I.*	SiO <sub>2</sub> ** R <sub>2</sub> O <sub>3</sub>
		SiO <sub>2</sub>	Al <sub>2</sub> O <sub>3</sub>	TiO <sub>2</sub>	Fe <sub>2</sub> O <sub>3</sub>	MnO	MgO	CaO	K <sub>2</sub> O	Na <sub>2</sub> O	Li <sub>2</sub> O	H <sub>2</sub> O			
<i>Cruiser</i>	60 318	32.60	47.23	1.24	5.18	.11	1.38	.57	3.75	.24	.33	1.85	5.52	1.1	
<i>Hasler</i>	60/138	51.09	25.69	.99	6.06	.05	1.51	.70	4.10	.28	.28	2.51	6.74	3.0	
<i>Commotion</i>	59/89	36.73	30.31	.94	13.67	.04	.80	.35	3.34	.34	.04	1.54	11.90	1.6	
<i>Moosebar</i>	61 301	55.31	19.43	1.06	8.12	.07	2.56	2.01	3.85	.33	.27	2.05	4.94	4.1	
<i>Gething</i>	<i>Besa River</i> ****	64/437, 440, 441, 443, 450	57.72	20.83	1.19	7.32	.05	1.06	.13	4.77	.16	.13	1.66	4.98	4.0
		64/458	69.44	16.11	1.26	2.93	.05	.69	.26	3.26	.18	.32	1.18	4.32	7.1
		64/465	56.77	17.95	.98	5.44	.10	4.14	5.95	3.36	.37	.20	1.46	3.28	4.7
	<i>Prophet River</i> ****	64/515	54.95	23.14	1.18	2.28	.09	2.43	4.25	5.35	.50	.23	1.11	4.49	3.8
		64/542	58.21	21.09	.95	5.08	.07	1.42	1.08	4.35	.39	.27	1.69	5.40	4.2
	<i>Bat Creek</i> ****	64 653	53.65	26.32	1.32	2.25	.08	1.38	.22	6.54	.08	.20	1.97	5.99	3.3
64/670		56.57	23.12	1.09	5.18	.06	1.75	.42	4.82	.36	.25	1.17	5.21	3.8	
<i>Buckinghorse</i>	<i>Tetsa River</i> ****	64 88-92	56.78	23.87	1.30	3.97	.05	1.45	1.13	5.49	.29	.26	2.09	3.32	3.8
		64/109	56.65	21.08	1.78	5.15	.08	1.97	2.12	4.75	.53	.17	1.59	4.13	4.0
		64/201	51.75	20.36	1.30	11.92	.08	1.39	2.47	2.96	.22	.29	1.75	5.51	3.2
		65/128	40.86	16.86	.94	20.79	.13	.95	6.27	2.45	.16	.17	2.63	7.79	2.4
		64 223	68.23	13.74	1.45	6.86	.09	1.39	.84	2.53	.44	.24	1.11	3.08	6.5
		64 278	66.46	16.27	1.24	5.31	.07	1.37	.39	3.04	.39	.20	1.28	3.98	6.0
	<i>Muskwa River</i> ****	64 757***	-	-	-	-	-	-	-	-	-	-	-	-	-
		64/822	53.46	22.63	.97	6.64	.05	1.43	.09	4.44	.29	.21	2.73	7.06	3.5
		64/999	52.18	22.96	1.19	9.08	.17	1.61	.45	3.21	.21	.34	1.76	6.84	3.2
		64/1063	59.18	21.66	1.12	4.54	.03	1.42	.65	3.54	.05	.40	1.89	5.52	4.2
<i>Middle Scatter</i>	<i>Bear Island, Liard River</i>	65/869	57.23	20.05	.94	5.69	.03	1.57	1.78	3.78	.32	.31	2.00	6.30	4.2
	<i>North of Scatter River</i>	65 800	57.06	20.89	.76	5.82	.03	1.54	1.51	4.07	.23	.26	2.21	5.62	4.2
<i>Scatter</i>	65 634	50.62	22.24	1.25	8.08	.03	1.61	1.16	3.58	.10	.43	3.54	7.36	3.2	
	65/666***	-	-	-	-	-	-	-	-	-	-	-	-	-	
	65/691	57.81	19.57	1.06	8.00	.04	1.81	.36	4.26	.16	.36	1.06	5.51	4.2	
<i>Garbutt</i>	65/756	58.10	21.57	.92	4.73	.04	1.23	.27	3.60	.19	.41	2.53	6.41	4.2	
<i>Lepine</i>	65 241	59.92	21.10	1.05	3.83	.03	1.18	.14	3.42	.14	.34	2.23	6.62	4.4	
	65 291	55.89	23.84	1.16	5.41	.03	1.48	.09	3.96	.09	.39	1.93	5.73	3.5	
<i>Lepine-Sikanni-Sully</i>	65/389	57.44	21.84	1.07	5.18	.05	1.22	.08	3.34	.00	.27	1.98	7.53	4.0	
	65/469	50.55	23.75	1.43	8.39	.04	1.72	.21	3.43	.11	.36	2.39	7.62	3.0	
	65/592	53.37	23.17	1.04	6.58	.06	1.93	.64	3.88	.06	.39	2.64	6.24	3.5	

GSC

\* L.O.I. = Net weight loss due to crystal lattice H<sub>2</sub>O, cavity water and gain in weight due to oxidation of Fe<sup>2+</sup> → Fe<sup>3+</sup>

\*\*\* Analysis not carried out due to lack of sample

\*\*\*\* Localities

$$** \text{ The ratio of SiO}_2 \text{ to sesquioxides (R}_2\text{O}_3) = \frac{\% \text{SiO}_2}{\text{M.W.}} \div \left( \frac{\% \text{Al}_2\text{O}_3}{\text{M.W.}} + \frac{\% \text{Fe}_2\text{O}_3}{\text{M.W.}} \right)$$

TABLE 10. Elemental analyses and molar ratio of SiO<sub>2</sub> to sesquioxides (R<sub>2</sub>O<sub>3</sub>), in salt-free, Li+-saturated samples after the removal of quartz and feldspars in fifteen Lower Cretaceous shale formations of northeastern British Columbia

position of the mixed layers (Table 7). Illite is the only discrete layer lattice silicate with 45 per cent 2M illite polymorphs. The pH value of this zone is very low indicating the possibility of free acidity. As a result, hydroxyaluminum and/or hydrogen should be the predominant ions on the clay surface. Exchange acidity and per cent base saturation show that this is true (Table 7). The molar ratio of  $\text{SiO}_2/\text{R}_2\text{O}_3$  is 4.0, which is high for illite. Therefore, it is deduced that amorphous silica also is present in the sample. In addition, free  $\text{Fe}_2\text{O}_3$ , that is, iron which is not in the layer silicates, is high (2.63%).

In the middle part of this formation (5, II; samples 64/453 to 64/461), the mineralogy consists of 40.78 per cent quartz, 0.33 per cent K-feldspar, 1.42 per cent Na-feldspar, illite and traces of chlorite. In the mixed layers, illite and 2:1 expandable clay minerals are in the proportion of 87:13 as indicated by the  $d_{001}$  peak position of the mixed layers (Table 6). Discrete illite is the predominant layer lattice silicate with 40 per cent 2M illite polymorphs. The pH value of this unit rises to 7.3 which indicates a neutral reaction. As a result, the per cent base saturation of the clays is 100, with  $\text{Ca}^{2+}$  being the predominant ion on the clay surface. The  $\text{K}_2\text{O}$  of the sample after the removal of quartz, feldspars, organic matter,  $\text{CO}_2$  and sulphur is low due to the presence of amorphous  $\text{SiO}_2$  as shown from the molar ratio of  $\text{SiO}_2$  to  $\text{R}_2\text{O}_3$  (Table 10). The  $\text{SiO}_2$  to  $\text{R}_2\text{O}_3$  ratio in this formation is 7.1 whereas in illite it is approximately 3 (Brown, 1961). The low  $\text{Al}_2\text{O}_3$  and  $\text{Fe}_2\text{O}_3$  content is notable (Table 10).

The upper Gething Formation (5, III; samples 64/462 to 64/465) contains 39.21 per cent quartz, 0.26 per cent K-feldspar, 3.73 per cent Na-feldspar, with dolomite, calcite, siderite, pyrite, illite and chlorite. The ratio of illite to 2:1 expandable clay minerals in the mixed layers is 85:13 as indicated by the  $d_{001}$  peak of the mixed layers; discrete illite is composed of 40 per cent 2M illite polymorphs and the ratio of illite to chlorite is 16.9 (Table 5). The pH value (8.1) is alkaline, owing to the predominance of the carbonates; as a result, the per cent base saturation is 100 with  $\text{Ca}^{2+}$  the predominant ion on the clay surface. The chemical analysis indicates high concentration of CaO and MgO, 5.95 and 4.14 per cent, respectively, due to the presence of calcite and dolomite. The molar ratio of  $\text{SiO}_2$  to  $\text{R}_2\text{O}_3$  is again above 4.7, indicating the presence of amorphous  $\text{SiO}_2$ .

#### GETHING FORMATION, PROPHET RIVER (SECTION 6)

Two very similar mineral groups occurring in the formation at this locality have the following characteristics.

The lower part of the sampled section\* at Prophet River (6, I; samples 64/505 to 64/526) contains 36.46 per cent quartz, 0.20 per cent K-feldspar, 2.40 per cent Na-feldspar, with dolomite, pyrite, illite and traces of siderite, and chlorite. In the mixed layers, the ratio of illite to 2:1 expandable clay minerals is 87:13 and the percentage of 2M

illite polymorphs in the discrete illite is 50. The pH value of the rock is 8.5 reflecting the presence of dolomite. As a result, the surface of the clay minerals is saturated with  $\text{Ca}^{2+}$  and  $\text{Mg}^{2+}$  ions. Also the per cent base saturation is 100.00.

The upper Gething Formation at Prophet River and basal Buckingham Formation (6, II; samples 64/527 to 64/596) contain 25.23 per cent quartz, 1.42 per cent Na-feldspar, with dolomite, calcite, siderite, pyrite, illite and chlorite. The ratio of the end members in the mixture of illite to 2:1 expandable clay minerals is identical to that of the lower part. However, the percentage of 2M illite polymorphs in the discrete illite drops to 40. The ratio of illite to chlorite is 16.9 which is the same as in the shale of the upper Gething Formation at Besa River. The pH of the rock (7.7) is slightly alkaline, owing to the presence of carbonates. As a result, the per cent base saturation of the clays is 100 and the predominant ions on the clay surfaces are  $\text{Ca}^{2+}$  and  $\text{Mg}^{2+}$ .

The molar ratio of  $\text{SiO}_2$  to  $\text{R}_2\text{O}_3$  is 4.2, indicating that amorphous oxides can be hydrated because the loss on ignition is higher than what the clay minerals can contribute. This can be deduced from the  $\text{K}_2\text{O}$  content, and the ratio of illite to chlorite (Tables 10 and 5, respectively). Also, in this group the amount of iron which is not combined with silicates, that is free  $\text{Fe}_2\text{O}_3$ , is 1.59 per cent, a relatively high value.

#### GETHING FORMATION, BAT CREEK (SECTION 7)

This formation is divided into two mineral zones. The lower Gething Formation (7, I; samples 64/647 to 64/652) contains 34.42 per cent quartz, 0.78 per cent K-feldspar, 0.62 per cent Na-feldspar, with dolomite, illite, and traces of siderite. In the mixed layers, the ratio of illite to 2:1 expandable clay minerals is 88:12. Illite is the only discrete clay mineral in this group with a composition of 55 per cent 2M illite polymorphs. The pH of the group (7.4) is alkaline, reflecting the presence of carbonates, especially dolomite. As a result, the ions on the clay surfaces are predominantly  $\text{Ca}^{2+}$  and  $\text{Mg}^{2+}$ . Organic matter content is very high in this zone (12.56%). The  $\text{K}_2\text{O}$  content is 6.54 per cent, indicating that this concentration is the minimum potassium content that can be assumed for the illites of the Gething Formation (Table 10) since it is the only mineral that can have potassium after the removal of K-feldspar.

The upper part\*\* of the formation at Bat Creek (7, II; samples 64/653 to 64/673) contains 25.81 per cent quartz, 0.26 per cent K-feldspar, 2.49 per cent Na-feldspar, with illite and chlorite. In the mixed layers, illite to 2:1 expandable clay minerals are combined at a ratio of 87:13. The percentage of 2M illite polymorphs in discrete illite is 40 and

\* Samples from the lower half of the formation at this locality are not available.

\*\* Samples from the middle part of the section are not available.

the ratio of  $d_{001}$  illite to  $d_{002}$  chlorite is 7.5. The pH of this sequence of shales is almost neutral (6.7) with  $\text{Ca}^{2+}$  ions occupying most of the exchange positions on the clay surfaces. The amount of hydroxyaluminum and/or hydrogen on the clay surface is 0.76 meq/100 g yielding a 93.29 per cent base saturation (Table 7).

BUCKINGHORSE FORMATION,  
TETSA RIVER (SECTION 8)

At Tetsa River, the Buckingham Formation is divided into six mineral zones on the basis on mineralogy and chemistry. The characteristics of each zone are as follows.

The lowest shale of the Buckingham Formation at Tetsa River (8, I; samples 64/88 to 64/93) contains 34.38 per cent quartz, 0.26 per cent K-feldspar, 3.38 per cent Na-feldspar, with illite, dolomite, and siderite. In the mixed layers, illite to 2:1 expandable clay minerals are combined at a ratio of 87:13 whereas the percentage of 2M illite polymorphs in discrete illite increases to 55. The pH of the rock is nearly neutral (6.9) with almost 100 per cent base saturation. Organic matter, at 3.21 per cent, is relatively high, and the loss on ignition very low, 3.32 per cent, indicating that other oxides, besides free  $\text{Fe}_2\text{O}_3$ , exist in an amorphous state. Illite, the only mineral with crystal-lattice  $\text{H}_2\text{O}$  in this group, yields a loss on ignition of between 5.73 and 6.03 per cent (Barshad, 1965). Therefore, even if all iron is in the ferrous state and then oxidized, by heating, to ferric, this cannot account for the low L.O.I. value. As a result, the low L.O.I. value must be attributed to amorphous oxides as well as to oxidation of ferrous iron to ferric.

Immediately above the first zone of shale there is another zone (8, II; samples 64/94 to 64/119) containing 44.77 per cent quartz, 0.52 per cent K-feldspar, 4.71 per cent Na-feldspar, dolomite, siderite, pyrite, illite and chlorite in traces. The amount of illite in the mixed layers drops to 84 per cent, as indicated by the  $10.5\text{\AA}$  spacing of the  $d_{001}$  peak position (Table 6), and the percentage of 2M illite polymorphs in discrete illite decreases to 50. Illite is the main layer silicate in this interval of shale. The pH of the rock is again on the alkaline side (8.3) as a result of the presence of carbonates. The presence of amorphous oxides, especially  $\text{SiO}_2$ , must be assumed because of the high molar ratio of  $\text{SiO}_2$  to  $\text{R}_2\text{O}_3$  and the relatively low L.O.I. value.

The third mineral association in the Buckingham Formation at Tetsa River (8, III; samples 64/120 to 64/201) contains 30.83 per cent quartz, 0.26 per cent K-feldspars, 1.61 per cent Na-feldspar, illite, chlorite and kaolinite, siderite, and pyrite. The percentage of illite in the mixed layers decreases to 79, the percentage of 2M illite polymorphs in discrete illite decreases to 40, and the ratio of  $d_{001}$  illite to  $d_{001}$  kaolinite +  $d_{002}$  chlorite increases to 2.1. The pH value of the rock decreases to 4.4, and the ratio of sulphur to inorganic carbon increases to 1.28 (Table 4). The clay becomes saturated with hydroxyaluminum and/or hydrogen ions, 3.19 meq/100 g, which occupy second place after

$\text{Na}^+$  ions, the predominant cations on the clay surface. The latter is due to high sodium concentration in the interstitial water, 28.00 meq/liter, as determined in the water extracts of the shale. Another important observation in this zone is the high iron content, 11.92 per cent  $\text{Fe}_2\text{O}_3$ . This mineral association, in conjunction with the previously described shales of the Buckingham and Gething Formations, differs substantially from the shales which will be discussed because the mineralogy and chemistry change drastically. For example, the percentage of 2M illite polymorphs in discrete illite decreases from 50 to 20, the sharpness ratio drops from 1.8 to 1.2, the crystallinity index, which is the width of the illite peak at half height expressed in mm, increases from 15 mm to 28 mm, the percentage of illite in the mixed layers decreases from 84 to 70, the pH values of the rocks become acidic to highly acidic and, finally, hydroxyaluminum and/or hydrogen ions become the most important ions on the clay surface.

The fourth zone (8, IV; samples 65/125 to 65/165), occurring in the middle part of the Buckingham Formation at Tetsa River, contains 24.52 per cent quartz, 0.33 per cent K-feldspar, 0.62 per cent Na-feldspar, with illite, vermiculite, kaolinite, calcite, siderite and pyrite. In the mixed layers, the proportion of illite decreases to 70 per cent, the 2M illite polymorphs in discrete illite decrease to 30 per cent, whereas the ratio of  $d_{001}$  illite to  $d_{001}$  kaolinite +  $d_{002}$  chlorite remains at 2.1 as in the previously described zone. The pH of the rock decreases to 4.1 while the ratio of sulphur to inorganic carbon increases to 2.65. The interrelation between high sulphur to inorganic carbon ratios, the pH, and the mineralogy will be discussed later. In this mineral zone, the predominant ion on the clay surface is again  $\text{Na}^+$ , as a result of the presence of  $\text{Na}^+$  ions in the interstitial water, 10.00 meq/liter. The molar ratio of  $\text{SiO}_2$  to  $\text{R}_2\text{O}_3$  is very low (2.4) due to high iron content (20.79%). However, the L.O.I. value is high (7.79%), much higher than what illite, kaolinite and chlorite can contribute, indicating that some amorphous  $\text{SiO}_2$ ,  $\text{Al}_2\text{O}_3$  and  $\text{Fe}_2\text{O}_3$  must be present in a hydrated state.

The fifth zone (8, V; samples 64/202 to 64/273) has a very high content of quartz (60.74%), 0.33 per cent K-feldspar, 3.73 per cent Na-feldspar, illite and chlorite. In the mixed layers, illite drops to 77 per cent as indicated by the  $11.2\text{\AA}$   $d_{001}$  peak position of the mixed layers (Table 6). The percentage of 2M illite polymorphs in discrete illite remains at 30 and the ratio of illite to chlorite drops to 1.0 which means that illite and chlorite are in equal proportion. The pH value of the rock (5.5) stays on the acidic side. The percentage of  $\text{SiO}_2$  (68.23%) is very high, the molar ratio of  $\text{SiO}_2$  to  $\text{R}_2\text{O}_3$  (6.5) is also high, and the L.O.I. value (3.08%) is very low (Table 10), indicating that amorphous  $\text{SiO}_2$  must be present in substantial amounts.

The sixth or uppermost shale zone of the Buckingham Formation at Tetsa River (8, VI; samples 64/274 to 64/310) contains 41.58 per cent quartz, 0.10 per cent K-feldspar, 1.28 per cent Na-feldspar, illite and chlorite. Thus, the mineralogy is the same as in the previously discussed zone. In addition, the percentage of illite in the mixed

layers and the percentage of 2M vs 1M + 1Md illite polymorphs are the same as in the previously discussed shales. However, the ratio of illite to chlorite increases to 2.9. The pH of the shale rises to almost neutrality (6.8), whereas the per cent base saturation decreases to 78.41, indicating that substantial amounts of hydroxyaluminum and/or hydrogen ions occupy exchange sites on the clay surfaces. Again a substantial amount of Na<sup>+</sup> occurs on the clay surface indicating that Na ions are predominant in the interstitial water. The amount of SiO<sub>2</sub> is high (66.46%, Table 7), the molar ratio of SiO<sub>2</sub> to R<sub>2</sub>O<sub>3</sub> (6.0) is also high, and the L.O.I. value low (3.98%), indicating that amorphous SiO<sub>2</sub> is present in this shale.

BUCKINGHORSE FORMATION,  
MUSKWA RIVER (SECTION 9)

Only the upper part of the Buckinghorse Formation was exposed at this locality. Four different mineral associations are recognized.

The lowest zone (9, I; samples 64/748 to 64/815) contains quartz, feldspars, illite and chlorite. The percentage of illite in the mixed layers is 77, the 2M illite polymorphs in discrete illite form 30 per cent and the ratio of illite to chlorite is 2.9. Mineralogically this zone is similar to the uppermost or sixth zone described in the Buckinghorse Formation at Tetsa River. However, the pH of the shale (3.5) is very low, and the ratio of sulphur to inorganic carbon is high (16.50) (Table 4).

The second zone of shale at this locality (9, II; samples 64/816 to 64/862) contains 25.59 per cent quartz, 1.07 per cent Na-feldspar, with illite, chlorite and kaolinite. In the mixed layers, the percentage of illite is 77, whereas the percentage of 2M illite polymorphs is 30, and the ratio of d<sub>001</sub> illite to d<sub>001</sub> kaolinite + d<sub>002</sub> chlorite decreases slightly to 2.7. The pH value of the rock (2.8) is very acidic, and the ratio of sulphur to inorganic carbon is 22.00. As a result, the predominant ions on the clay surface are hydroxyaluminum and/or hydrogen. This is indicated also by the per cent base saturation which is 27.10. The L.O.I. value (7.06%) is high, indicating that some amorphous oxides exist in a hydrated state. Also, in this zone the percentage of organic matter is relatively high (4.03%).

The third zone (9, III; samples 64/863 to 64/1092) is subdivided into two subzones. The lower subzone (9, IIIa; samples 64/863 to 64/1049) contains 22.03 per cent quartz, 0.26 per cent K-feldspar, 3.11 per cent Na-feldspar, with illite, kaolinite, dolomite, siderite, pyrite and traces of chlorite. The percentage of illite in the mixed layers decreases slightly to 76, although the 2M illite polymorph content in discrete illite is constant at 30, as in the previously described zone. The ratio of d<sub>001</sub> illite to d<sub>001</sub> kaolinite + d<sub>002</sub> chlorite increases to 6.7 indicating that illite is predominant in the layer lattice silicate assemblages. Owing to the presence of carbonates, the pH value rises to 6.0 and the ratio of sulphur to inorganic carbon drops to less than unity. Also Ca and Mg ions predominate at the exchange sites, raising the per cent base

saturation to 90.11 and leaving 1.58 meq/100 g of hydroxyaluminum and/or hydrogen ions to occupy positions on the adsorptive surfaces of the layer silicates. Iron content expressed as Fe<sub>2</sub>O<sub>3</sub> is high (9.08%) due to the presence of siderite and pyrite. Also, the L.O.I. value is high (6.84%), indicating that some amorphous oxides may exist in a hydrated state. In this and the overlying subzone, the cation exchange capacity (C.E.C.) of clay minerals in shale increases substantially. For example, in the second zone the C.E.C. value is 14.00 meq/100 g, whereas in this subzone the C.E.C. value rises to 22.65 meq/100 g and in the next subzone goes even higher to 26.65 meq/100 g (Table 10)\*. This pattern follows the per cent increase of the 2:1 expandable layer silicates in the shale.

The upper subzone (9, IIb; samples 64/1050 to 64/1092) contains 34.15 per cent quartz, 0.52 per cent K-feldspar, 2.04 per cent Na-feldspar, with siderite, pyrite, illite, chlorite and kaolinite and traces of dolomite. The percentage contribution of the illite in the mixed layers is 76, the percentage of 2M illite polymorphs in discrete illite is 30 and the ratio of the d<sub>001</sub> illite to d<sub>001</sub> kaolinite + d<sub>002</sub> chlorite is 3.9. The pH value of the shales (6.7) is close to neutrality due to the presence of carbonates. The percentage of SiO<sub>2</sub> and the molar ratio of SiO<sub>2</sub> to R<sub>2</sub>O<sub>3</sub> is high, 59.18 and 4.2, respectively, indicating the presence of amorphous SiO<sub>2</sub>.

MIDDLE SCATTER FORMATION,  
BEAR ISLAND, LIARD RIVER (SECTION 12)

Shale from the middle Scatter Formation contains 33.65 per cent quartz, 0.20 per cent K-feldspar, 1.95 per cent Na-feldspar, illite, kaolinite and chlorite. The contribution of illite in the mixed layers is 77 per cent, the percentage of 2M illite polymorphs in discrete illite decreases to 25 and the ratio of d<sub>001</sub> illite to d<sub>001</sub> kaolinite + d<sub>002</sub> chlorite increases to 10.7. The pH value of the rock (4.7) is acidic, whereas the sulphur to inorganic carbon ratio increases above 1.00 (Table 8). As a result, the base saturation decreases to 59.90 per cent due to saturation of the clay surfaces by hydroxyaluminum and/or hydrogen ions. The molar ratio of SiO<sub>2</sub> to R<sub>2</sub>O<sub>3</sub> is 4.2. This, in combination with the relatively high value of SiO<sub>2</sub> (57.23%) indicates that amorphous SiO<sub>2</sub> exists, some of which might be in a hydrated form.

The pH value of the rocks in Scatter, Garbutt, Lepine, Sikanni and Sully Formations becomes acidic to very acidic, hydroxyaluminum and/or hydrogen ions predominate on most clay surfaces, the base saturation drops drastically, except in the uppermost zone of shale of the Sully Formation (15, IV; samples 65/497 to 65/620), and the ratio of sulphur to inorganic carbon is always above unity, indicating the presence of either oxidative products of free sulphur or, probably, of hydrotroilite (amorphous FeS).

\* Cation exchange capacity (C.E.C.) in meq/100 g is obtained by dividing the per cent Li<sub>2</sub>O by its equivalent weight, 14.94, and multiplying the result by 100.

MIDDLE SCATTER FORMATION,  
NORTH OF SCATTER RIVER (SECTION 13)

Shale at this locality has the following mineralogical and chemical characteristics: 30.91 per cent quartz, 0.20 per cent K-feldspar, 1.69 per cent Na-feldspar, illite and chlorite. The illite contribution in the mixed layers is 77 per cent, the percentage of 2M illite polymorphs in discrete illite is 25, and the ratio of  $d_{001}$  illite to  $d_{002}$  chlorite is 6.3. The pH of the shale in this formation is 4.5, and the ratio of sulphur to inorganic carbon is 1.25. The exchange acidity yields 7.06 meq/100 g of hydroxyaluminum and/or hydrogen on the clay surface resulting in a 37.68 per cent base saturation. The molar ratio of  $\text{SiO}_2$  to sesquioxides is 4.2, indicating, as in the previous formation, the presence of amorphous  $\text{SiO}_2$ .

SCATTER FORMATION,  
SCATTER RIVER (SECTION 11)

Shale of this formation is differentiated into three mineral zones with the following characteristics.

The first zone (11, I; samples 65/628 to 65/630) consists of 31.68 per cent quartz, 1.04 per cent K-feldspar, 1.95 per cent Na-feldspar, with dolomite, calcite, gypsum, pyrite, illite, montmorillonite and kaolinite. It is the only mineral association in which montmorillonite has been identified. The percentage of illite contribution in the mixed layers decreases to 32, the per cent ratio of 2M illite polymorphs in discrete illite decreases to 20 and the ratio of  $d_{001}$  illite to  $d_{002}$  chlorite is measured at 3.5. The pH value of the shale is 2.7 and the sulphur to inorganic carbon ratio is 4.84. As a result, the surface of the clays is loaded mainly with hydrogen ions and secondarily with hydroxyaluminum and aluminum cations. This is shown also by the per cent base saturation which is 25.20. Due to the presence of montmorillonite, the adsorbed water  $\text{H}_2\text{O}^-$  value increases to 3.54 per cent (Table 10) and the C.E.C. to 28.65 meq/100 g (Table 7).

The middle part of this formation (11, II; samples 65/640 to 65/686) contains quartz, feldspars, illite, chlorite and kaolinite. The percentage contribution of illite in the mixed layers increases to 77, while the percentage of 2M illite polymorphs in discrete illite remains at 20, and the ratio of  $d_{001}$  illite to  $d_{001}$  kaolinite +  $d_{002}$  chlorite increases to 10.2, indicating the prominence of illite in the layer silicates. The pH value of the shale increases to 4.5, the per cent base saturation to 57.10 and the ratio of sulphur to inorganic carbon is calculated at 4.0.

The upper part of the Scatter Formation, Scatter River (11, III; samples 65/687 to 65/707) consists of 47.60 per cent quartz, 0.91 per cent K-feldspar, 2.75 per cent Na-feldspar, illite and chlorite. The percentage contribution of illite in the mixed layers is 78, the percentage of 2M illite polymorphs in discrete illite is the same as in the previously described shale of the same formation, and the ratio of  $d_{001}$  illite to  $d_{002}$  chlorite is measured at 4.4. The pH value of the shale is 4.8, and the ratio of sulphur to inorganic carbon is 1.26.

As a result, the exchange acidity amounts to 3.32 meq/100 g and the base saturation to 70.69 per cent. The percentage of  $\text{SiO}_2$  is relatively high (4.2%). Both values indicate that amorphous  $\text{SiO}_2$  should exist in the shale of this zone.

GARBUTT FORMATION  
(SECTION 10, SAMPLES 65/721 to 65/765)

This formation contains 40.74 per cent quartz, 2.49 per cent Na-feldspar, illite, chlorite and kaolinite. The percentage contribution of illite in the mixed layers is 76, the percentage of 2M illite polymorphs in discrete illite is 25, and the ratio of  $d_{001}$  illite to  $d_{001}$  kaolinite +  $d_{002}$  chlorite is 3.0. The pH of the shale is 3.9 and the ratio of sulphur to inorganic carbon 2.0. As a result, the exchange acidity, that is the exchangeable hydroxyaluminum and/or hydrogen ions, increases to 10.81 meq/100 g, and the base saturation decreases to 26.31 per cent. The percentage of  $\text{SiO}_2$  is 58.10 (Table 10) and the molar ratio of  $\text{SiO}_2$  to sesquioxides is 4.2, both of which are high, indicating the presence of amorphous  $\text{SiO}_2$ .

LEPINE FORMATION,  
LIARD RIVER (SECTION 14)

This formation is subdivided into three mineralogical associations.

The lower zone (14, I; samples 65/234 to 65/243) contains 40.74 per cent quartz, 2.04 per cent Na-feldspar, 3.46 per cent organic matter, with gypsum, illite, vermiculite and kaolinite. The contribution of the illite in the mixed layers is 76 per cent, the percentage of 2M illite polymorphs in discrete illite is 25 and the ratio of  $d_{001}$  illite to  $d_{001}$  kaolinite is 3.8. The pH value of the shale is very low (3.0), and the ratio of sulphur to inorganic carbon is 6.4, indicating that free acidity must be present. An analysis of the original sample gave 0.48 per cent CaO or 0.34 per cent  $\text{Ca}^{2+}$  which yields 1.48 per cent  $\text{CaSO}_4 \cdot 2\text{H}_2\text{O}$ , if all  $\text{Ca}^{2+}$  is in gypsum. This ties up approximately 0.27 per cent sulphur leaving .37 per cent sulphur (.64-.27, Table 7) free for other compounds. These compounds must be oxidative products of sulphur generating the acidity. The results of this process are the high exchange acidity (9.06 meq/100 g), and low base saturation (28.4%). In this zone, the percentage of  $\text{SiO}_2$  is high (60.31%), and the molar ratio of  $\text{SiO}_2$  to  $\text{R}_2\text{O}_3$  is also high (4.4), indicating free amorphous  $\text{SiO}_2$ .

The second zone in the Lepine Formation (14, II: samples 65/244 to 65/372) contains 38.25 per cent quartz, 3.02 per cent Na-feldspar, with illite, vermiculite, kaolinite and traces of chlorite. The contribution of illite in the mixed layers drops to 74 per cent, the percentage of 2M illite polymorphs in discrete illite remains at 25 as in the previously described group of shales, and the ratio of  $d_{001}$  illite to  $d_{001}$  kaolinite +  $d_{002}$  chlorite is 3.2. The pH value of the shale increases slightly to 3.4 from the previous value of 3.0 which was encountered in the lower zone of shale, whereas the ratio of sulphur to inorganic carbon drops to 3.13. The exchange acidity rises to 14.25 meq/100 g, and the

base saturation drops to 14.40 per cent; these are the highest exchange acidity and lowest base saturation values encountered in the whole study.

The third or upper zone of this formation (14, III; samples 65/373 to 65/411) has identical mineralogy and very similar chemistry to the lower zone of shale of the Lepine-Sikanni-Sully Formations, which is discussed immediately below.

LEPINE, SIKANNI AND SULLY  
FORMATIONS, SCATTER RIVER (SECTION 15)

This sequence of formations is divided into three separate zones which have the following characteristics.

The lower zone (15, I; samples 65/408 to 65/450) contains 14.97 per cent quartz, 0.25 per cent K-feldspar, 3.64 per cent Na-feldspar, with dolomite, illite, vermiculite, kaolinite and traces of chlorite. The contribution of illite in the mixed layers is 74 per cent, the percentage of 2M illite polymorphs in discrete illite is 25, and the ratio of  $d_{001}$  illite to  $d_{001}$  kaolinite +  $d_{002}$  chlorite reaches a value of 3.7. The pH value of the shale increases to 3.8 while the ratio of sulphur to inorganic carbon decreases to 1.70. The per cent base saturation increases to 57.00 while the exchange acidity decreases to 6.02 meq/100 g. However, hydroxy-aluminum and/or hydrogen are still predominant on the exchange surfaces. The percentage of  $\text{SiO}_2$  is high (57.44%; Table 10), and the molar ratio of  $\text{SiO}_2$  to sesquioxides is also high (4.0), indicating that amorphous  $\text{SiO}_2$  must exist in the shale.

The second zone (15, II; samples 65/451 to 65/496) contains 37.94 per cent quartz, 2.34 per cent K-feldspar, 5.60 per cent Na-feldspar, illite, vermiculite, chlorite and kaolinite. The contribution of the illite in the mixed layer decreases to 70 per cent, the percentage of 2M illite polymorphs in discrete illite decreases to 20, and the ratio of  $d_{001}$  illite to  $d_{001}$  kaolinite +  $d_{002}$  chlorite becomes 1.9. The pH value of the shale increases to 4.0 and the per cent base saturation stays approximately at the same level (54.71%) as in the previously described zone. The percentages of  $\text{Fe}_2\text{O}_3$  and  $\text{Al}_2\text{O}_3$  are relatively high (8.39% and 23.75%, respectively). The L.O.I. value is also high (7.62%; Table 10). However, this value is acceptable since vermiculite, with substantial cavity water, and chlorite and kaolinite with substantial amounts of crystal-lattice water contribute in the making of the layer lattice silicate assemblages.

The upper zone in the Lepine-Sikanni-Sully Formations (15, III; samples 65/497 to 65/620) contains 29.87 per cent quartz, 1.23 per cent K-feldspar, 2.04 per cent Na-feldspar, illite, vermiculite, chlorite and kaolinite. The contribution of illite is 76 per cent, the percentage of 2M illite polymorphs in discrete illite is 20, and the ratio of  $d_{001}$  illite to  $d_{001}$  kaolinite +  $d_{002}$  chlorite is 3.5. The pH value of the shale becomes very close to neutral (6.8) and the ratio of sulphur to inorganic carbon drops to 1.90. As a result, the per cent base saturation increases to 91.72 and  $\text{Ca}^{2+}$  and  $\text{Mg}^{2+}$  become again predominant on the clay surface

with the exchange acidity dropping to 1.38 meq/100 g.

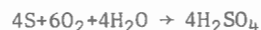
DISCUSSION AND  
INTERPRETATION OF THE RESULTS

INORGANIC GEOCHEMISTRY,  
MINERALOGY AND LAYER LATTICE SILICATES

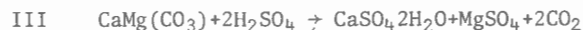
The Lower Cretaceous shale of northeastern British Columbia shows a wide spectrum of pH values (Table 7) ranging from 2.8 up to 8.3. The low pH values indicate the presence of free hydrogen, whereas the high pH values indicate the presence of carbonates. The presence of free hydrogen is attributed to the oxidation products of pyrite (Quispel *et al.*, 1952; Harmsen, 1954; Baas Becking *et al.*, 1960). The reactions which take place are:



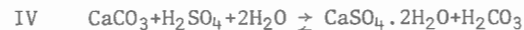
or



Reaction I or II can be used to explain the low pH values of the studied shale. For example, in the Lepine, Sikanni, and Sully Formations, though pyrite and/or gypsum are absent (Table 6), sulphur concentration is higher (Table 7) than the organic matter can accommodate (Smith, 1961; Smith and Young, 1967). To explain this, it has been assumed that a black amorphous precursor of the sulphides, collectively referred to as hydrotroilite ( $\text{FeS}$ ; Berner, 1970), undergoes reaction I or II. However, the hydrogen ion concentration of the shale, which plays an important role in the destruction or formation of certain minerals, depends on the presence or absence of carbonates. If carbonates, such as calcite and/or dolomite and/or ankerite, are present then the following reactions may take place:



or

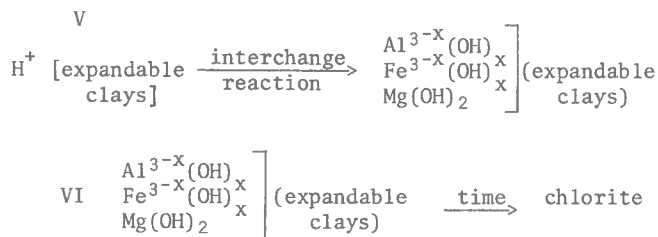


The above reactions show that the final pH value of the shale depends on the concentration of the reactants, specifically pyrite or hydrotroilite, dolomite and/or calcite.

If carbonates are absent, hydrogen ions are absorbed on the clay surfaces, specifically on the expandable 2:1 layer silicates. The absorbed protons move inward, interchanging with aluminum, iron and/or magnesium mainly from the octahedral layers. The factors governing these reactions are discussed by Foscolos (1964) and Foscolos and Barshad (1969). Finally, aluminum and iron which are adsorbed on the clay surface are polymerized leading, with time, to the formation of sedimentary chlorites in a way



similar to those discussed by Barnishel and Rich (1963), Brydon and Kodama (1966), Rich (1968), Gupta and Malik (1969), and Carstea *et al.* (1970). Therefore, the overall reaction can be summarized as follows:



If the pH value of the shale is below 3.00, chlorite is destroyed and is therefore absent from the rock. This property is used to destroy sedimentary chlorites in a mixture of clays (Brown, 1961).

Reactions I to VI can be used to explain the presence or absence of certain minerals in sedimentary rocks as well as the epigenetic formation of gypsum and siderite. For example, in the Lepine, Sikanni and Sully Formations (Tables 6 and 7), chlorite is absent in the lower zone due to the high hydrogen concentration, and present in the higher zones due to the low hydrogen concentration in the shale.

From the preceding discussion it is obvious that sedimentary rocks are chemically very active. Hydrogen ion concentration, geothermal temperature, pressure and time are acting simultaneously to destroy certain minerals and create others. This conclusion can be verified from the molar ratio of  $\text{SiO}_2$  to  $\text{R}_2\text{O}_3$  (Table 10). This molar ratio for layer silicates ranges from 2.0 for kaolinities to 3.3 for illites (Grim, 1953). Values below 2.0 and above 3.3 indicate the presence of amorphous components resulting from the destruction of layer silicates. Table 10 shows that most shale contains amorphous material and, therefore, is chemically very active.

PEAK MIGRATION OF MIXED LAYERS,  
ILLITE POLYMORPHS, SHARPNESS RATIO,  
CRYSTALLINITY INDEX, AND PRESENCE  
OF 1:1 LAYER SILICATES

Peak migration of mixed layers

The proportion of illite in the mixed layers which are composed of illite and 2:1 expandable clay minerals was used as an indicator for the degree of sediment diagenesis. To quantize the percentage of illite in the interstratified clays, the peak migration method was used.

Two end components have been identified in the mixed layer lattice silicate assemblages of the Lower Cretaceous shale of northeastern British Columbia. The first one is illite, a non-expandable component with  $d_{001} = 9.98\text{\AA}$ ; the second is an expandable 2:1 layer lattice silicate component with two members both having  $d_{001} = 15.3\text{\AA}$  at 50 per

cent R.H. These members are vermiculite and montmorillonite (Foscolos and Kodama, 1974). Because the peak position in the binary or ternary mixed layer silicates in the diffractogram is a function of the composition of the end members, the closer the  $d_{001}$  peak position is to the  $d_{001} = 9.98\text{\AA}$ , the richer the mixture is in illite. Based on the diffraction curves for 10/15.4 $\text{\AA}$  random interstratification calculated by Hendricks and Teller (1942) for infinite crystallites (*see* MacEwan, Ruiz Amil and Brown *in* Brown, 1961, Fig. XI.19), the percentage composition of the end members has been obtained.

In the Lepine, Sikanni and Sully Formations, the  $d_{001}$  peak position of the mixed layers migrates from 12.3 $\text{\AA}$  in the stratigraphically higher group of shales to 11.7 $\text{\AA}$  in the stratigraphically lower part, yielding 30 and 24 per cent expandables, respectively. In the Buckingham Formation, the  $d_{001}$  peak migrates from 11.7 $\text{\AA}$  in the uppermost group of shales of Muskwa River to 10.3 $\text{\AA}$  in the lowest portion of Tetsa River, yielding 24 and 13 per cent expandables, respectively. Thus, from the bottom of the Buckingham Formation to the upper part of the Lepine, Sikanni and Sully Formations there is a decrease of the illite percentage from 87 to 70. A reverse trend is observed with the cation exchange capacity (Table 10). The decrease in percentage of illite is associated with an increase of the percentage of the expandable layer lattice silicates and of the cation exchange capacity.

In the middle Scatter Formation, Liard River, the  $d_{001}$  peak position of mixed layers yields a value of 11.2 $\text{\AA}$ . This indicates 77 per cent illite concentration in the mixed layers. The same illite composition in the mixed layers is encountered in the middle Scatter Formation, north of Scatter River. The middle Scatter Formation, at Scatter River, shows the following peculiarity. The  $d_{001}$  peak of the interstratified clays migrates from 11.1 $\text{\AA}$  in the uppermost zone to 14.7 $\text{\AA}$  in the lowest zone, indicating that the percentage of illite in the interstratified clays is lower in the bottom portion of the formation and higher in the upper. This trend is contrary to what has been observed in all other formations and it can be explained by assuming that the lower portion of the sediment was derived from a mature source, while the middle and upper parts were derived from a younger terrain. This explanation satisfies also the presence of kaolinite and montmorillonite in the lower portion of the formation and their absence from the uppermost zone of shales.

In the Garbutt Formation, at Scatter River, the  $d_{001}$  peak position of the mixed layers is at 11.7 $\text{\AA}$ . This yields 76 per cent illite and 24 per cent expandables in the interstratified clays. The same composition is encountered in the clays of the lower part of the Lepine Formation.

The Gething Formation has the lowest percentage of expandable layer silicates, therefore the highest percentage of illites. The  $d_{001}$  spacing of the mixed layer ranges from 10.2 $\text{\AA}$  to 10.4 $\text{\AA}$ . Thus, illite contribution in the mixed layers ranges from 85 to 88 per cent. Cruiser, Hasler, Commotion and Moosebar Formations at Peace River show a narrow band of  $d_{001}$  peak migration. This ranges from 10.4 $\text{\AA}$  to 10.6 $\text{\AA}$ .

On the basis of the illite to 2:1 expandable layer silicate mixtures, the shale of Lepine, Sikanni and Sully Formations has undergone less diagenetic alteration than the shale which forms the middle Buckingham Formation at Tetsa River and the middle to upper shale of the Buckingham Formation at Muskwa River. The latter has undergone less diagenetic change than the shale encountered in the Cruiser, Hasler, Commotion and Moosebar Formations. Diagenetically, the shale of the middle Scatter, Scatter and Garbutt Formations is very close to the shale of the middle Buckingham Formation at Tetsa River and the shale of middle to upper Buckingham Formation at Muskwa River. Most of the Gething Formation and the lowermost part of the Buckingham Formation in the vicinity of Prophet and Tetsa Rivers have the highest degree of diagenesis.

#### Illite polymorphs

The study of illite polymorphs yields the same diagenetic trend as the study of the mixed layer silicates. Thus, the percentage of 2M polymorphs in the Lepine, Sikanni and Sully Formations ranges from 20 to 25 whereas in the Buckingham Formation the variation is from 30 per cent in the upper zone of shale at Muskwa River to 55 per cent in the lowest part at Tetsa River. Because Maxwell and Hower (1967) demonstrated that increasing temperature and pressure accompanying deep burial apparently cause transformation of the 1Md to 2M polymorphs, it might be assumed that the shale of Lepine, Sikanni and Sully Formations has undergone less diagenetic alteration than the shale of the Buckingham Formation. On the same basis, the shale of the Gething Formation and the lowermost part of the Buckingham Formation at Tetsa River are most altered diagenetically because the percentage of 2M polymorphs ranges from 40 to 55. The shale of the Cruiser, Hasler, Commotion and Moosebar Formations is diagenetically younger than the shale of the Gething Formation and the lower Buckingham Formation at Prophet and Tetsa Rivers, but is similar to the middle and upper parts of the Buckingham Formation because the percentage of 2M illite polymorphs varies between 25 and 30. The shale of the Scatter and Garbutt Formations has a percentage of 2M illite polymorphs of between 20 and 25 which classifies them diagenetically in the same facies with the shale of Lepine, Sikanni and Sully Formations.

#### Crystallinity index and sharpness ratio of the illite $d_{001}$ peak

The sharpness ratio (S.R.) of the  $d_{001}$  illite diffraction peak has been used in the present study as a parameter for the degree of diagenesis (Weaver, 1961). In addition, the crystallinity index (C.I.), which is the measure of the width of  $d_{001}$  illite peak at half height, has been used for the same purpose (Kubler, 1966). Their relationship is shown in Table 11. The larger the S.R. value, or the smaller the C.I., the better the crystallinity of illites. This implies increasing temperature and rising pressure conditions which accompany deep burial.

The trend of S.R. and C.I. values, as far as the diagenetic stage of each formation is concerned, follows the pattern which has been established with the previous two factors, namely the percentage of illite in the mixed layers and the percentage of 2M illite polymorphs. Thus the  $d_{001}$  illite peak in Garbutt, Lepine, Sikanni and Sully Formations yields a range of S.R. and C.I. values of between 1.2 and 1.4 and between 22 mm and 28 mm, respectively, whereas for the shale of the middle and upper parts of Buckingham Formation at Tetsa and Muskwa Rivers they range from 1.2 to 1.6 and from 18 mm to 26 mm, respectively. This implies that the latter formation has been subjected to more advance diagenesis than the others. The S.R. and C.I. values of the shale of the Gething Formation and of the lower part of the Buckingham Formation at Tetsa River range from 1.8 to 3.0 and from 13 mm to 15 mm, respectively, indicating that they have been altered diagenetically more than any other shale of any formation studied here. The Cruiser, Hasler, Commotion and Moosebar Formations yield S.R. and C.I. values between 1.4 and 1.7 and between 17 mm and 19 mm, respectively, thus placing their shales diagenetically between those of the middle and upper parts of the Buckingham Formation at Tetsa and Muskwa Rivers, and those of the Gething and the lowermost part of the Buckingham Formation. The shale in the Scatter Formation, with the exception of that in the lower part, is classified diagenetically between that of the Lepine, Sikanni and Sully Formations and that of the middle and upper Buckingham Formations at Tetsa and Muskwa Rivers, because the S.R. and C.I. values ranges from 1.3 to 1.5 and from 21 mm to 24 mm, respectively.

#### Presence of kaolinite in shales

In this study, the presence of kaolinite has been used as a secondary factor in establishing the diagenetic stage of shale, since limits of stability for this mineral are known. The occurrence of kaolinite, however, is related not only to regular pressure and temperature gradients but also to geochemical factors (Dunoyer de Seconzac, 1970). As a result, this mineral cannot be used independently for evaluating the stages of diagenesis.

Kaolinite is absent from the Gething Formation, and from the lower and middle zones of the Buckingham Formation at Tetsa and Muskwa Rivers, but present in the Garbutt, Lepine, Sikanni and Sully Formations. Therefore, the latter formations have undergone less diagenesis than the previous ones. This also is in accordance with the conclusions derived from the study of the primary indices of diagenesis, namely the percentage of illite in the interstratified binary mixtures of illite to 2:1 expandable layer lattice silicates, the type of illite polymorphs, the crystallinity index, and the sharpness ratio. Erratic occurrences of kaolinite appear in the remaining formations (Table 6); their diagenetic stages are therefore evaluated on the basis of the primary factors.

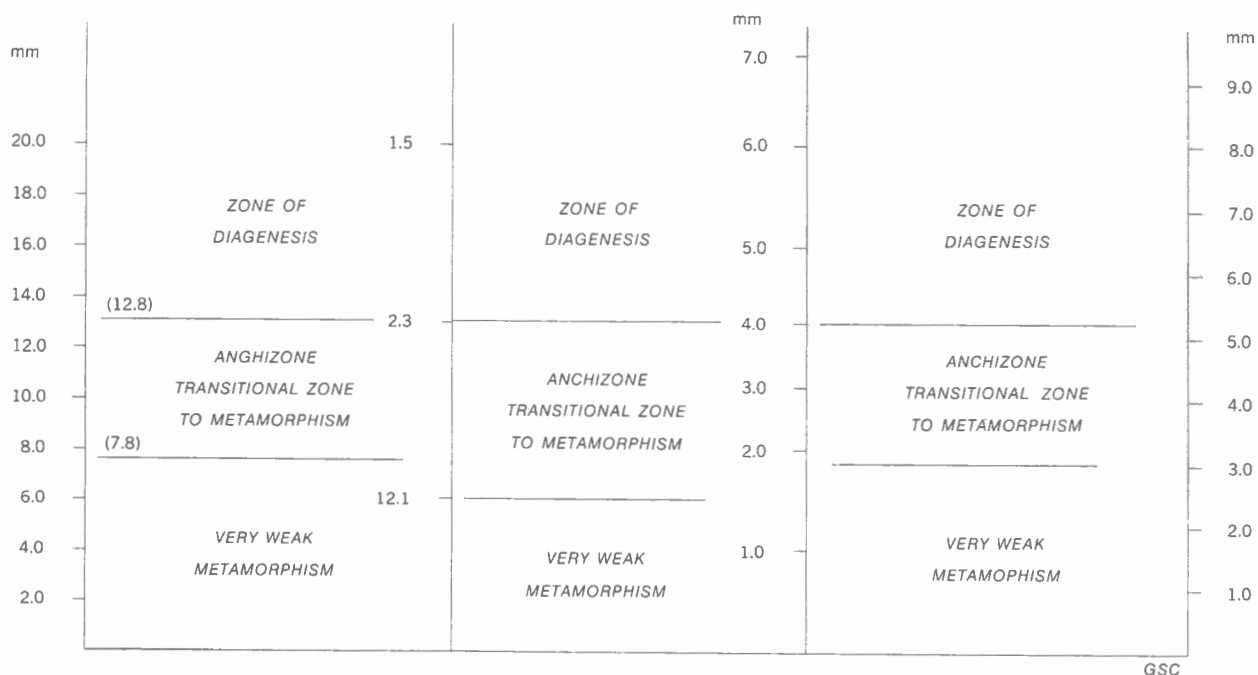


TABLE 11. Crystallinity indices of illites, their relation to sharpness ratio of illites, and their use in evaluating the stages of diagenesis and early metamorphism

#### DIAGENESIS

To evaluate the degree of diagenesis of the Lower Cretaceous shale formations of northeastern British Columbia, five parameters, which have been derived from the study of the  $<2\mu$  clay fraction (Tables 5, 6), were combined with the data and information of Burst (1959, 1969), Dunoyer de Seconzac (1969, 1970), Khitarov and Pugin (1966), Kubler (1964, 1966, 1968), Long *et al.* (1964, 1966), Long and Neglia (1968), Muffler and White (1969), Perry and Hower (1972), Scherp (1963), van Moort (1971) and Weaver (1960, 1961). Diagenetic stages were defined to best fit the data of the previously mentioned authors. Results are presented in Table 12 and are summarized as follows.

1. Discrete expandable clays do not occur below 4,500 feet (1500 m) unless a special geochemical condition or hydrothermal phenomenon occurs. Therefore, as a rule, their presence is confined to those rocks which belong to the early diagenetic stage.

2. In general, kaolinite disappears below 9,000 feet (3000 m).
3. Illite to 2:1 expandable clays generally occur between 3,000 and 12,000 feet (1000 m - 4000 m). The maximum reported depth is around 15,000 feet (5000 m) (Burst, 1969).
4. In general, 2M illite polymorphs predominate over the 1M + 1Md illite polymorphs in late diagenesis.

The boundary between late and middle diagenesis is defined when:

- (a) the illite content in the interstratified clays is 80 per cent;
- (b) fifty per cent of the illite is the 2M polymorph;
- (c) crystallinity index is  $\leq 15$  mm;
- (d) sharpness ratio is  $\geq 2.0$ ; and

(e) kaolinite just disappears from the clay mineral facies.

The division between early and middle diagenesis cannot be sharply drawn but has been defined as the point at which:

- (a) discrete expandable layer silicates and kaolinite are present;
- (b) 1M + 1Md illite polymorphs comprise 75 per cent of the illite or more;
- (c) illite contribution in the interstratified clays equals 25 per cent, or less;
- (d) crystallinity index is  $\geq 20$  mm; and
- (e) sharpness ratio is  $\leq 1.5$ .

Using the five diagenetic criteria (Table 12), four main mineralogical facies can be recognized in the fifteen sections.

The first facies, which includes the Gething Formation at Besa and Prophet Rivers and Bat Creek, and the basal Buckinghamshire Formation at Prophet and Tetsa Rivers, has the following characteristics: a) illite in mixed layers ranges from 84 to 88 per cent; b) 2M illite polymorphs range from 40 to 55 per cent; c) S.R. and C.I. values 1.8 to 3.0, and

from 13 mm to 15 mm, respectively; and d) kaolinite is absent.

The second facies, which includes the lower (but not lowermost) and middle Buckinghamshire Formation at Tetsa River, the upper Buckinghamshire Formation at Muskwa River, in the Scatter and Garbutt Formations, has the following characteristics: a) illite content in the mixed layers ranges from 76 to 79 per cent; b) 2M illite polymorphs vary between 25 to 30 per cent; c) the S.R. and C.I. values fluctuate from 1.4 to 1.6, and from 19 to 26 mm, respectively; and d) kaolinite appears erratically in these formations.

The third facies, which includes the Lepine, Sikanni, and Sully Formations at Scatter and Liard Rivers, has the following characteristics: a) illite in the mixed layers ranges from 70 to 75 per cent; b) 2M illite polymorphs vary from 20 to 25 per cent; c) the S.R. and C.I. values fluctuate between 1.2 and 1.4, and from 24 mm to 27 mm, respectively; and d) kaolinite is present.

The fourth facies, which comprises the Moosebar, Commotion, Hasler and Cruiser Formations, has the following characteristics: a) illite in the mixed layers varies from 79 to 82 per cent; b) 2M illite polymorphs range from 25 to 35 per cent; c) the S.R. and C.I. values fluctuate between 1.4 and 1.7, and from 17 to 19 mm, respectively; and d) kaolinite is encountered in the Cruiser, Hasler, and Commotion

DIAGENETIC STAGES	CRYSTALLINITY INDEX (C.I.)	SHARPNESS RATIO (S.R.)	PER CENT 2M ILLITE POLYMORPHS	LAYER LATTICE SILICATES		
				Per Cent Illite in Illite - 2:1 expandables	Discrete Layers	
					Expandables	Kaolinite
EARLY DIAGENESIS	20	1.5	20	20-25	Present	Present
MIDDLE DIAGENESIS	19				Usually Absent	Present
	18		35			
				40-50		
	17				Usually Absent	Usually Present
	16	1.9			Absent	Usually Absent or transformed to Dickite
LATE DIAGENESIS			50	80-90		
	15			Discrete expandables and kaolin absent		
	14			Randomly interstratified are absent		
	13			Regular interstratified are present 1. Corrensite in Mg rich environment 2. Rectorite in K rich environment		
METAGENESIS OR ANCHIZONE	12.8	2.3	65			
	7.8	12.1		Illites and/or Chlorites		

GSC

TABLE 12. A tentative scheme for correlating the crystallinity index, sharpness ratio, per cent 2M illite polymorphs, per cent illite in the illite-2:1 expandables random mixed layers, presence and absence of discrete layer lattice silicates and regular interstratified layer silicates with diagenetic stages

Formations, whereas it is absent from the Moosebar Formation.

As a result, the four facies can be classified diagenetically as follows. The first one is at the beginning of advanced diagenesis, the second and fourth facies at the intermediate stages of diagenesis, the second facies being less advanced than the fourth, and the third at the early stages of middle or intermediate diagenesis.

#### STRATIGRAPHIC RELATIONSHIPS

On the basis of mineralogy, primarily, and chemistry, secondarily, the following stratigraphic relationships are suggested for the Lower Cretaceous shale formations of northeastern British Columbia (Fig. 36).

The clay mineralogy of the lower Gething Formation at Besa River (5, I; samples 64/437 to 64/452) is similar to that of the lower Gething Formation at Bat Creek (7, I; samples 64/647 to 64/653), and to that of the basal Buckinghamshire Formation at Tetsa River (8, I; samples 64/88 to 64/93). The middle part of the Gething Formation at Besa River (5, II; samples 64/453 to 64/461) is similar to the upper Gething at Bat Creek (7, II; samples 65/654 to 65/673). The upper zone of the Gething Formation at Besa River (5, III; samples 64/462 to 64/465) is similar to that of the upper Gething at Prophet River (6; samples 64/505 to 64/596) and that of the second lowest zone in the Buckinghamshire Formation at Tetsa River (8, II; samples 64/94 to 64/119). All the zones of the above formations seem to have close relationships because the combined indicators of C.I., S.R., percentage of 2M illite polymorphs, percentage of illite in the mixed layer, as well as the absence of expandable layer silicates and kaolinite, are very similar.

The Moosebar Formation (4) has the same mineralogy and chemistry as the upper part of the Gething at Besa River (5, III), Gething Formation at Prophet River (6) and the second lowest zone of the Buckinghamshire Formation at Tetsa River (8, II). However, the percentage of 2M illite and the percentage of illite in the mixed layers differ.

The facies in the lower-middle Buckinghamshire Formation at Tetsa River (8, IV; samples 65/125 to 65/165) is similar to the lower zone encountered in the Scatter Formation (11, I; samples 65/628 to 65/639). However, differences do exist, such as two kinds of expandable layer silicates, namely montmorillonite in the Scatter Formation and vermiculite in the Buckinghamshire Formation. Gypsum in the lower zone of the Scatter Formation can be explained as a by-product from the reaction between the oxidative products of pyrite and calcite or dolomite.

The clay mineralogy of zones V and VI of the Buckinghamshire Formation at Tetsa River (8, V and VI; samples 64/202 to 64/310) is similar to that of the lower zone of the middle Buckinghamshire Formation at Muskwa River (9, I; samples 64/748 to 64/815), the middle to upper Scatter Formation at Scatter River (11, III; samples 65/687 to 65/707), and to the shale of the middle Scatter Formation north of Scatter River (13; samples 65/794 to 65/809).

The shale of the Cruiser, Hasler, Commotion and Moosebar Formations is mineralogically similar to some shale encountered in the Buckinghamshire Formation (9, II and III; samples 64/816 to 64/862 and 64/683 to 64/1049). Nevertheless, the sharpness ratio, crystallinity index, percentage of 2M illite polymorphs, the percentage of illite, chemistry and non-layer lattice silicate minerals do differ.

The upper zones of the Buckinghamshire Formation at Muskwa River (9, II and III; samples 64/816 to 64/1049) are related to the upper shale of the Lepine Formation (14, III; samples 65/373 to 65/411) because both groups have illite, chlorite, kaolinite, carbonates, and FeS (crystalline in the Buckinghamshire Formation and amorphous in the Lepine). However, vermiculite occurs in the Lepine Formation whereas chlorite is present in the Buckinghamshire. As previously explained, one can be derived from the other. Therefore, assuming such alteration, these shales are quite similar.

The lower, but not lowermost shale of the Lepine Formation at Liard River (14, II; samples 65/244 to 65/372) has mineralogy similar to that of the upper Lepine, Sikanni and Sully Formations (15, I and II; samples 65/451 to 65/620), whereas the lowermost part of the Lepine, Sikanni and Sully Formations (15, I; samples 65/408 to 65/450) has mineralogy identical to the uppermost zone of the Lepine Formation, Liard River (14, III; samples 65/373 to 65/411).

The lowermost part of the Lepine Formation (14, I; samples 65/234 to 65/243) cannot be correlated with any zone of any other formation, because the mineralogy and chemistry differ substantially.

#### POSSIBLE SEDIMENT SOURCES

Combined mineralogical and chemical data indicate that the fifteen formations studied may be divided into three groups, each with different source characteristics (Fig. 37).

The sediments of the Lepine, Sikanni and Sully Formations probably were derived from the same source terrain because the chemical and mineralogical variations within the formations can be explained on the basis of diagenesis. As the burial depth of the sediment increases, the sharpness ratio, the percentage of 2M illite polymorphs and the percentage of illite in the mixed layer increase (Table 12).

Sediments which comprise the shale of middle and upper Buckinghamshire Formation at Tetsa River, the Buckinghamshire Formation at Muskwa River, Scatter and Garbutt Formations also may have been derived from the same source area that supplied the sediments of the Lepine, Sikanni and Sully Formations. Not only the mineral assemblages and the overall inorganic chemistry of the shale rocks are similar but also the gradual changes of the ratio of illite to expandable layer lattice silicates in the interstratified clays, the percentage of 2M illite polymorph, the crystallinity index and sharpness ratio (Tables 5, 10) can be explained on the basis of diagenetic changes.



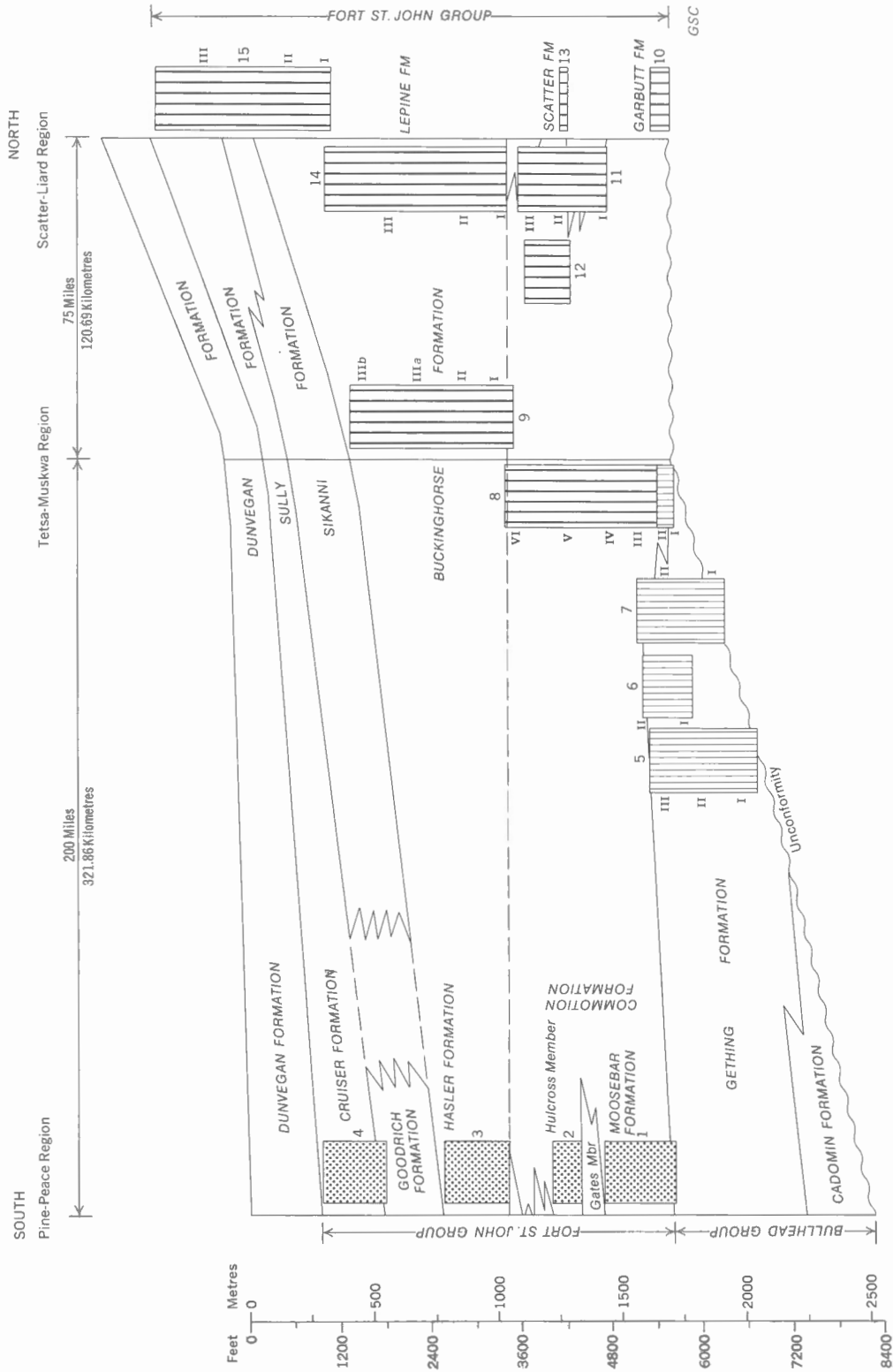


FIGURE 37. Columnar sections of fifteen Lower Cretaceous shale formations of northeastern British Columbia. The various patterns indicate sediments having different source characteristics

The sediments encountered in the Gething Formation, the lowermost Buckingham Formation between Besa River and Bat Creek and the lower shale of the Buckingham Formation at Tetsa River appear to have been derived from another source terrain because the mineralogy, clay mineralogy and chemistry differ substantially (Tables 6, 7). In addition, the five diagenetic indicators show an abrupt change (Tables 5, 6). For example, in the latter group, carbonates and pyrite are present while kaolinite and expandable clays are absent. The opposite is the case with the group described previously.

Finally, the sediments of Cruiser, Hasler, Compton and, probably, Moosebar Formations seem to have been derived from another area. The chemistry of these formations after the removal of quartz and feldspars (Table 10) differs substantially from the chemistry of the other formations. Silica on one hand is very low whereas aluminum and iron on the other are very high. Furthermore, the five diagenetic factors yield values which cannot be correlated diagenetically with the other two groups.

#### BIBLIOGRAPHY

- Aguilera, N.H. and Jackson, M.L.  
1953: Iron oxide removal from soils and clays; Soil Sci. Soc. Am. Proc., v. 17, p. 359-364.
- Andreev, P.F., Bogomolov, A.I., Dobyanskii, A.F. and Kartsev, A.A.  
1968: Transformation of petroleum in nature; Pergamon Press, New York.
- Baas Beeking, L.G.M., Kaplan, I.R. and Moore, D.  
1960: Limits of the natural environment in terms of pH and oxidation-reduction potentials; J. Geol., v. 68, p. 243-384.
- Barnishel, R.I. and Rich, C.I.  
1963: Gibbsite formation from aluminum interlayers in montmorillonite; Soil Sci. Soc. Am. Proc., v. 27, p. 632-635.
- Barshad, I.  
1948: Vermiculite and its relation to biotite; Am. Mineralogist, v. 33, p. 655-678.  
1950: Effect of interlayer cations on expansion of mica lattice; Am. Mineralogist, v. 35, p. 225-238.  
1954: Cation exchange in micaceous minerals I. Replaceability of the interlayer cations of vermiculite with ammonium and potassium ions; Soil. Sci., v. 76, p. 463-472.  
1965: Thermal analysis techniques for mineral identification and mineralogical composition in Methods of Soil Analysis (C.A. Black, ed.-in-chief); Part 1, p. 699-742.
- Berner, R.A.  
1970: Sedimentary pyrite formation; Am. J. Sci., v. 268, p. 1-23.
- Bower, C.A. and Wilcox, L.V.  
1965: Soluble salts in Methods of Soil Analysis (C.A. Black, ed.-in-chief); Part 2, p. 933-951.
- Brooks, R.  
1960: Dissolution of silicate rocks; Nature, v. 185, p. 837-838.
- Brown, G.  
1961: X-ray identification and crystal structure of clay minerals, 2nd edition; Mineralogical Soc., London.
- Brydon, J.E. and Kodama, H.  
1966: The nature of aluminum hydroxide-montmorillonite complexes; Am. Mineralogist, v. 51, p. 875-889.
- Burst, J.F.  
1959: Postdiagenetic clay-mineral environmental relationship in the Gulf Coast Eocene; Proc. Nat. Conf. Clays and Clay Minerals, 6th Nat. Acad. Sci., Nat. Res. Council, Publ. 1957, p. 327-341.  
1969: Diagenesis of Gulf Coast clayey sediments and its possible relation to petroleum migration; Bull. Am. Assoc. Petrol. Geologists, v. 53, p. 73-93.
- Carstea, D.D., Harward, M.E. and Knox, E.C.  
1970: Formation and stability of hydroxy-magnesium interlayers in phyllosilicates; Clays and Clay Minerals, v. 18, p. 213-223.
- Cassidy, M.M. and Mankin, C.J.  
1960: Chlorox use in preparation of black shales for clay mineral analysis; Oklahoma Geology Notes, v. 20, p. 275-281.
- Chapman, H.D.  
1965a: Cation exchange capacity in Methods of Soil Analysis (C.A. Black, ed.-in-chief); Part 2, p. 891-901.  
1965b: Total exchangeable bases in Methods of Soil Analysis (C.A. Black, ed.-in-chief); Part 2, p. 902-904.
- Colombo, V.  
1967: Origin and evolution of petroleum, in Fundamental Aspects of Petroleum Geochemistry (Nagy, G., and Colombo, V., eds.); Elsevier Publishing Co., New York, p. 321-336.
- Cordell, R.J.  
1972: Depths of oil origin and primary migration: A review and critique; Bull. Am. Assoc. Petrol. Geologists, v. 56, p. 2029-2067.
- Cupta, G.C. and Malik, W.V.  
1969: Chloritization of montmorillonite by its co-precipitation with magnesium hydroxide; Clays and Clay Minerals, v. 17, p. 331-338.
- Dudas, M.J. and Harward, M.E.  
1971: Effect of dissolution treatment on standard and soil clays; Soil Sci. Soc. Am. Proc., v. 35, p. 134-139.



- Dunoyer de Seconzac, G.  
1969: Les Minéraux argileux dans la diagenèse. Passage au Métamorphisme (Thesis Univ. Strasbourg); Mém. Serv. Carte Géol. Alsace-Lorraine, no. 29, p. 1-320.  
1970: The transformation of clay minerals during diagenesis and lower grade metamorphism. A review; *Sedimentology*, v. 15, p. 281-346.
- Forsman, J.P. and Hunt, J.M.  
1958: Insoluble organic matter (kerogen) in sedimentary rocks of marine origin *in* Habitat of Oil, a Symposium; Alberta Soc. Petrol. Geologists, p. 747-778.
- Foscolos, A.E.  
1964: Factors affecting replaceability of octahedral  $Mg^{2+}$  ion of various soil minerals with  $H^{+}$  ion; M.Sc. Thesis, Univ. of California, Berkeley.
- Foscolos, A.E. and Barshad, I.  
1969: Equilibrium constants between both freshly prepared and aged H. montmorillonites and chloride salt solutions; *Soil. Sci. Soc. Am. Proc.*, v. 33, p. 242-247.
- Foscolos, A.E. and Barefoot, R.R.  
1970a: A rapid determination of total, organic and inorganic carbon in shales and carbonates. A rapid determination of total sulphur in rocks and minerals; *Geol. Surv. Can.*, Paper 70-11.  
1970b: A buffering and standard addition technique as an aid in the comprehensive analysis of silicates by atomic absorption spectroscopy; *Geol. Surv. Can.*, Paper 70-16.
- Foscolos, A.E. and Kodama, H.  
1974: Diagenesis of clay minerals from Lower Cretaceous shales of northeastern British Columbia, *Clay and clay minerals*, v. 22, p. 319-335.
- Galwey, A.K.  
1972: The rate of hydrocarbon desorption from mineral surfaces and the contribution of heterogenous catalytic-type processes to petroleum genesis; *Geochim., et Geochem., Acta* 36, p. 1115-1130.
- Gehman, H.M.  
1962: Organic matter in limestones; *Geochim. et Cosmochim., Acta* 26, p. 885-897.
- Greene-Kelly, R.  
1953: The identification of montmorillonoids; *J. Soil Sci.*, v. 4, p. 233-237.
- Grim, R.E.  
1953: *Clay Mineralogy*; McGraw-Hill, New York.
- Harmsen, G.W.  
1954: Observations on the formation and oxidation of pyrite in the soil; *Plant and Soil*, v. 4, p. 324-328.
- Hendricks, S.B. and Teller, E.  
1942: X-ray interference in partially ordered layer lattices; *J. Chem. Phys.*, v. 10, p. 147-167.
- Jackson, M.L.  
1956: *Soil chemical analysis*; Advanced course Mimeo published by the author, Dept. Soil. Sci., Univ. Wisconsin, Madison, Wisconsin.  
1965: Free oxides, hydroxides, and amorphous aluminosilicates *in* *Methods of Soil Analysis* (C.A. Black, ed.-in-chief); Part 1, p. 578-603.
- Jones, F.W.  
1938: The measurement of particle size by X-ray method; *Proc. Roy. Soc. London A.*, v. 166, p. 16-43.
- Kartsev, A.A. Vassoevich, N.B., Geodekian, A.A., Neruchev, S.G., and Sokolov, V.A.  
1971: The principal stage in the formation of petroleum; Preprint of the Proceedings of the Eighth World Petroleum Congress, Panel Discussion #1, Elsevier Publishing Company, Essex, England, p. 1-17.
- Khitarov, N.J. and Pugin, V.A.  
1966: Behaviour of montmorillonite under elevated temperatures and pressures; *Geokhim S.S.S.R.*, v. 7, p. 790-795, *Geochem. Intern.*, v. 3, no. 4, p. 621-626.
- Kodama, H. and Brydon, J.E.  
1968: A study of clay minerals in podzol soils in New Brunswick, Eastern Canada; *Clay Minerals, Bull.* 7, p. 295-309.
- Kubler, B.  
1964: Les argiles indicateurs de métamorphisme; *Rev. Inst. Franç. Pétrole*, v. 19, p. 1093-1112.  
1966: La cristallinité d'illite et les zones tout a fait supérieure du métamorphisme *in* *Colloque sur les étages tectoniques à la Baconnière*; Neuchatel, p. 105-122.  
1968: Evaluation quantitative du métamorphisme par la cristallinité de l'illite; *Bull. Centre Rech. Pau - S.N.P.A.*, v. 2, p. 385-397.
- Long, G. and Neglia, S.  
1968: Composition de l'eau interstitielle des argiles et diagenèse des minéraux argilleux; *Rev. Inst. Franç. Pétrole*, v. 25, p. 53-69.
- Long, G., Neglia, S. and Favretto, L.  
1964: Geochemical contribution to research for the reconstruction of the paleogeography of a sedimentary basin *in* *Advanced Organic Geochemistry* (V. Colombo and G.D. Hobson, eds.); Pergamon Press, London, p. 239-259.  
1966: Geochemical studies on the Cretaceous black shales of the Cyrenaica Basin; *Intern., Ser. Monogr. Earth Sci. G.B.*, v. 24, p. 101-113.
- Louis, M. and Tissot, B.  
1967: Influence de la température et de la pression sur la formation des hydrocarbures dans les argiles à kerogene; 7th World Petroleum Congr. Proc., v. 2, p. 47-60.

- MacEwan, D.M.C., Ruiz Amil, A. and Brown, G.  
1961: Interstratified clay minerals *in* The X-ray identification and crystal structure of clay minerals (G. Brown, ed.); Mineralogical Society, London, p. 393-445.
- Maxwell, D.T. and Hower, J.  
1967: High-grade diagenesis and low grade metamorphism of illite in the Precambrian Belt Series; *Am. Mineralogist*, v. 52, p. 843-857.
- Mirchink, M.F., Ali-Zade, A.A. Bakirov, A.A., Veber, V.V., Vassoevich, N.B., Dvali, M.F., Maximov, S.P., Simakov, S.N., Sokolov, V.Z., and Trofimuk, A.A.  
1971: Main concepts of the theory of oil and gas origin and their accumulation in the light of the most recent investigations; Preprint of the Proceedings of the Eighth World Petroleum Congress, Panel Discussion No. 1, Elsevier Publishing Company, Essex, England, p. 3-1 to 3-13.
- Mooney, R.W., Keenan, A.G. and Wood, L.A.  
1952: Adsorption of water vapour by montmorillonite; *J. Am. Chem. Soc.*, v. 74, p. 1367-1374.
- Muffler, L.J.P. and White, D.E.  
1969: Active metamorphism of Upper Cenozoic sediments in the Salton Sea-geothermal field and the Salton trough, southeastern California; *Bull. Geol. Soc. Am.*, v. 80, p. 157-182.
- Parham, W.E.  
1966: Lateral variation of clay mineral assemblages in modern and ancient sediments; *Proc. Intern. Clay Conf.*, Jerusalem, Israel, v. 1, p. 135-145.
- Peech, M.  
1965: Exchange Acidity *in* Methods of Soil Analysis (C.A. Black, ed.-in-chief); Part 2, p. 905-913.  
1965: Hydrogen-Ion Activity *in* Methods of Soil Analysis (C.A. Black, ed.-in-chief); Part 2, p. 914-926.
- Perry, E. and Hower, J.  
1970: Burial diagenesis in Gulf Coast pelitic sediments; *Clays and Clay Minerals*, v. 18, p. 165-177.  
1972: Late stage dehydration in deeply buried pelitic sediments; *Am. Assoc. Petrol. Geologists, Bull.* 56, p. 2013-2021.
- Powers, M.C.  
1959: Adjustment of clays to chemical change and the concept of equivalence level; *Proc. Natl. Conf. Clays and Clay Minerals*, 6th Natl. Acad. Sci. Natl. Res. Council, Publ. 1957, p. 309-326.  
1967: Fluid release mechanisms in compacting marine mudrocks and their importance in oil exploration; *Am. Assoc. Petrol. Geologists, Bull.* 51, p. 1240-1253.
- Price, L.C.  
1973: Solubility of hydrocarbons and petroleum in water as applied to primary migration of petroleum; Ph.D. Thesis, Univ. Calif., Riverside.
- Quispel, A., Harmsen, G.W. and Otzen, D.  
1952: Contribution to the chemical and bacteriological oxidation of pyrite in soil; *Plant and Soil*, v. IV, no. 1, p. 43-56.
- Reynolds, R.C.  
1968: The effect of particle size on apparent lattice spacings; *Acta Cryst.*, v. A24, p. 319-320.
- Rich, C.I.  
1968: Hydroxy-interlayers in expandable layer silicates; *Clays and Clay Minerals*, v. 16, p. 15-30.
- Sarkisjan, S.G.  
1972: Origin of authigenic clay minerals and their significance in petroleum geology; *Sediment. Geol.*, v. 7, p. 1-22.
- Scherp, A.  
1963: Die petrographie der paläozoischen Sandsteine in der Bohrung Münsterland I and ihre Diagenese in Abhängigkeit von der Teufe; *Fortschr. Geol. Rheinland Westfalen*, v. 11, p. 251-282.
- Smith, J.W.  
1961: Ultimate composition of organic material in Green River oil shales; *U.S. Bur. Mines Rept. Investig.*, v. 5725, p. 16.
- Smith, J.W. and Young, N.R.  
1967: Organic composition of Kentucky's new Albany shale. Determination and uses; *Chem. Geol.*, v. 2, p. 157-170.
- Stott, D.F.  
1967: Jurassic and Cretaceous stratigraphy between Peace and Tetsa Rivers, northeastern British Columbia; *Geol. Surv. Can.*, Paper 66-7.  
1968a: Lower Cretaceous Bullhead and Fort St. John Groups, between Smoky and Peace Rivers, Rocky Mountain Foothills, Alberta and British Columbia; *Geol. Surv. Can., Bull.* 152.  
1968b: Cretaceous stratigraphy between Tetsa and La Biche Rivers, Northeastern British Columbia; *Geol. Surv. Can.*, Paper 68-14.  
1972: Cretaceous stratigraphy, Northeastern British Columbia; *Proc. 1st Geol. Conf. Western Canada, Coal. Res. Council Alberta*, p. 137-150.  
1973: Lower Cretaceous Bullhead Group between Bullmoose Mountain and Tetsa River, Rocky Mountain Foothills, northeastern British Columbia; *Geol. Surv. Can., Bull.* 219.

- Teodorovich, G.E. and Konyukhov, A.I.  
1970: Mixed layer minerals in sedimentary rocks as indicators of the depth of their catagenetic alteration, *Doklady Akad. Nauk SSSR*, v. 191, p. 174-176.
- Tissot, B., Califet-Debyser, Y., Deroo, G., and Oudin, J.L.  
1971: Origin and evolution of hydrocarbons in early Toarcian shales, Paris basin, France; *Am. Assoc. Petroleum Geologists, Bull.* 55, p. 2177-2193.
- Tissot, B., Durand, B., Espitalié, J. and Combaz, A.  
1974: Influence of nature and diagenesis of organic matter in formation of petroleum; *Am. Assoc. Petroleum Geologists, Bull.* 58, p. 499-506.
- Van der Speck, I.  
1952: The loss of calcium carbonate from sea clay deposits by oxidation of sulphides in these deposits; *Landbouwkundig Tijdschrift*, v. 64, no. 7, p. 473-478.
- van Moort, J.C.  
1971: A comparative study of the diagenetic alteration of clay minerals in Mesozoic shales from Papua, New Guinea, and in Tertiary shales from Louisiana, U.S.A.; *Clays and Clay Minerals*, v. 19, p. 1-20.
- Velde, B. and Hower, S.  
1963: Petrological significance of illite and polymorphism in Paleozoic sedimentary rocks; *Am. Mineralogist*, v. 48, p. 1239-1254.
- Weaver, C.E.  
1960: Possible uses of clay minerals in search for oil; *Bull. Am. Assoc. Petrol. Geologists*, v. 44, p. 1505-1518.
- Weaver, C.E.  
1961: Minerals of the Ouachita structural belt and adjacent foreland *in* The Ouachita System (P.T. Flawn *et al.*, eds.); University of Texas, Bur. Econ. Geol., Publ. 6120, p. 147-162.
- 1967: The significance of clay minerals in sediments *in* Fundamental Aspects of Petroleum Geochemistry (Nagy, B. and Colombo, V., eds.); Elsevier Publishing Company, New York, p. 37-75.
- Weaver, C.E., Beck, K.C. and Pollard, C.O.  
1971: Clay water diagenesis during burial: How mud becomes gneiss; *Geol. Soc. Am., Spec. Paper* 134, p. 1-78.
- Weaver, C.E. and Wampler, J.M.  
1970: K, Ar, illite burial; *Bull. Geol. Soc. Am.*, v. 81, p. 3423-3430.
- Weiss, A.  
1969: Organic derivatives of clay minerals, zeolites and related minerals *in* Organic Geochemistry (Eglinton, C. and Murphy, M.T., eds.); p. 737-781.
- Weiss, A. and Roloff, G.  
1965: Die Rolle organischer Derivate von glimmerartigen Schichtsilikaten bei der Bildung von Erdöl *in* Intern. Clay Conf., Stockholm, 1963, v. 2, p. 373-378.
- Yerofeyev, V.F.  
1972: Geothermal activity at depth and distribution of deposits of hydrocarbons; *Intern. Geol. Review*, v. 14, p. 49-53.

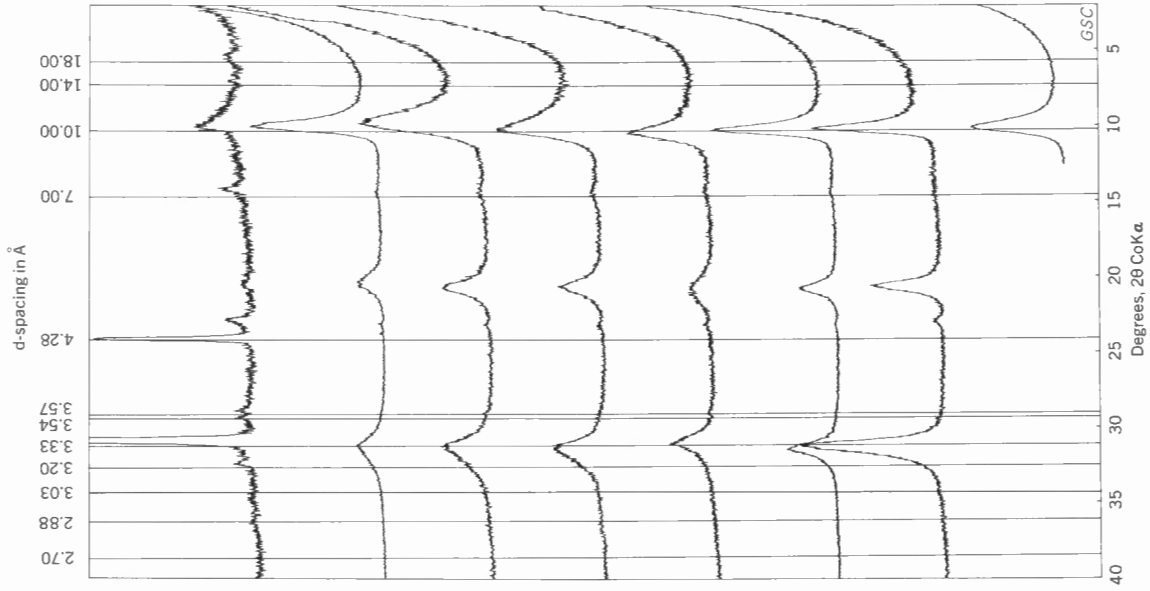


FIGURE 5. X-ray diffraction patterns of the whole rock,  $\text{Ca}^{2+}$  and  $\text{K}^{+}$  saturated  $<.2\mu$  oriented specimens from Comotion Formation, North Wolverine Ridge (Section 2)

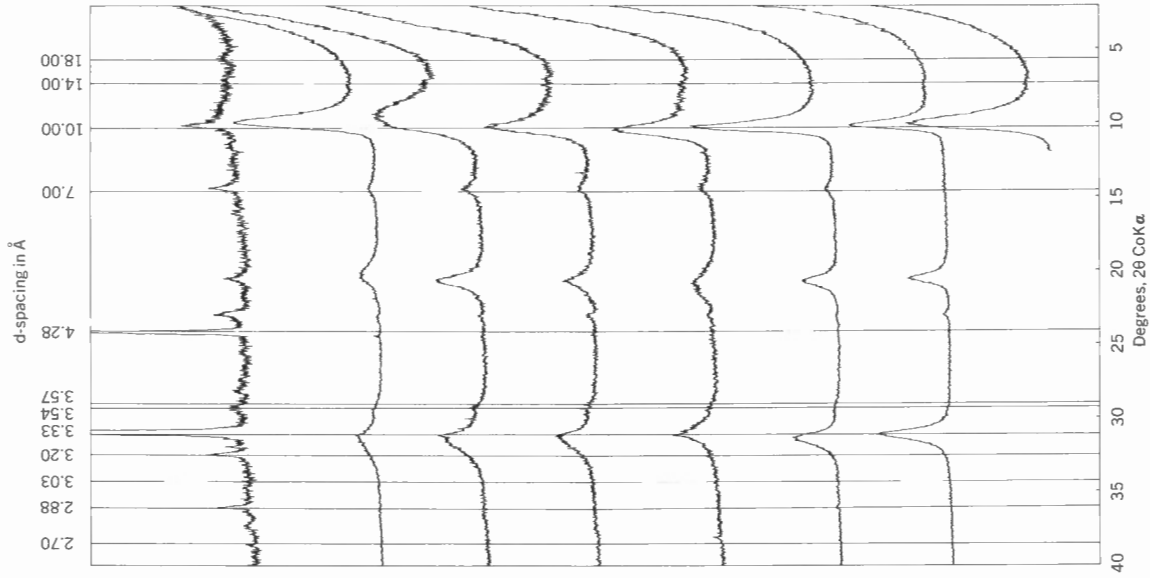


FIGURE 4. X-ray diffraction patterns of the whole rock,  $\text{Ca}^{2+}$  and  $\text{K}^{+}$  saturated  $<.2\mu$  oriented specimens from Moosebar Formation, Peace River (Section 1)

Whole rock

Ca  $<.2\mu$  oriented specimen at 0% R.H.

Ca  $<.2\mu$  oriented specimen at 50% R.H.

Ca  $<.2\mu$  oriented specimen at 85% R.H.

Ca  $<.2\mu$  oriented specimen with glycerol

Ca  $<.2\mu$  oriented specimen at 350°C

Ca  $<.2\mu$  oriented specimen at 600°C

K  $<.2\mu$  oriented specimen at 85% R.H.

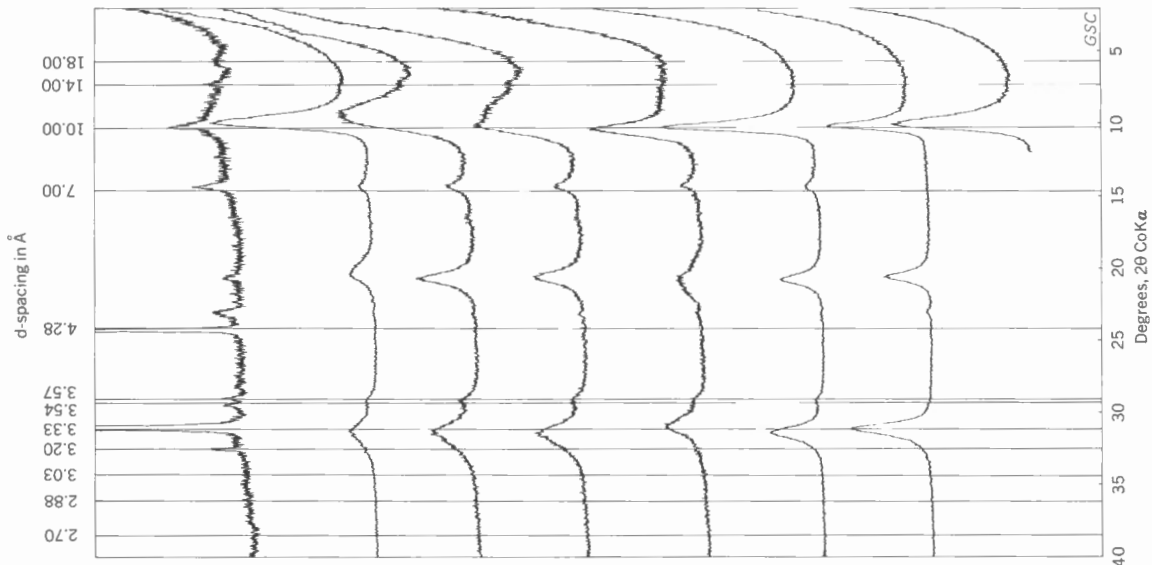


FIGURE 7. X-ray diffraction patterns of the whole rock,  $\text{Ca}^{2+}$  and  $\text{K}^{+}$  saturated  $<.2\mu$  oriented specimens from Cruiser Formation (Section 4)

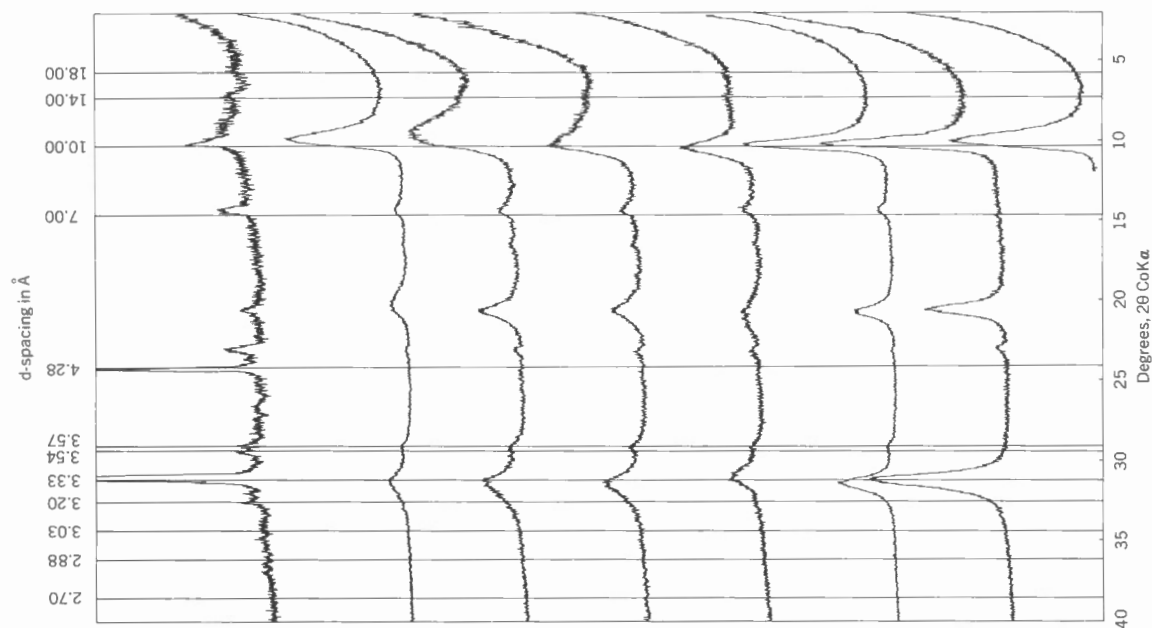


FIGURE 6. X-ray diffraction patterns of the whole rock,  $\text{Ca}^{2+}$  and  $\text{K}^{+}$  saturated  $<.2\mu$  oriented specimens from Hasler Formation, Dokie Ridge (Section 3)

Whole rock

Ca  $<.2\mu$  oriented specimen at 0% R.H.

Ca  $<.2\mu$  oriented specimen at 50% R.H.

Ca  $<.2\mu$  oriented specimen at 85% R.H.

Ca  $<.2\mu$  oriented specimen with glycerol

Ca  $<.2\mu$  oriented specimen at 350°C

Ca  $<.2\mu$  oriented specimen at 600°C

K  $<.2\mu$  oriented specimen at 85% R.H.

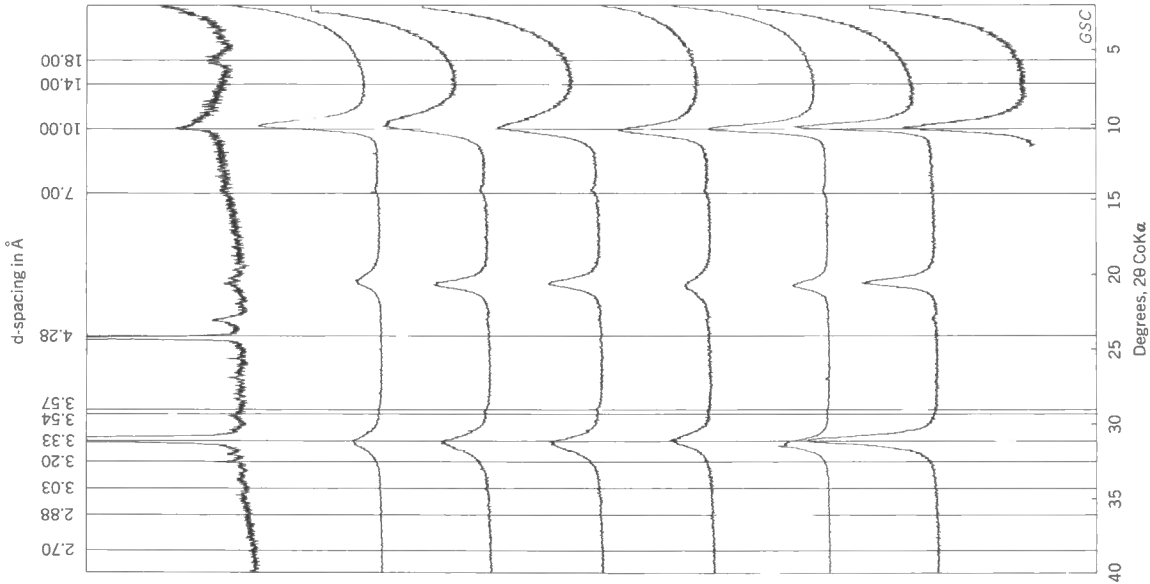


FIGURE 9. X-ray diffraction patterns of the whole rock,  $\text{Ca}^{2+}$  and  $\text{K}^+$  saturated  $<.2\mu$  oriented specimens from the middle zone of Gething Formation, Besa River (Section 5, II)

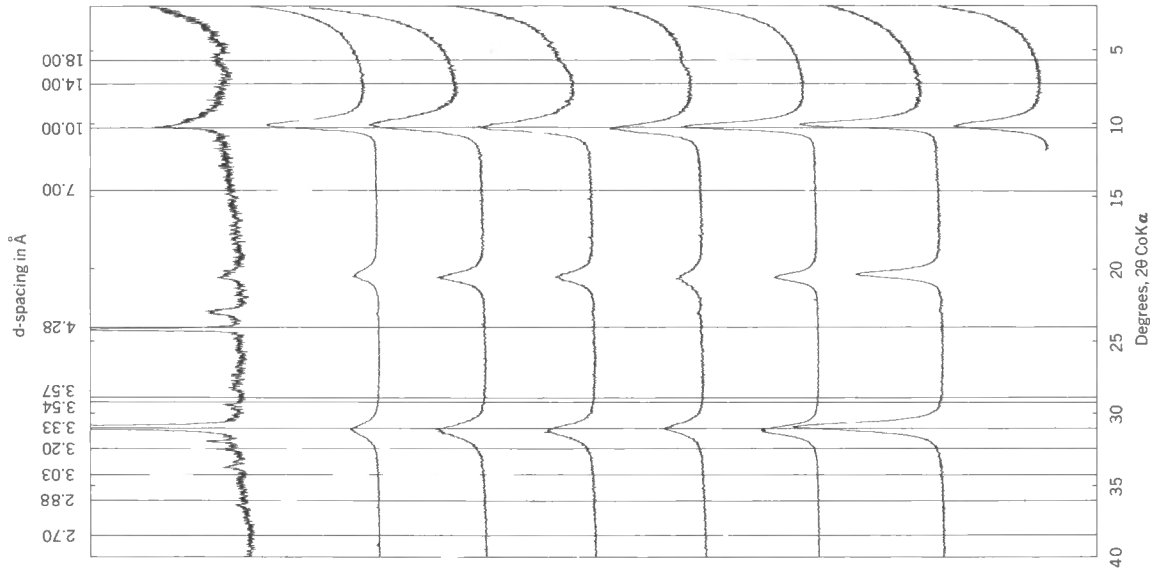


FIGURE 8. X-ray diffraction patterns of the whole rock,  $\text{Ca}^{2+}$  and  $\text{K}^+$  saturated  $<.2\mu$  oriented specimens from the lower zone of Gething Formation, Besa River (Section 5, I)

Whole rock

$\text{Ca} <.2\mu$  oriented specimen at 0% R.H.

$\text{Ca} <.2\mu$  oriented specimen at 50% R.H.

$\text{Ca} <.2\mu$  oriented specimen at 85% R.H.

$\text{Ca} <.2\mu$  oriented specimen with glycerol

$\text{Ca} <.2\mu$  oriented specimen at 350°C

$\text{Ca} <.2\mu$  oriented specimen at 600°C

$\text{K} <.2\mu$  oriented specimen at 85% R.H.

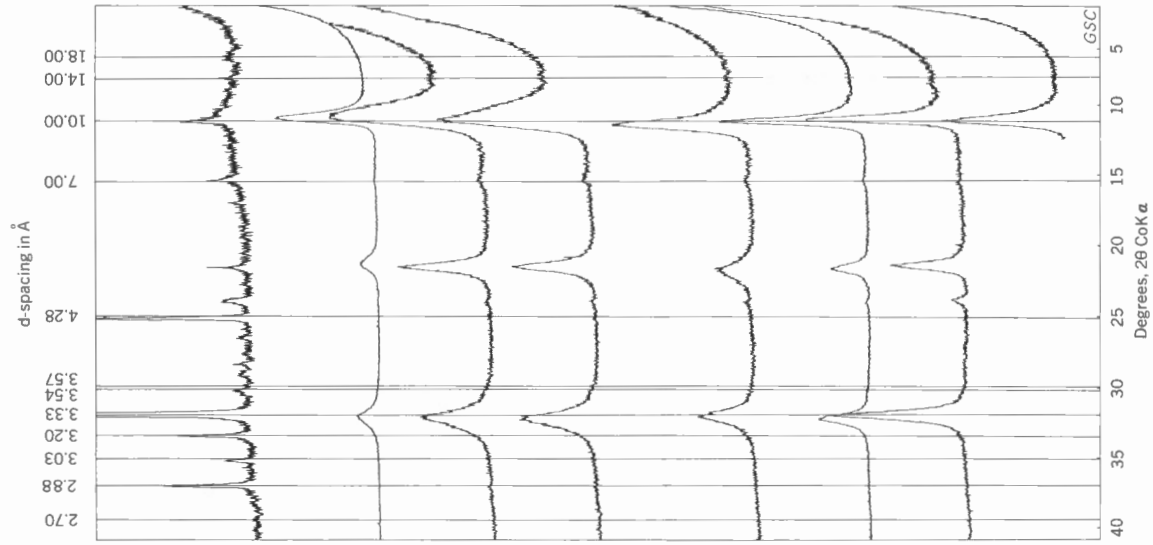


FIGURE 11. X-ray diffraction patterns of the whole rock,  $\text{Ca}^{2+}$  and  $\text{K}^+$  saturated  $<.2\mu$  oriented specimens from the lower zone of Gething Formation, Prophet River (Section 6, I)

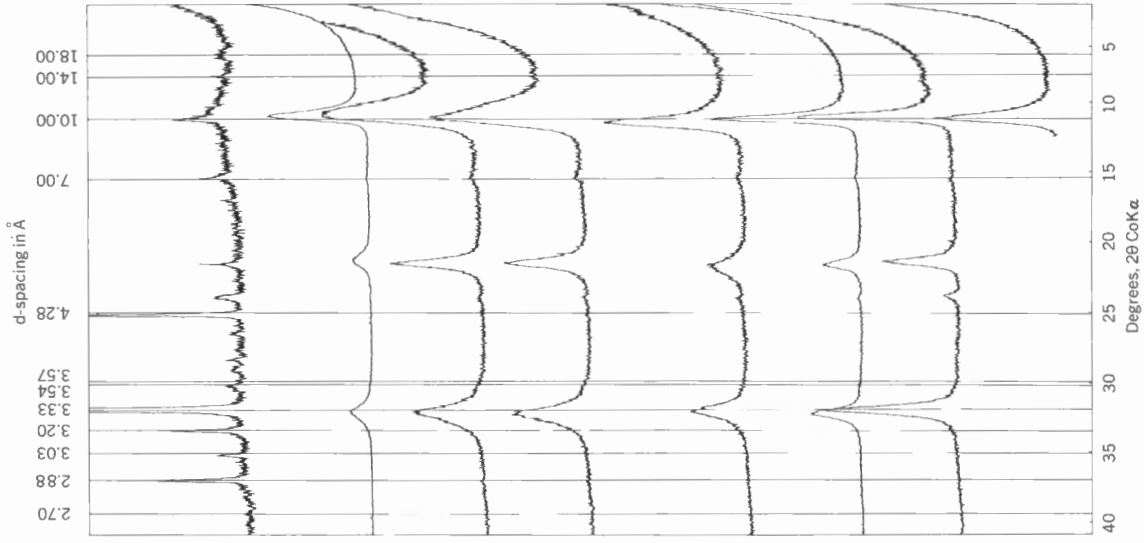


FIGURE 10. X-ray diffraction patterns of the whole rock,  $\text{Ca}^{2+}$  and  $\text{K}^+$  saturated  $<.2\mu$  oriented specimens from the upper zone of Gething Formation, Besa River (Section 5, III)

Whole rock

Ca  $<.2\mu$  oriented specimen at 0% R.H.

Ca  $<.2\mu$  oriented specimen at 50% R.H.

Ca  $<.2\mu$  oriented specimen at 85% R.H.

Ca  $<.2\mu$  oriented specimen with glycerol

Ca  $<.2\mu$  oriented specimen at 350°C

Ca  $<.2\mu$  oriented specimen at 600°C

K  $<.2\mu$  oriented specimen at 85% R.H.

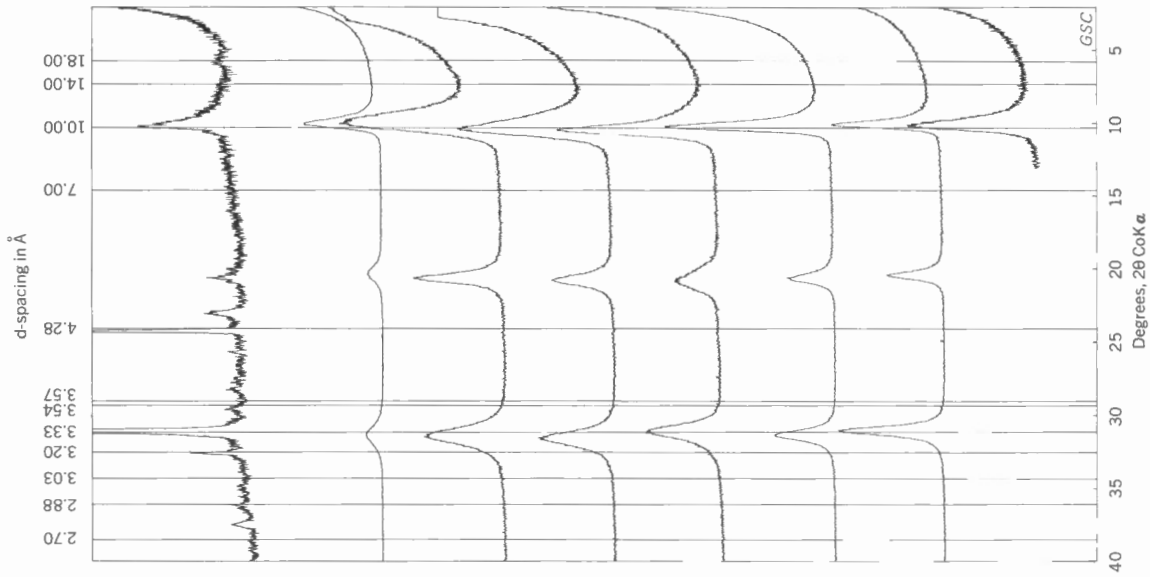


FIGURE 13. X-ray diffraction patterns of the whole rock,  $\text{Ca}^{2+}$  and  $\text{K}^+$  saturated  $<.2\mu$  oriented specimens from the lower zone of Gething Formation, Bat Creek (Section 7, I)

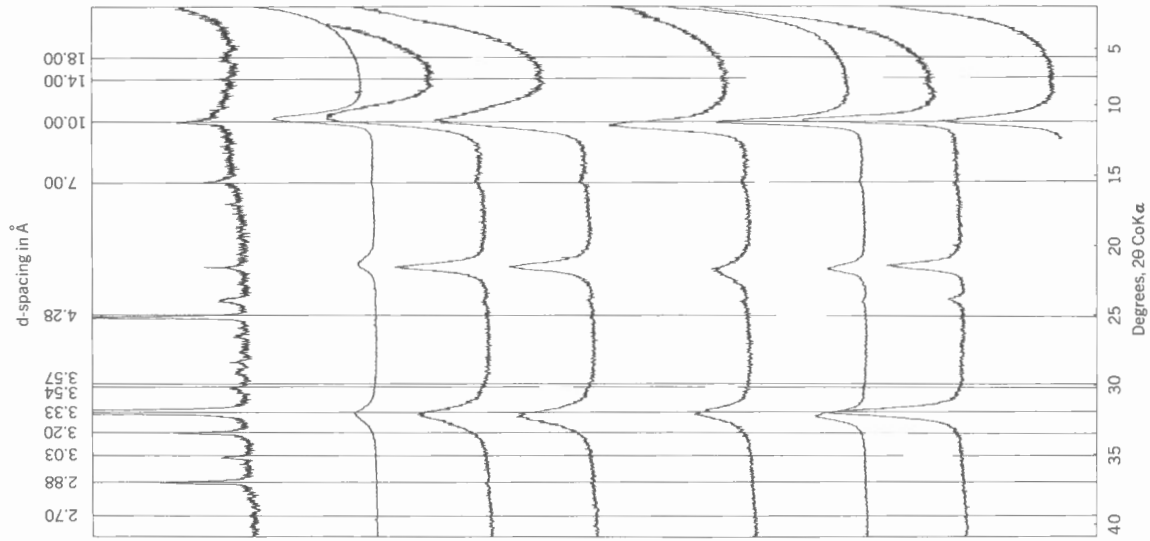


FIGURE 12. X-ray diffraction patterns of the whole rock,  $\text{Ca}^{2+}$  and  $\text{K}^+$  saturated  $<.2\mu$  oriented specimens from the upper zone of Gething Formation, Prophet River (Section 6, II)

Whole rock

$\text{Ca} <.2\mu$  oriented specimen at 0% R.H.

$\text{Ca} <.2\mu$  oriented specimen at 50% R.H.

$\text{Ca} <.2\mu$  oriented specimen at 85% R.H.

$\text{Ca} <.2\mu$  oriented specimen with glycerol

$\text{Ca} <.2\mu$  oriented specimen at 350°C

$\text{Ca} <.2\mu$  oriented specimen at 600°C

$\text{K} <.2\mu$  oriented specimen at 85% R.H.



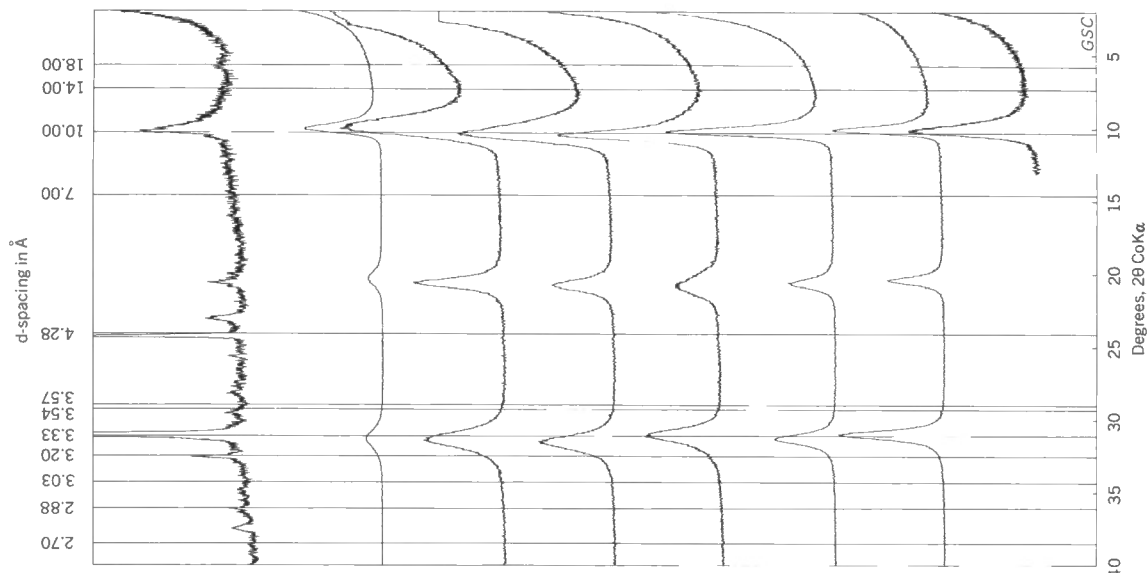


FIGURE 15. X-ray diffraction patterns of the whole rock,  $\text{Ca}^{2+}$  and  $\text{K}^{+}$  saturated  $<.2\mu$  oriented specimens from Buckinghamshire Formation, Tetsa River (Section 8, I)

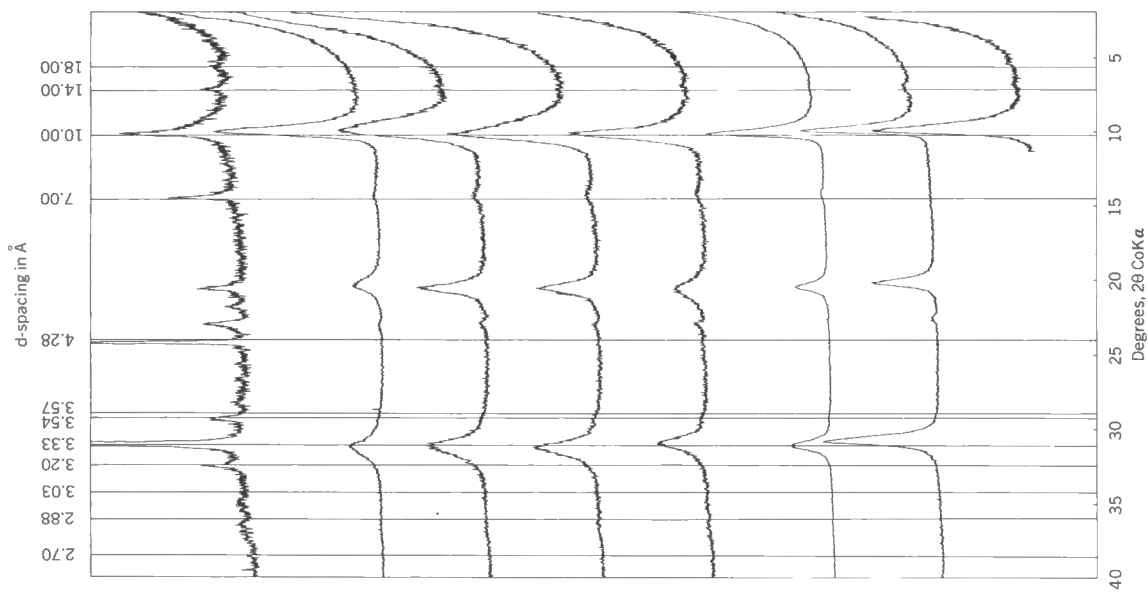


FIGURE 14. X-ray diffraction patterns of the whole rock,  $\text{Ca}^{2+}$  and  $\text{K}^{+}$  saturated  $<.2\mu$  oriented specimens from the upper zone of Gething Formation, Bat Creek (Section 7, II)

Whole rock

$\text{Ca} <.2\mu$  oriented specimen at 0% R.H.

$\text{Ca} <.2\mu$  oriented specimen at 50% R.H.

$\text{Ca} <.2\mu$  oriented specimen at 85% R.H.

$\text{Ca} <.2\mu$  oriented specimen with glycerol

$\text{Ca} <.2\mu$  oriented specimen at 350°C

$\text{Ca} <.2\mu$  oriented specimen at 600°C

$\text{K} <.2\mu$  oriented specimen at 85% R.H.

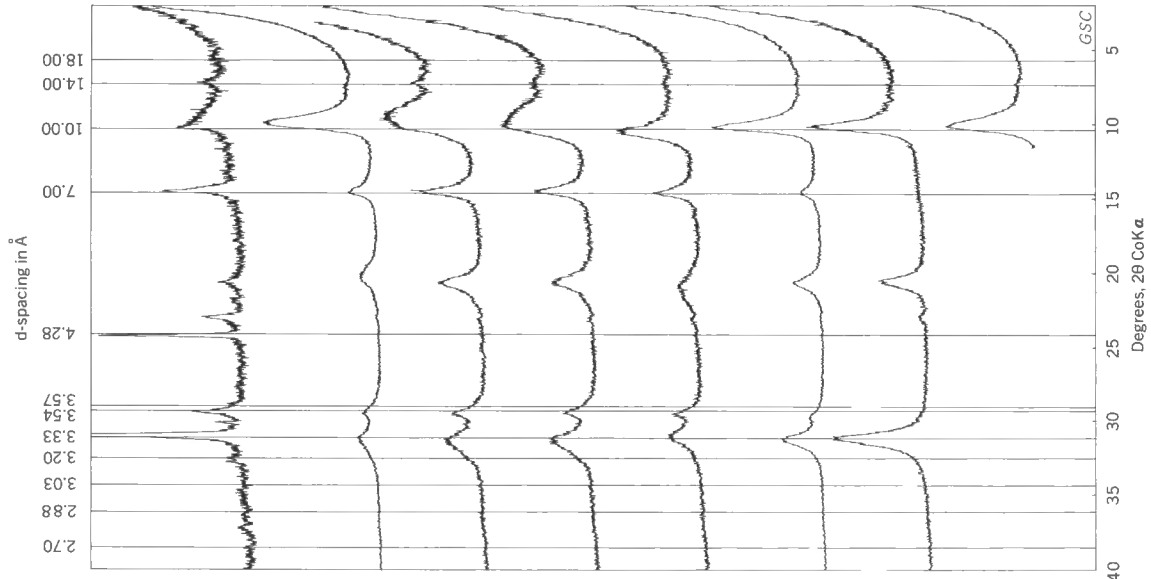


FIGURE 17. X-ray diffraction patterns of the whole rock,  $\text{Ca}^{2+}$  and  $\text{K}^{+}$  saturated  $<.2\mu$  oriented specimens from Buckinghamshire Formation, Tetsa River (Section 8, III)

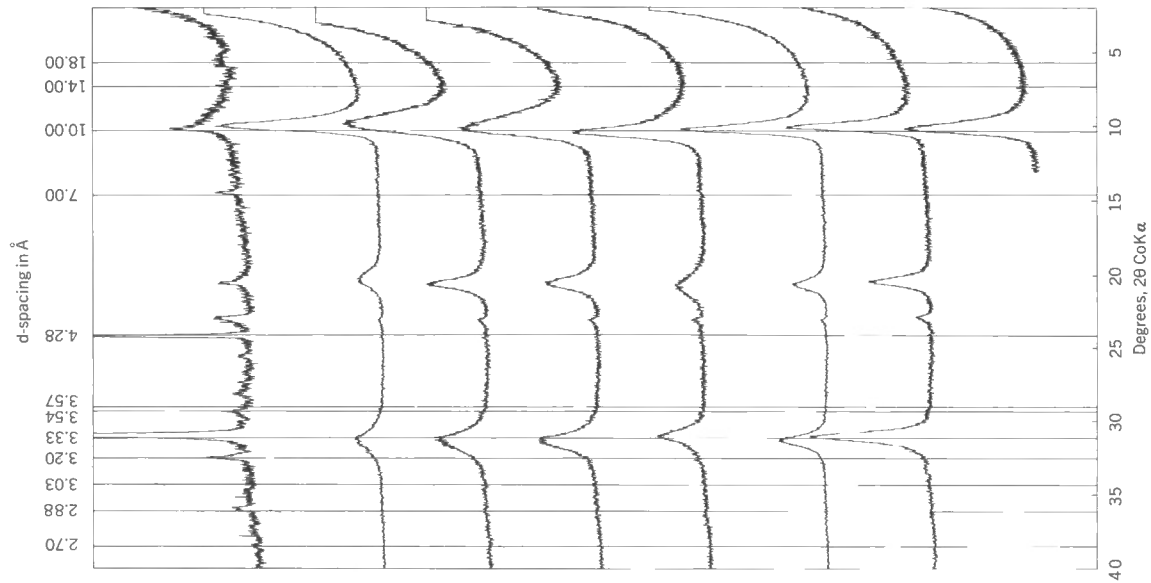


FIGURE 16. X-ray diffraction patterns of the whole rock,  $\text{Ca}^{2+}$  and  $\text{K}^{+}$  saturated  $<.2\mu$  oriented specimens from Buckinghamshire Formation, Tetsa River (Section 8, II)

Whole rock

Ca <math><.2\mu</math> oriented specimen at 0% R.H.

Ca <math><.2\mu</math> oriented specimen at 50% R.H.

Ca <math><.2\mu</math> oriented specimen at 85% R.H.

Ca <math><.2\mu</math> oriented specimen with glycerol

Ca <math><.2\mu</math> oriented specimen at 350°C

Ca <math><.2\mu</math> oriented specimen at 600°C

K <math><.2\mu</math> oriented specimen at 85% R.H.

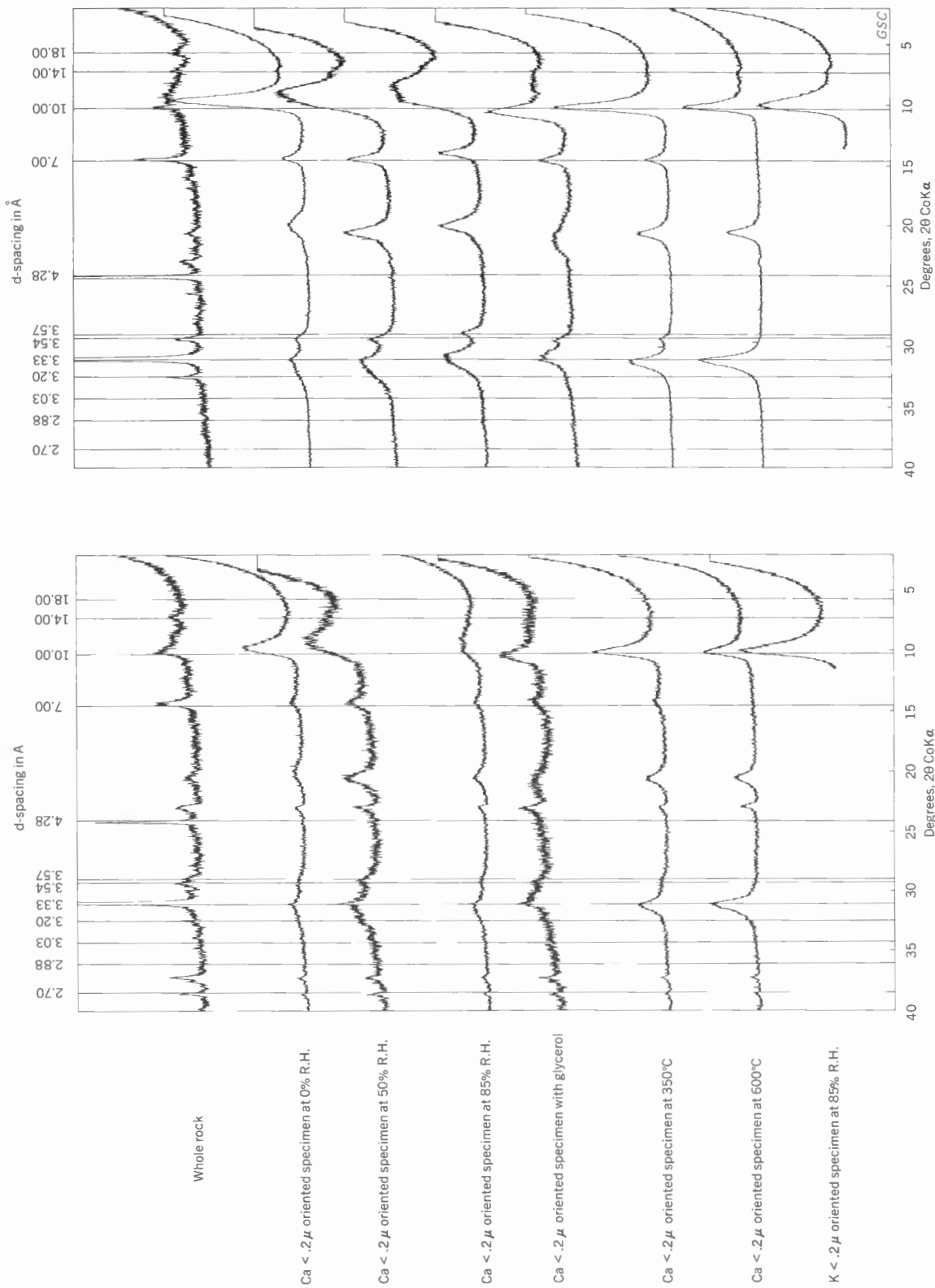


FIGURE 19. X-ray diffraction patterns of the whole rock, Ca<sup>2+</sup> and K<sup>+</sup> saturated <.2μ oriented specimens from Buckingham Formation, Tetsa River (Section 8, V)

FIGURE 18. X-ray diffraction patterns of the whole rock, Ca<sup>2+</sup> and K<sup>+</sup> saturated <.2μ oriented specimens from Buckingham Formation, Tetsa River (Section 8, IV)

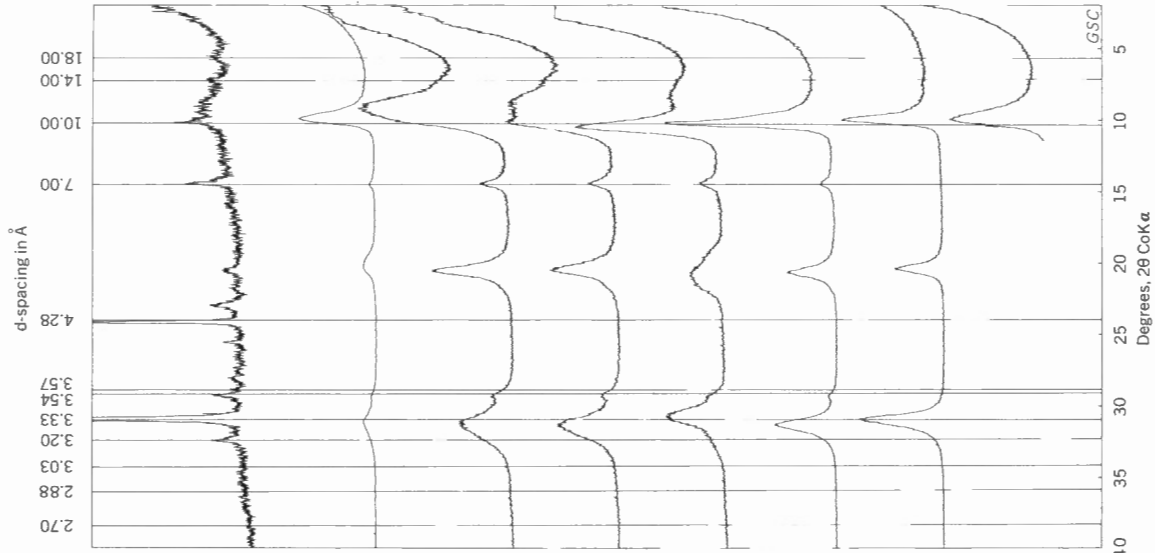


FIGURE 21. X-ray diffraction patterns of the whole rock,  $\text{Ca}^{2+}$  and  $\text{K}^{+}$  saturated  $<.2\mu$  oriented specimens from Buckinghamhorse Formation, Muskwa River (Section 9, I)

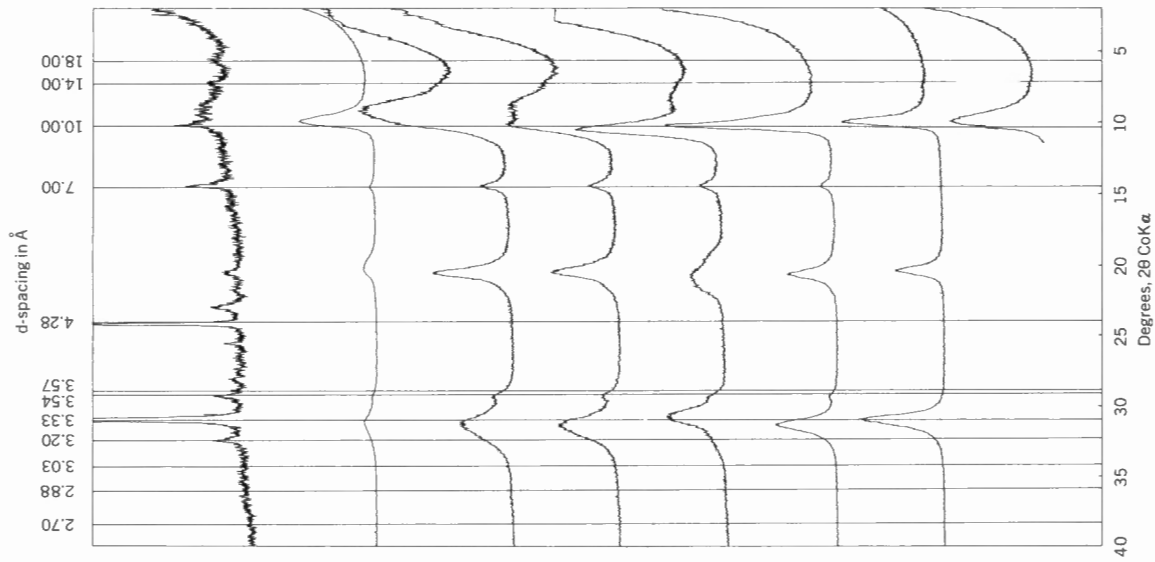


FIGURE 20. X-ray diffraction patterns of the whole rock,  $\text{Ca}^{2+}$  and  $\text{K}^{+}$  saturated  $<.2\mu$  oriented specimens from Buckinghamhorse Formation, Tetsa River (Section 8, VI)

Whole rock

Ca  $<.2\mu$  oriented specimen at 0% R.H.

Ca  $<.2\mu$  oriented specimen at 50% R.H.

Ca  $<.2\mu$  oriented specimen at 85% R.H.

Ca  $<.2\mu$  oriented specimen with glycerol

Ca  $<.2\mu$  oriented specimen at 350°C

Ca  $<.2\mu$  oriented specimen at 600°C

K  $<.2\mu$  oriented specimen at 85% R.H.

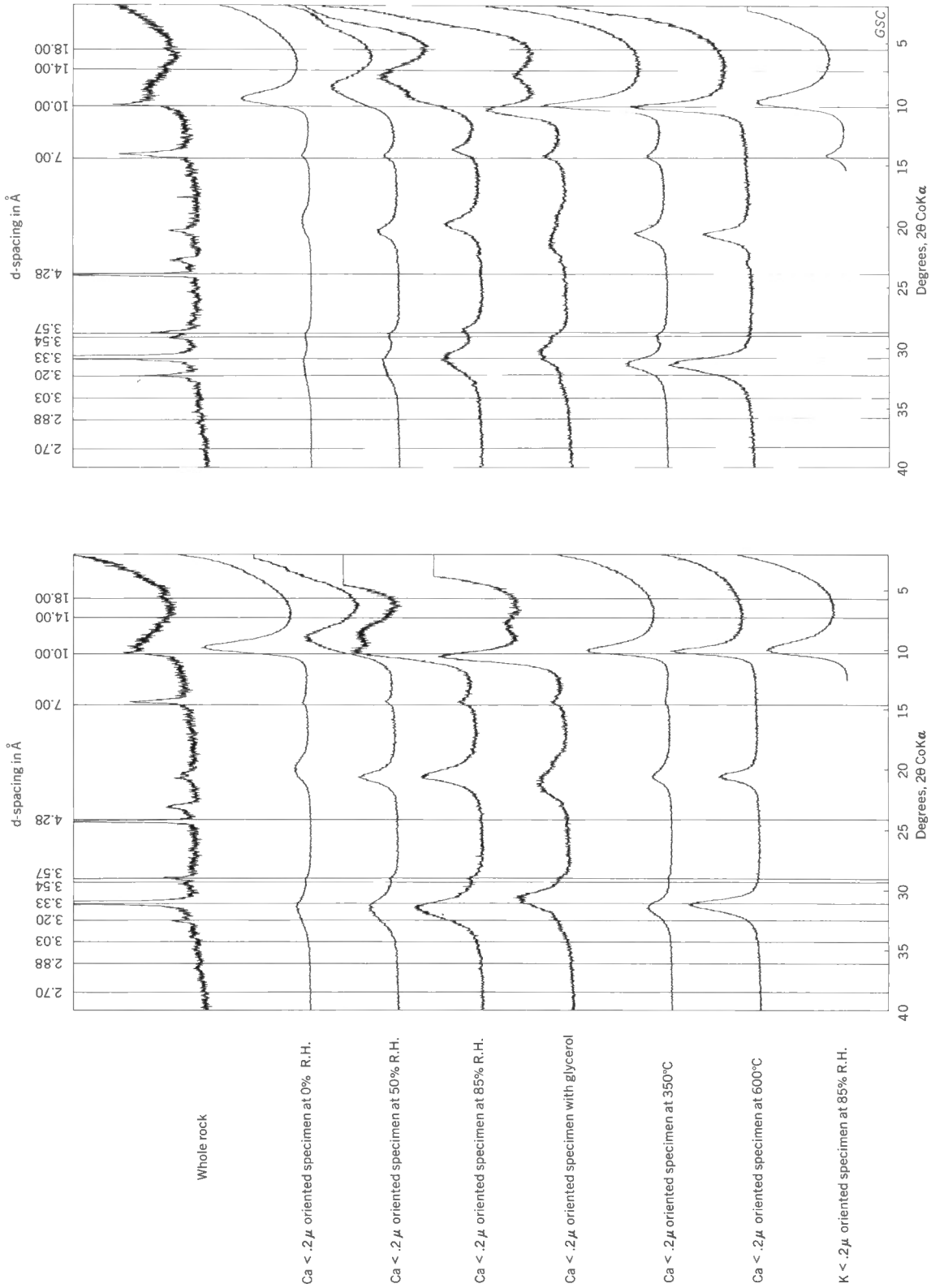


FIGURE 23. X-ray diffraction patterns of the whole rock, Ca<sup>2+</sup> and K<sup>+</sup> saturated <.2μ oriented specimens from Buckinghamhorse Formation, Muskwa River (Section 9, IIIa)

FIGURE 22. X-ray diffraction patterns of the whole rock, Ca<sup>2+</sup> and K<sup>+</sup> saturated <.2μ oriented specimens from Buckinghamhorse Formation, Muskwa River (Section 9, II)

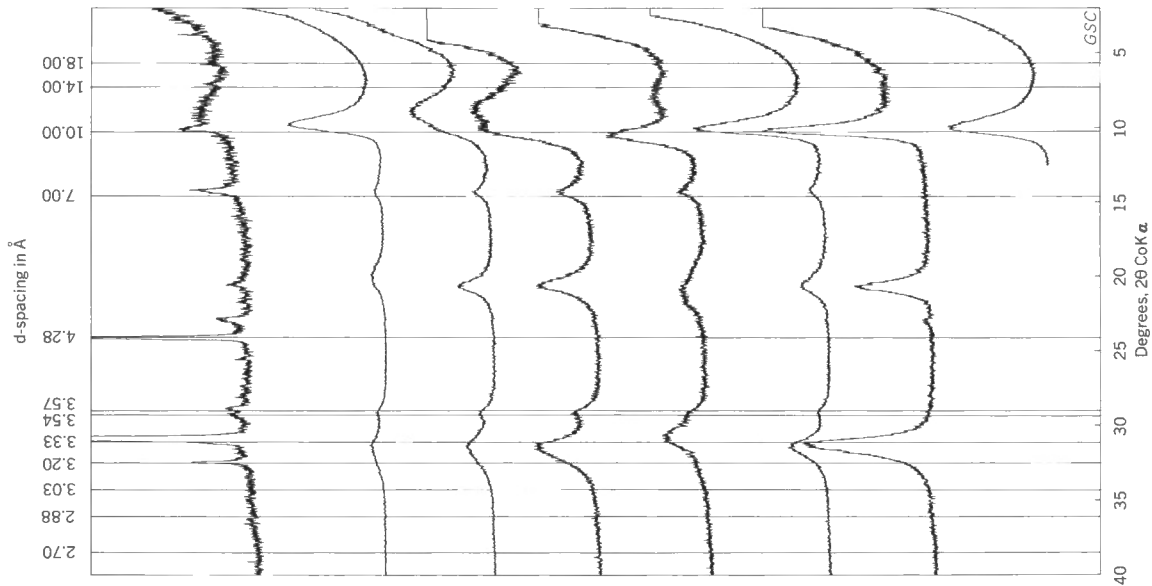


FIGURE 25. X-ray diffraction patterns of the whole rock,  $\text{Ca}_2^+$  and  $\text{K}^+$  saturated  $<.2\mu$  oriented specimens from Garbutt Formation (Section 10)

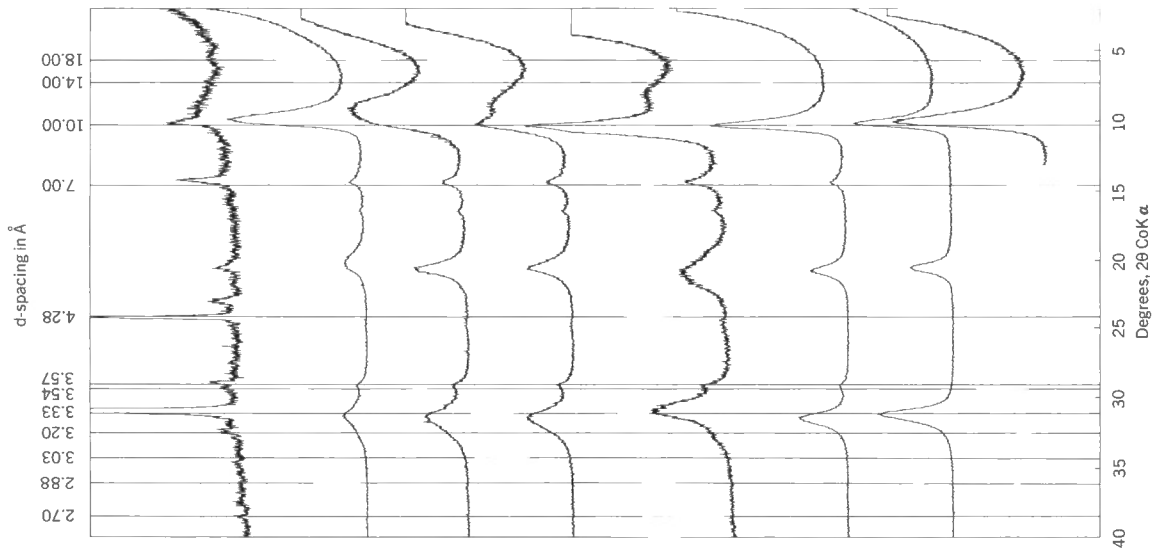


FIGURE 24. X-ray diffraction patterns of the whole rock,  $\text{Ca}_2^+$  and  $\text{K}^+$  saturated  $<.2\mu$  oriented specimens from Buckingham Formation, Muskwa River (Section 9, IIIb)

Whole rock

Ca  $<.2\mu$  oriented specimen at 0% R.H.

Ca  $<.2\mu$  oriented specimen at 50% R.H.

Ca  $<.2\mu$  oriented specimen at 85% R.H.

Ca  $<.2\mu$  oriented specimen with glycerol

Ca  $<.2\mu$  oriented specimen at 350°C

Ca  $<.2\mu$  oriented specimen at 600°C

K  $<.2\mu$  oriented specimen at 85% R.H.

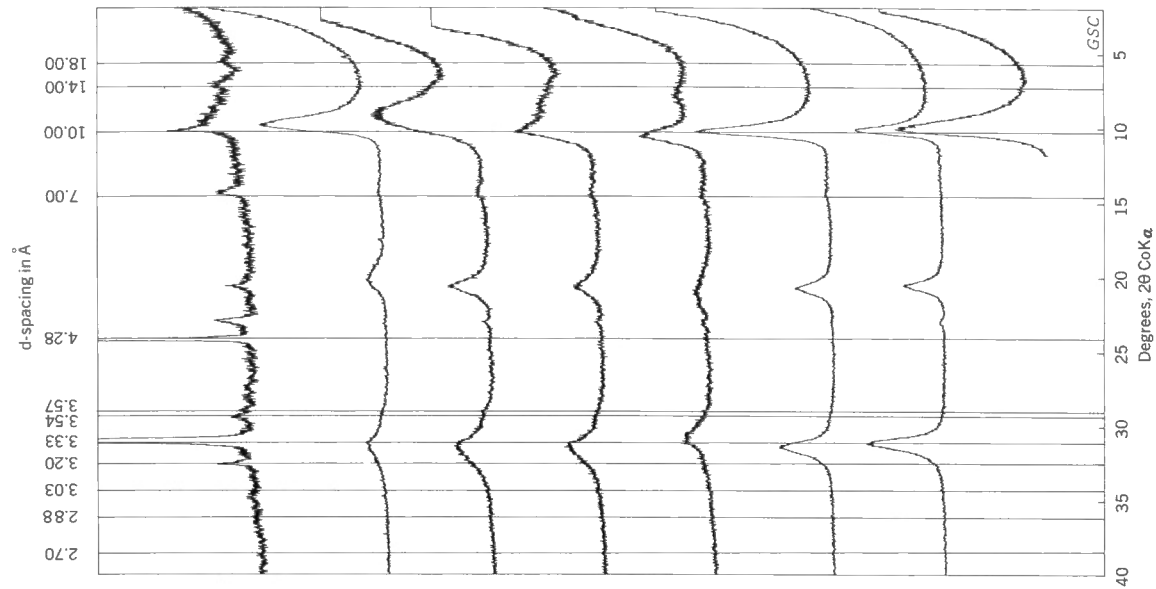


FIGURE 27. X-ray diffraction patterns of the whole rock,  $\text{Ca}^{2+}$  and  $\text{K}^+$  saturated  $<.2\mu$  oriented specimens from the middle zone of Scatter Formation, Scatter River (Section II, II)

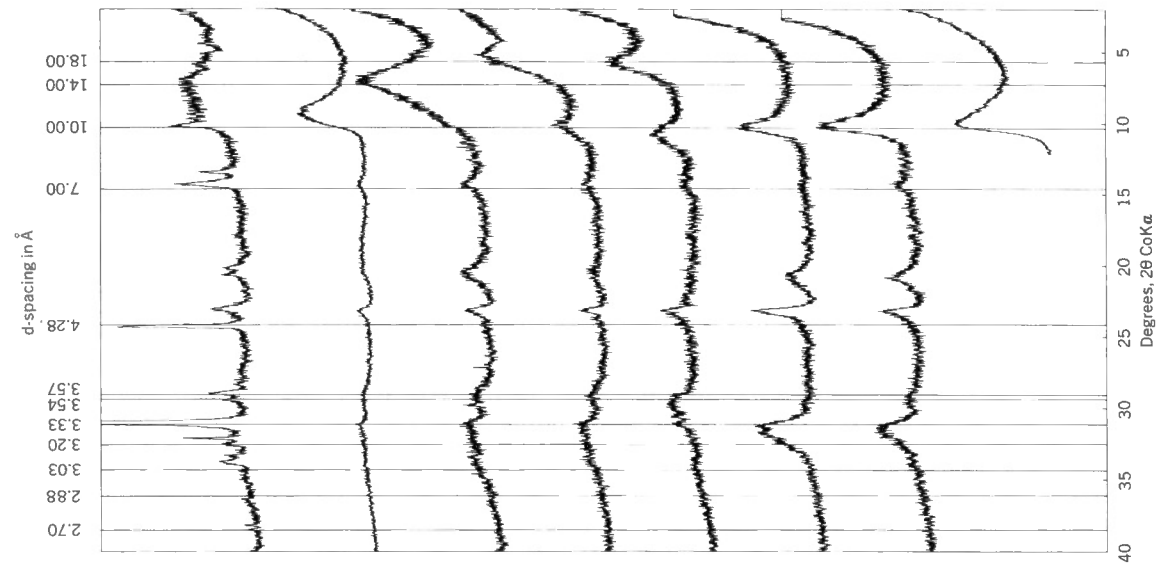


FIGURE 26. X-ray diffraction patterns of the whole rock,  $\text{Ca}^{2+}$  and  $\text{K}^+$  saturated  $<.2\mu$  oriented specimens from the lower zone of Scatter Formation, Scatter River (Section II, I)

- Whole rock
- $\text{Ca} <.2\mu$  oriented specimen at 0% R.H.
- $\text{Ca} <.2\mu$  oriented specimen at 50% R.H.
- $\text{Ca} <.2\mu$  oriented specimen at 85% R.H.
- $\text{Ca} <.2\mu$  oriented specimen with glycerol
- $\text{Ca} <.2\mu$  oriented specimen at 350°C
- $\text{Ca} <.2\mu$  oriented specimen at 600°C
- $\text{K} <.2\mu$  oriented specimen at 85% R.H.

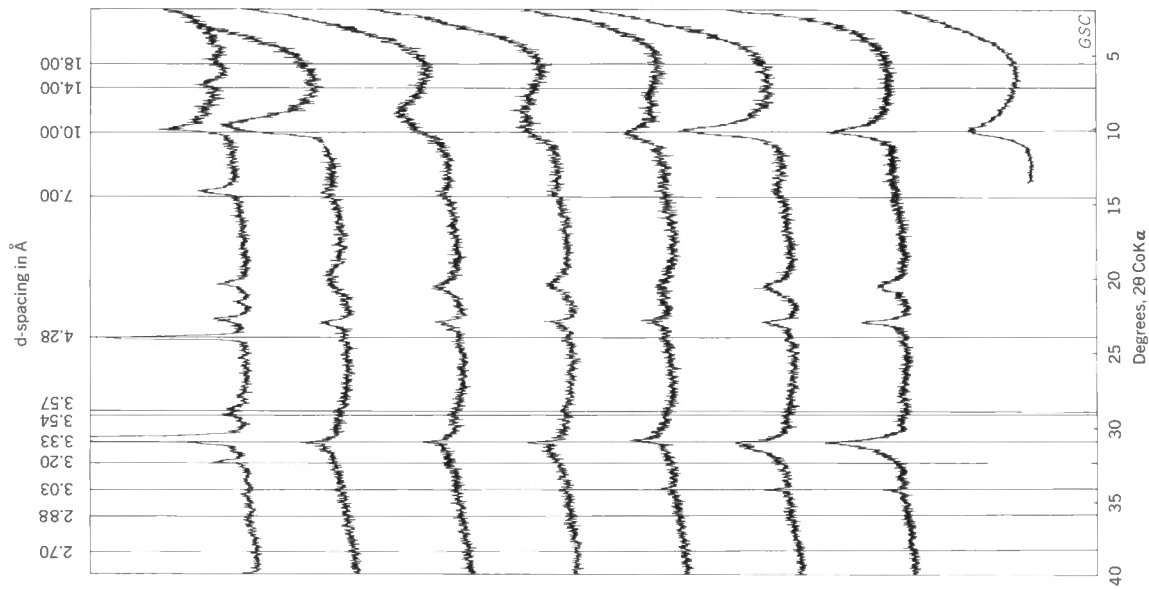


FIGURE 29. X-ray diffraction patterns of the whole rock,  $\text{Ca}^{2+}$  and  $\text{K}^+$  saturated  $< .2\mu$  oriented specimens from Middle Scatter Formation, Bear Island, Liard River (Section I2)

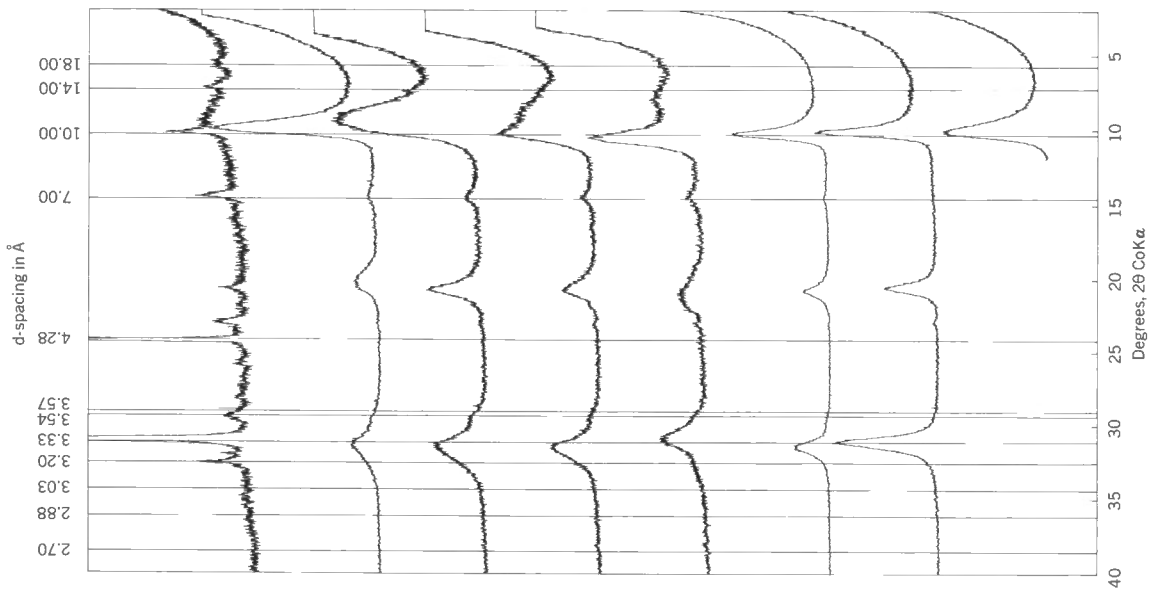


FIGURE 28. X-ray diffraction patterns of the whole rock,  $\text{Ca}^{2+}$  and  $\text{K}^+$  saturated  $< .2\mu$  oriented specimens from the upper zone of Scatter Formation, Scatter River (Section 11, III)

Whole rock

Ca <math>< .2\mu</math> oriented specimen at 0% R.H.

Ca <math>< .2\mu</math> oriented specimen at 50% R.H.

Ca <math>< .2\mu</math> oriented specimen at 85% R.H.

Ca <math>< .2\mu</math> oriented specimen with glycerol

Ca <math>< .2\mu</math> oriented specimen at 350°C

Ca <math>< .2\mu</math> oriented specimen at 600°C

K <math>< .2\mu</math> oriented specimen at 85% R.H.



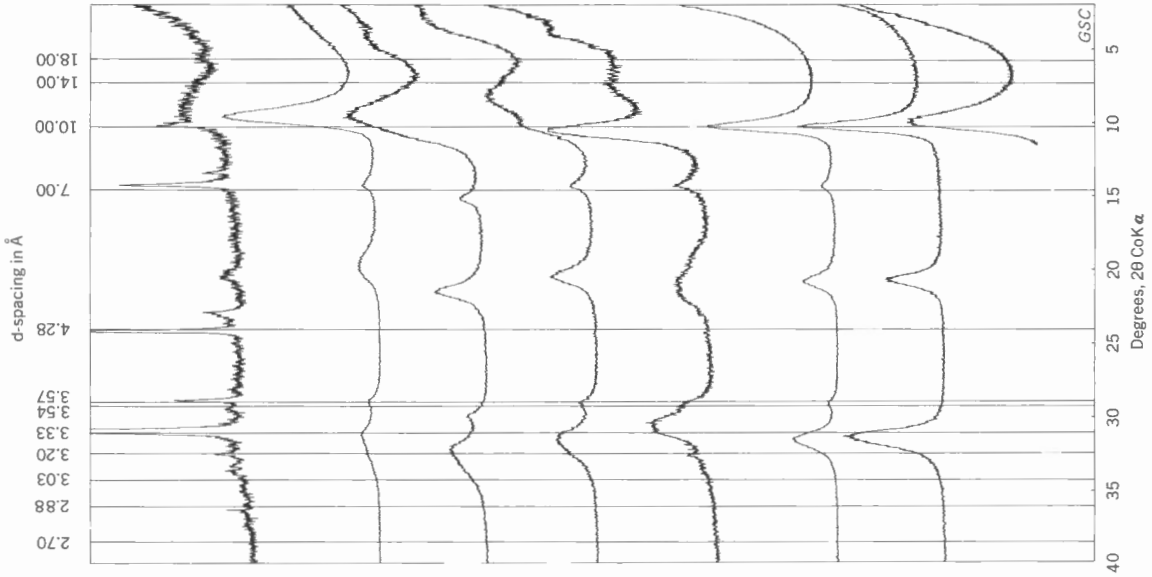


FIGURE 31. X-ray diffraction patterns of the whole rock,  $\text{Ca}^{2+}$  and  $\text{K}^{+}$  saturated  $<.2\mu$  oriented specimens from the lower zone of Lepine Formation, Liard River (Section 14, I)

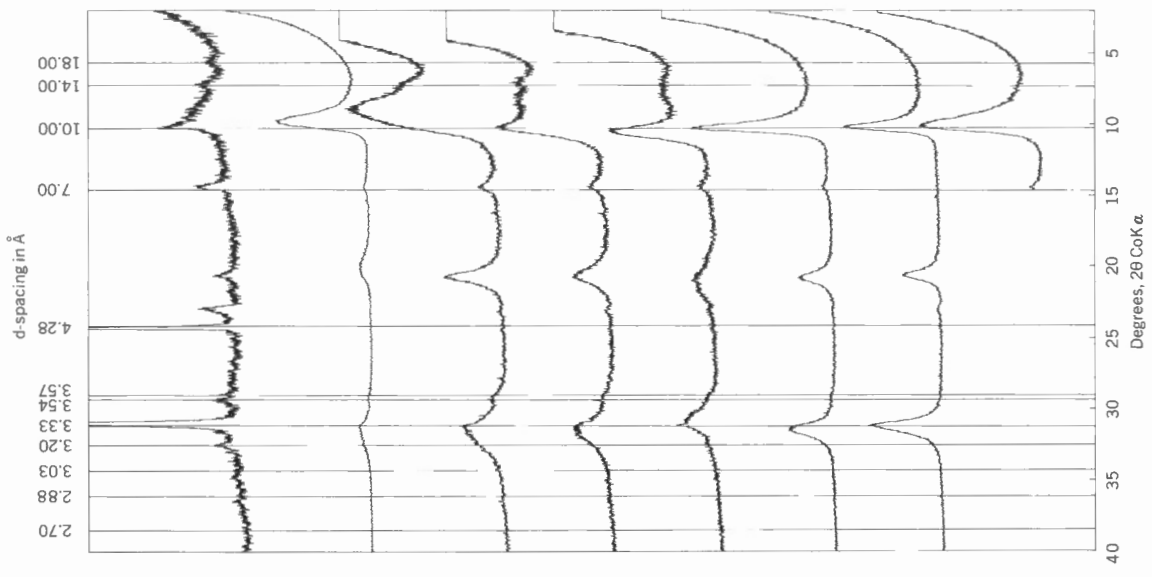


FIGURE 30. X-ray diffraction patterns of the whole rock,  $\text{Ca}^{2+}$  and  $\text{K}^{+}$  saturated  $<.2\mu$  oriented specimens from Middle Scatter Formation, north of Scatter River (Section 13)

Whole rock

Ca  $<.2\mu$  oriented specimen at 0% R.H.

Ca  $<.2\mu$  oriented specimen at 50% R.H.

Ca  $<.2\mu$  oriented specimen at 85% R.H.

Ca  $<.2\mu$  oriented specimen with glycerol

Ca  $<.2\mu$  oriented specimen at 350°C

Ca  $<.2\mu$  oriented specimen at 600°C

K  $<.2\mu$  oriented specimen at 85% R.H.

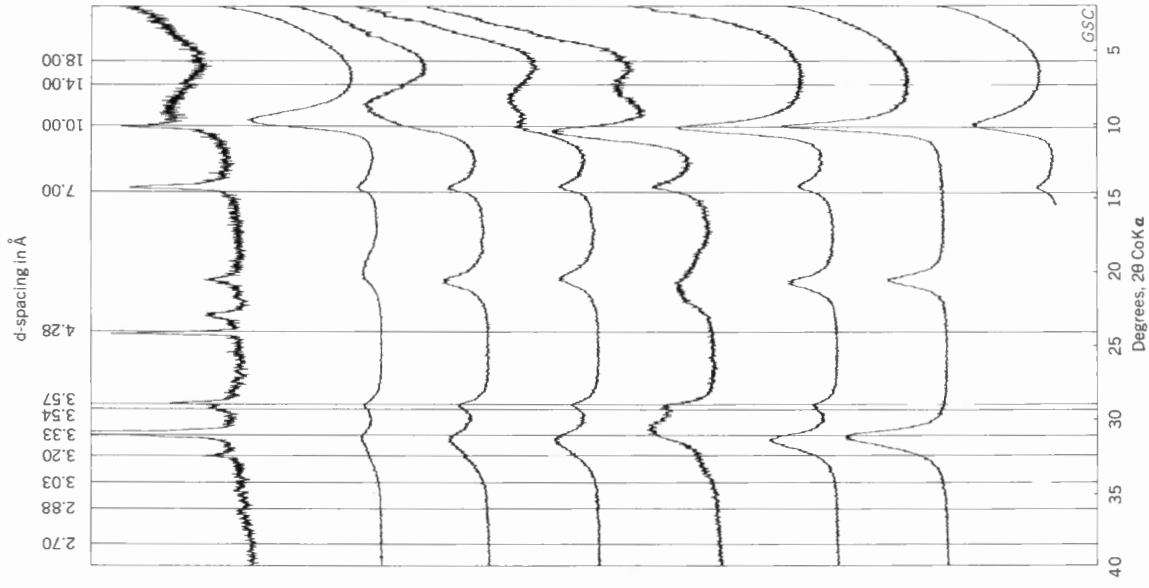


FIGURE 33. X-ray diffraction patterns of the whole rock,  $\text{Ca}^{2+}$  and  $\text{K}^{+}$  saturated  $<.2\mu$  oriented specimens from the lower zone of Lepine, Sikanni and Sully Formations, Scatter River (Section 14, III, and 15, I)

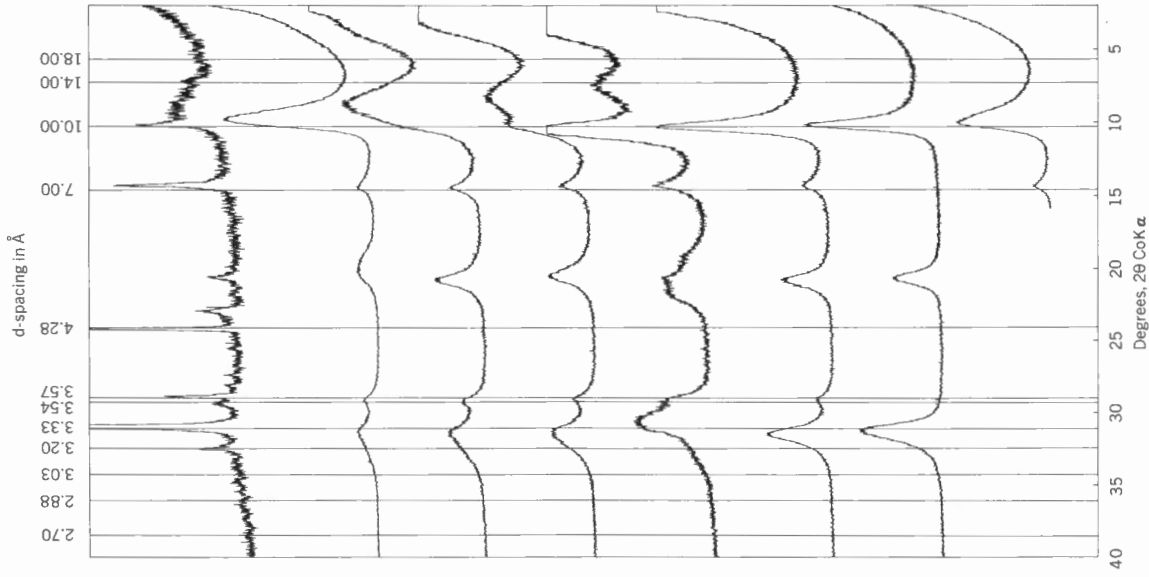


FIGURE 32. X-ray diffraction patterns of the whole rock,  $\text{Ca}^{2+}$  and  $\text{K}^{+}$  saturated  $<.2\mu$  oriented specimens from the middle zone of Lepine Formation, Liard River (Section 14, II)

- Whole rock
- Ca  $<.2\mu$  oriented specimen at 0% R.H.
- Ca  $<.2\mu$  oriented specimen at 50% R.H.
- Ca  $<.2\mu$  oriented specimen at 85% R.H.
- Ca  $<.2\mu$  oriented specimen with glycerol
- Ca  $<.2\mu$  oriented specimen at 350°C
- Ca  $<.2\mu$  oriented specimen at 600°C
- K  $<.2\mu$  oriented specimen at 85% R.H.

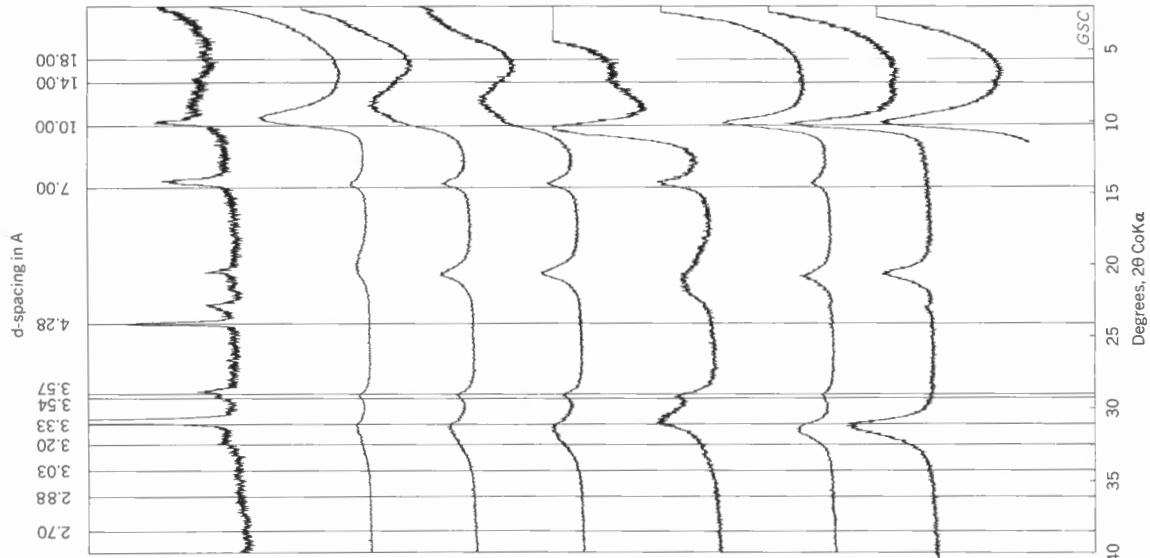


FIGURE 35. X-ray diffraction patterns of the whole rock,  $\text{Ca}^{2+}$  and  $\text{K}^+$  saturated  $<.2\mu$  oriented specimens from the upper zone of Lepine, Sikanni and Sully Formations, Scatter River (Section 15, III)

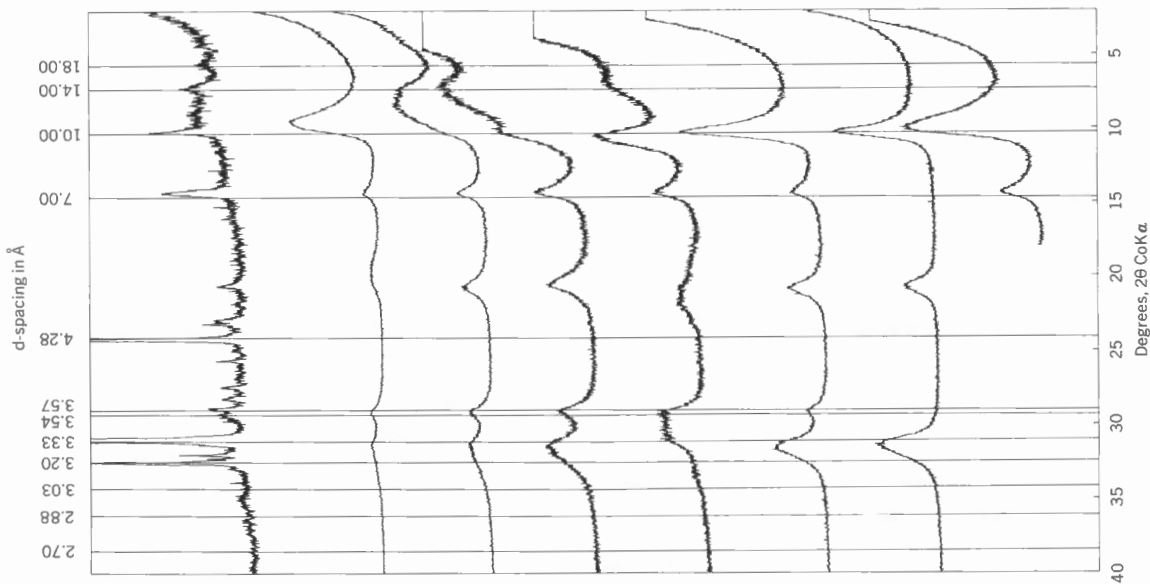


FIGURE 34. X-ray diffraction patterns of the whole rock,  $\text{Ca}^{2+}$  and  $\text{K}^+$  saturated  $<.2\mu$  oriented specimens from the middle zone of Lepine, Sikanni and Sully Formations, Scatter River (Section 15, II)

Whole rock

$\text{Ca} <.2\mu$  oriented specimen at 0% R.H.

$\text{Ca} <.2\mu$  oriented specimen at 50% R.H.

$\text{Ca} <.2\mu$  oriented specimen at 85% R.H.

$\text{Ca} <.2\mu$  oriented specimen with glycerol

$\text{Ca} <.2\mu$  oriented specimen at 350°C

$\text{Ca} <.2\mu$  oriented specimen at 600°C

$\text{K} <.2\mu$  oriented specimen at 85% R.H.